REVIEWS OF GEOPHYSICS, VOL. 26, NO. 3, PAGES 459–494, AUGUST 1988

Alternative Theories of Atmospheric Teleconnections and Low-Frequency Fluctuations

JORGEN S. FREDERIKSEN

Division of Atmospheric Research, Commonwealth Scientific and Industrial Research Organization Aspendale, Australia

PETER J. WEBSTER

Department of Meteorology, The Pennsylvania State University, University Park

Observational studies have revealed a rich low-frequency structure in the atmosphere. A review of the theories, observations, and model studies of this low-frequency atmospheric variability is presented. On time scales of weeks or longer the atmosphere appears to possess distinct oscillatory behavior in well-defined and persistent "centers of action." This behavior is also an endemic feature of surrogate atmospheric data sets emerging from experiments with complicated climate models. Many theories have attempted to determine the dominant physical processes responsible for the low-frequency variance but have usually failed when compared carefully with observations. For example, simple linear steady state and Rossby wave dispersion theories have been used in an attempt to explain the observed global response to low-latitude perturbation. However, the observed structures of mature anomalies are often quite distinct from the vertical structures of disturbances predicted in these theories. Also, in general circulation and model studies, the sign of the nonlinear response is not simply related to the sign of the forcing as predicted by linear steady state theories. It is argued that the theories fail because either the full three-dimensional complexity of the basic state is not considered or its inherent instability structure is not recognized or is, in fact, ignored. It is shown that three-dimensional instability theory provides a natural generalization and marriage of the zonally averaged instability theory of Charney and Eady and the Rossby wave dispersion theory of Rossby and Yeh. As such, it provides a formalism which may be used to understand a wide variety of atmospheric fluctuations including the locations of eddy flux covariance maxima and storm tracks in both the tropics and extratropics and the generation of blocking, teleconnection patterns, and other quasi-stationary anomaly features. Attention is focused on two particular mechanisms within this formalism for the formation of quasi-stationary low-frequency fluctuations. One of these is the baroclinic-barotropic dipole instability mechanism in which the formation of quasi-stationary mature anomalies is initiated by the upstream development of mid-latitude eastward propagating dipole wave trains which arise through the combined baroclinic-barotropic instability of the three-dimensional atmospheric flow. The other is the westerly duct mechanism in which the initiation of low-frequency variability is caused by tropical disturbances. According to this hypothesis, the longitudinal variation of the basic state flow near the equator causes a ducting of wave energy generated in the tropics to specific zones in the upper tropospheric westerlies; these zones then act as source regions for the emanation of waves into the extratropics. Furthermore, this duct also acts as a waveguide for extratropical modes propagating into or through the tropics.

CONTENTS

Paper number 8R0376.
8755-1209/88/008R-0376$05.00

1. INTRODUCTION

In recent years, two new avenues of research have developed in the atmospheric sciences, and each has required a better understanding of the low-frequency variability of the atmosphere. The first development is the extension of numerical weather prediction into the medium- (5–10 days) and low-frequency (> 10 days) ranges and the prospect of the extension of deterministic forecasting to the very long range. Here, low-frequency variability, defined generically as frequency lower than synoptic but higher than intraseasonal (10–90 days), is of importance as it is the major modulator of synoptic events within the extended forecast period. The second

research avenue is dynamic climatology, which has emerged as an important field through the growing interest in interannual variability and the hope of being able to forecast the variability or, at least, its statistics.

An example of a research avenue that has received considerable attention is that of the remote response of the climate system to changes in boundary forcing. This field emerged following the discovery of probable and intriguing relationships between anomalous tropical and extratropical climate and the warm events of the equatorial Pacific Ocean (of which the familiar El Niño is a notable manifestation) which were first raised, implicitly, by *Walker* [1924] and later, explicitly, by *Bjerknes* [1969]. Later we will see that such low-frequency variability is of importance in the context of dynamic climatology as it constitutes a major aggregation for intra-annual variability.

Both modeling and observational studies of low-frequency variability, the teleconnection of remote forcing, and anomalous climate response, in general, have proceeded with some vigor. (The term "teleconnection" was coined by *Bjerknes* [1969] to describe the remote response of the atmosphere to geographically removed forcing. Maps of teleconnectivity can be defined for fluctuations of all scales and period, including band-pass fluctuations (compare, for example, *Blackmon et al.* [1984*a*]). However, traditionally, the term has been applied primarily to the large-scale atmospheric fluctuations of low to very low frequency.)

However, as we shall develop subsequently, observations (here used generically to include surrogate atmospheric data fields generated by sophisticated climate models as well as fields derived from observed data obtained in the traditional manner) and theory appear to be some distance apart. In our review of both theory and observations we shall point out a number of such inconsistencies. Furthermore, we shall offer hypotheses that are, at the same time, we believe, more fundamental and physically consistent. Specifically, we shall suggest that the subject of low-frequency variability must be addressed in relation to a "full three-dimensional basic flow" which must follow from the realization that the basic flow is inherently unstable and possesses a whole hierarchy of modal structures that extends through the synoptic time scale to the low-frequency domain.

In our discussion of current theories aimed at explaining various aspects of the low-frequency variability of the atmosphere, we shall examine some of the observational studies of low-frequency fluctuations as well as the mechanisms which determine the three-dimensional atmospheric basic state. We then focus on theoretical, modeling, and observational studies of these phenomena pertinent to Rossby wave dispersion and steady state response theories and to three-dimensional instability theory. It will be emphasized that three-dimensional instability theory provides a natural generalization, and marriage, of the Rossby wave dispersion and steady state response theories of *Rossby* [1945] and *Yeh* [1949] and the zonally averaged instability theory of *Charney* [1947] and *Eady* [1949]. Within a linear context this more general instability theory thus provides a natural formalism for examining anomalies generated both through the evolution and amplification of internal "noise" and through the response to anomalous forcing. Within this theoretical framework we concentrate on two particular mechanisms for generating anomalies such as blocks and other teleconnection patterns, that we feel are consistent with both observational and model studies.

One of these mechanisms is the "baroclinic-barotropic dipole instability mechanism," in which the quasi-stationary mature anomalies are viewed as being initiated by the upstream development of mid-latitude eastward propagating dipole wave trains, arising through the combined baroclinic-barotropic instability of three-dimensional atmospheric flows. The other mechanism, in which the initiation is due to tropical disturbances, is the "wave energy accumulation-emanation region" (or "westerly duct") mechanism. In this hypothesis the longitudinal variation of the basic flow along the equator is considered to be of great significance. Energy generated remotely in other regions of the tropics is ducted toward and accumulated within specific zones which lie to the east of the upper tropospheric westerlies of the eastern Pacific Ocean and the Atlantic Ocean. Furthermore, these energy accumulation zones appear to act as source regions for the emanation of waves into the extratropics. The equatorial westerlies also appear to act as wave ducts for extratropical waves moving from higher latitudes to low latitudes or even through to the other hemisphere.

In section 2 we discuss the relationships between the rather complicated structure of the three-dimensional basic state and the global heating functions and orography, while in section 3 we examine the relationships between the observed eddy fields and the basic state. Section 4 considers the current theories which have been proposed to explain various aspects of low-frequency variability. In section 5 we examine Rossby wave dispersion and linear steady state theories with zonally averaged basic states which are implicitly or explicitly assumed to be stable. We show that these theories fail, in several aspects, to capture the observed structure of atmospheric variability. Here we also discuss the westerly duct mechanism, which emphasizes the longitudinal component of the stretching deformation (termed "longitudinal stretch") of the low-latitude basic flow as a focusing agent for the energy of the equatorial transients. Longitudinal stretch refers to the eastward component of the stretching deformation tensor $\partial\bar{u}/\partial x$, often referred to, incorrectly, as longitudinal shear, which is, of course, $\partial\bar{v}/\partial x$ and not $\partial\bar{u}/\partial x$.

In section 6 we describe the baroclinic-barotropic dipole instability mechanism for the initiation of mature anomalies and examine the instability properties of both three-dimensional climatological and instantaneous basic states. We also consider the role of barotropic instability in mature anomaly formation. The relationships between three-dimensional instability theory and Rossby wave dispersion and linear steady state theories are examined in section 7. Here we also consider observational and model studies which throw light on the role of anomalous forcing in the formation of anomalous circulation features.

In section 8, two studies of the time evolution of anomalies in baroclinic models with longitudinal stretch are discussed. In one study the large-scale anomaly evolves from a small-scale mid-latitude disturbance, while in the other, anomalies are generated from initial tropical disturbances. Section 9 provides a summary and conclusions.

2. Mechanisms Determining the Three-Dimensional Time-Mean State of the Atmosphere

Figure 1 shows the 200-mbar field of the zonal and meridional wind components ($\bar{u}$ and $\bar{v}$, respectively) for the boreal summer (June, July, and August (JJA)) and the boreal winter (December, January, and February (DJF)) from *Webster*

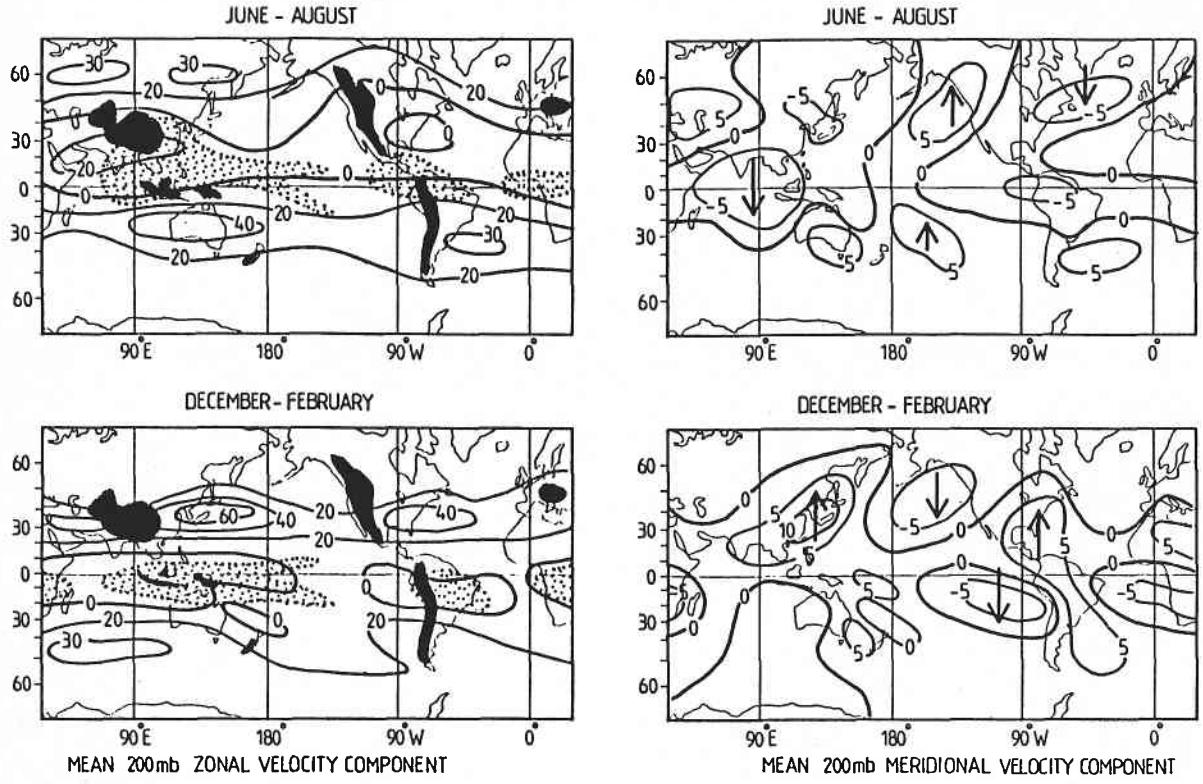

Fig. 1. Global distributions of the 200-mbar time-mean zonal velocity component ($\bar{u}$, m s^{-1}, left panels) and meridional components ($\bar{v}$, m s^{-1}, right panels) for the boreal summer (upper panels) and boreal winter (lower panels). The stippled regions indicate cold outgoing long-wave radiation (i.e., convection), and the solid areas show the major orographic features [after *Webster*, 1983].

[1983]. Areas of maximum convection (minima in outgoing long-wave radiation) are stippled, and the major orographic features are shaded. Arrows on the $\bar{v}$ field charts show the direction of the maximum values.

In the boreal winter extratropics, localized jet maxima exist downstream of all major orographic features. The colocation of orography and wind speed maxima has led to a very prevalent conclusion that the longitudinal variation of the mean flow (i.e., the phase and amplitude of the seasonal stationary waves of the atmosphere) is mainly a function of orographic forcing (*Wallace* [1983], *Held* [1983], and many others). These conclusions would appear to be supported by the inefficiency of surface heating gradients in the extratropics, to perturb, in an effective manner, regions of strong westerlies [*Webster*, 1982]. Yet, a closer inspection of Figure 1 shows that there is a further effect to be considered. The extratropical jet maxima are also across the equator and poleward of the low-latitude convection maxima. In fact, in the austral winter the strongest jet stream lies to the south of a very large south Asian heating maximum. There are no local orographic features on a scale that could produce a jet of this scale within the southern hemisphere.

Webster [1982] has argued that in the strong winter westerlies (boreal or austral) the surface heating differential is a very inefficient forcing function. It is inefficient because the flow approaches an "advective limit" as distinct from the efficient "diabatic limit" of low latitudes [*Webster*, 1982]. From the steady state first law of thermodynamics the vertical velocity is determined by the residual of the temperature advection and the diabatic heating. If the winds are sufficiently strong, the advective term increases relatively, and the energy transformation between the potential and kinetic energy becomes less direct and thus less efficient. Such is the advective limit. On the other hand, near the equator, with weaker winds and smaller advection, the vertical velocity is determined almost exactly by the diabatic heating [*Webster*, 1982, 1983]. There the energy transformed is almost perfectly direct (i.e., the diabatic limit), and a strong response may be expected.

The physical connections between the tropics and the extratropics can be seen in the $\bar{v}$ component diagrams of Figure 1. Equatorward of each winter hemisphere jet stream is a strong (>5 m s^{-1}) cross-equatorial flow originating in the region of low-latitude summer heating and extending to the region upstream of the winter jet. This is the ageostrophic flow moving down the heating gradient between regions of maximum latent heating toward the regions of maximum radiational cooling. The flow is most notable across the equator in the Indian Ocean in JJA.

The mean basic flow in the equatorial regions appears to be closely correlated with the distribution of heating and, in turn, with the sea surface temperature distribution. Figure 2 [*Webster*, 1987; *Arkin and Webster*, 1985] shows the vertical distributions of $\bar{u}^*$ and $\bar{v}^*$ (i.e., the spatial deviations of the time mean from the zonal average) along the equator for both JJA and DJF. Below each panel are the corresponding mean infrared temperatures (i.e., the satellite-sensed outgoing long-wave radiation effective temperature plotted on an inverse scale) for 15°N, 0°, and 15°S. We note in the $\bar{u}^*$ fields that there is little seasonal variation. The flow shows a strong anticorrelation between the surface and the upper troposphere with divergence overlying convergence, and vice versa. Comparing the circulation with the convection along the equator, we note a

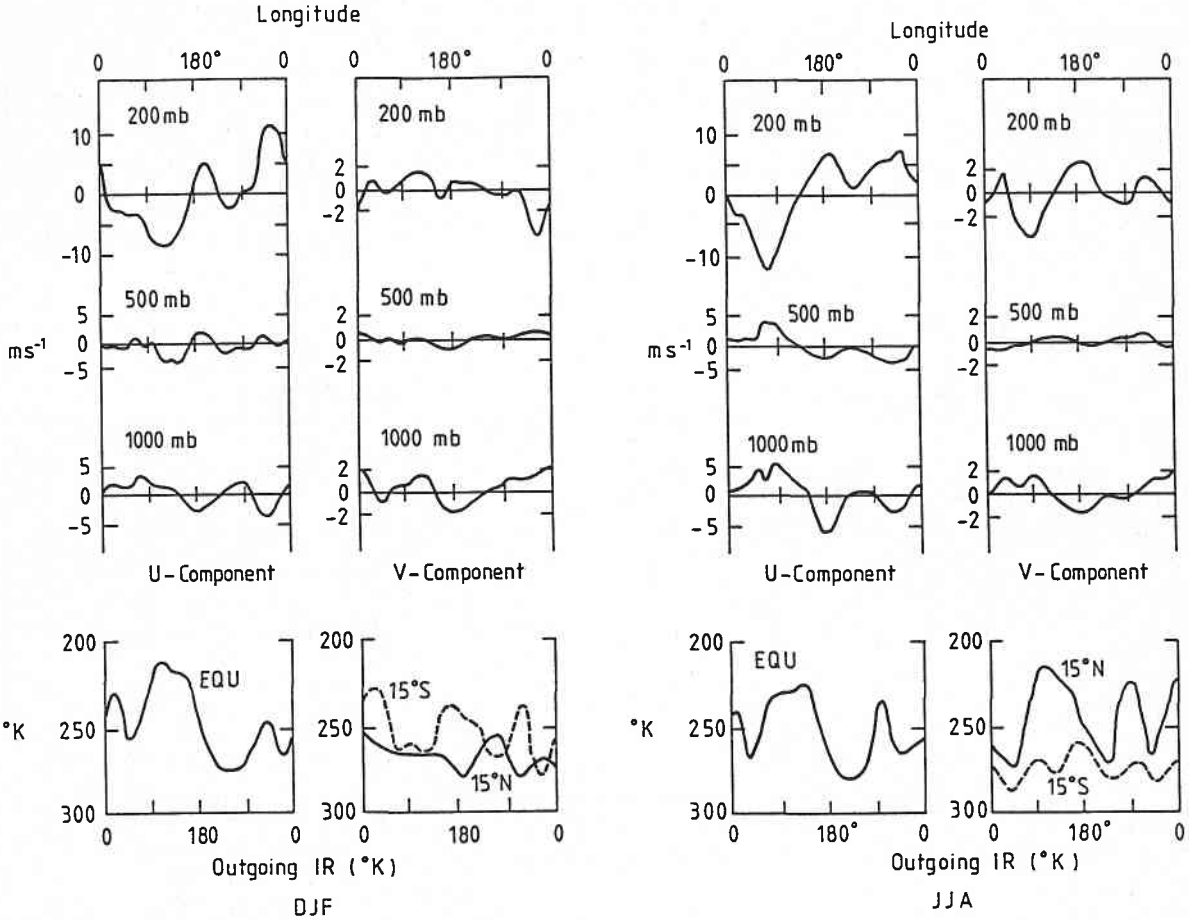

Fig. 2. Height-longitude sections along the equator of the spatial deviations from the zonal average of the time mean flow at 1000, 500, and 200 mbar. The lower panels show the infrared effective temperatures (degrees Kelvin on an inverted scale) along the equator, 15°N, and 15°S [after *Arkin and Webster*, 1985].

strong correlation between cool IR temperatures (maximum convection) at 0° and low level convergence and upper level divergence. On the other hand, the $\bar{v}^*$ field shows a reversal between seasons and a correlation, not with the equatorial IR temperature, but with the IR temperature in the summer subtropics. That is, the cross-equatorial flow appears to be driven by the monsoon subtropical heating of the summer hemisphere.

The dynamic structure of the quasi-stationary flow of Figure 2 was discussed by *Matsuno* [1966], *Webster* [1972, 1973*b*], and *Gill* [1980]. *Webster* [1972] and *Gill* [1980] showed that the near-equatorial flow can be thought of as a very large scale and dissipative equatorially trapped Kelvin wave. The properties of the Kelvin wave are such that the meridional flow is nearly zero [*Webster*, 1972]. Thus at low latitudes the zonal wind component is determined, in the long-term mean, by the local equatorial heating.

It is important to note that the basic state also possesses considerable interannual variability, especially in relation to the El Niño–Southern Oscillation signal [*van Loon and Rogers*, 1978, 1981; *van Loon and Madden*, 1981; *Pittock*, 1984; *van Loon and Labitzke*, 1987]. Changes in the near-equatorial circulation occurring between the extremes of the Southern Oscillation Index (the SOI) can be seen in the schematic of Figure 3 [*Webster*, 1987]. *Troup* [1965] noted that the unwieldly SOI was essentially the pressure difference between Tahiti and Darwin. With the change in the location of the warm water (stippled area) the major ascending and convective region moves from the Indonesian/western Pacific Ocean to the central Pacific. With this eastward slip, the entire tropical circulation changes, with regions of easterlies being replaced by westerlies, and vice versa.

Figure 4 presents another depiction of the planetary scale variability unearthed by Walker. The top panel shows the variation over a number of years of the SOI or the surface pressure difference between Tahiti and Darwin. The lower panel shows the spatial variability associated with the oscillation plotted as simultaneous correlations with the Darwin sea level pressure. For future reference a number of features are worth noting. First, the scale of variability in the tropics is very large. That is, if the sign of the pressure difference between Darwin and Tahiti changes, then the change is transmitted completely around the equator. Clearly, Walker's Southern Oscillation is primarily an equatorial teleconnection pattern. Second, weaker teleconnections are apparent between the low latitudes and the extratropics. For example, a correlation "ridge" extends across the United States. Walker, of course, noted all of these correlations. What was not apparent in Walker's calculations, or in Figure 4, is that transients also appear to possess similar spatial variabilities.

3. Observations of Low-Frequency Variability

Considerable effort by the scientific community has provided climate data sets of the northern hemisphere atmospheric

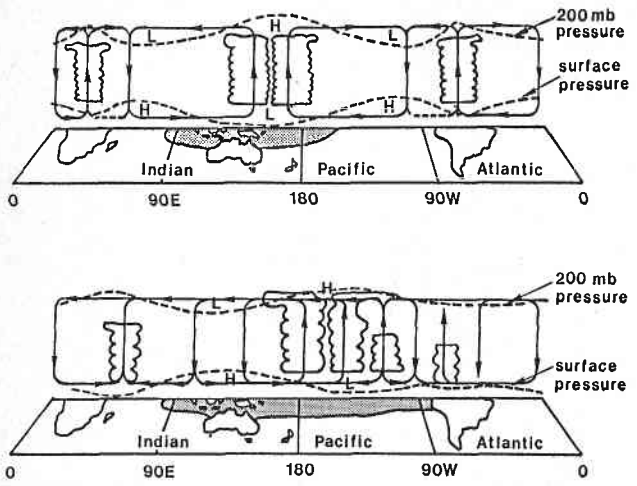

Fig. 3. Schematic diagram of the longitude-height-circulation along the equator typical of a strong positive (upper panel) and strong negative Southern Oscillation Index (lower panel). The surface and 200-mbar pressure derivatives are shown as dashed lines. Clouds indicate region of convection, and sea surface temperature warmer than 27°C is stippled [from *Webster*, 1987].

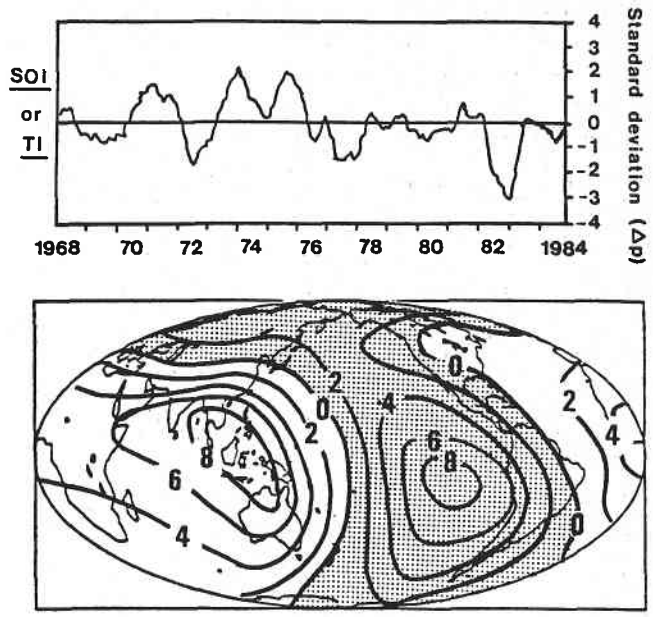

Fig. 4. Variation of the normalized Tahiti-Darwin pressure difference or the Southern Oscillation Index (upper panel) and the spatial variation (lower panel) of the simultaneous correlation of surface pressure variations at all points with the Darwin surface pressure. Shaded areas show negative correlations [after *Webster*, 1987].

circulation which possess both substantial length and spatial continuity, allowing, for the first time, detailed analyses of the three-dimensional structure of the evolving atmosphere. Now, with the advent of a nearly complete and continual satellite coverage, similar data sets are being created for the southern hemisphere. Thus observational studies in both hemispheres and the tropics have shifted from a focus on the zonal average [e.g., *Oort and Rasmussen*, 1971] to that of the three-dimensional structure of the atmosphere and its fluctuations (*Blackmon et al.* [1977] and many others). Furthermore, the length and quality of the data sets have allowed the analyses of the fluctuations to be extended from a case study perspective to that of four-dimensional analysis [e.g., *Blackmon et al.*, 1977, 1984*a*; *Kushnir*, 1987].

The fluctuations to which we refer, and which now can be studied in great detail, are the cyclones, blocking events, and other mature anomalies as well as the response of the extratropics to remote forcing from the tropical latitudes discussed before.

An overview of the colocation of the geographic distribution of atmospheric variability can be seen in Figure 5*a*, showing the colocation of the seasonal mean $\bar{u}$ field at 200 mbar (upper panel) and the perturbation kinetic energy (PKE) (lower panel) for the boreal winter (left) and summer (right) at 200 mbar. Figure 5*b* shows the boreal winter distributions for two climate epochs: the 1971/1972 non–El Niño and the 1972/1973 El Niño period. For ease of comparison the PKE and $\bar{u}$ fields are superimposed. Even a casual inspection will show different $\bar{u}$-PKE relationship at different latitude and different correlations between different seasons and years. We will now examine this variability in greater detail.

3.1. *Synoptic Variability and Mature Anomalies*

The use of filter techniques (*Blackmon et al.* [1977, 1984*a*], *Trenberth* [1981, 1984], and others) has provided evidence of great differences in the character of the high-frequency (periods less than about 1 week and also described as band pass) and low-frequency (10–90 days) atmospheric variations. Not only are their spatial scales quite different, but they also have distinct relationships with respect to the background basic state within which they are immersed. The three-dimensional instability studies discussed in later sections produce modes resembling the band-pass and low-pass filtered observations but in addition suggest that there are many other modes of fluctuation which may be missed by using the rather broad low-pass filter. *Blackmon et al.* [1984*b*] have replaced the low-pass filter by two filters, one having a period of 10–30 days and the other of 30–90 days, while *Schubert* [1986] used a total of five filters. He found within the observations that there existed a richer variety of fluctuations, some of which are similar to the additional instability modes such as the "onset-of-blocking" (periods of 6–10 days or so) and intermediate modes (periods of 10–20 days or so) [*Frederiksen*, 1982*a*, 1983*c*]. Analogues of such modes also occur in composite analyses using unfiltered data [e.g., *Dole*, 1983, 1986].

The studies listed above show distinct regions of synoptic activity slightly poleward and downstream of the winter zonal wind maxima of the northern hemisphere. Similar relationships have been found for the summer season by *White* [1982]. The southern hemisphere is slightly different, with the PKE maxima being more in phase with the jet streams. This may be due to the poorer data base in the southern hemisphere but more probably is because of the different nature of the quasi-stationary long waves, which are essentially equivalent barotropic as distinct from the more baroclinic nature of the northern hemisphere waves.

Blackmon et al. [1977, 1984*a*] showed the relative location of the band-pass and the low-pass fluctuation fields against the background time-mean zonal wind component for the northern hemisphere. Both fields possess very distinct maxima, but each is located in a unique position relative to the time-mean jet streams. Maxima in the band-pass fields, (i.e., in the regions of synoptic activity) occur slightly poleward and to the east of the mean jets. These centers, over the Pacific Ocean, over eastern North America, and (more weakly) over the Mediterranean, represent the locations of the winter storm tracks. The low-pass maxima, on the other hand, lie in the belt

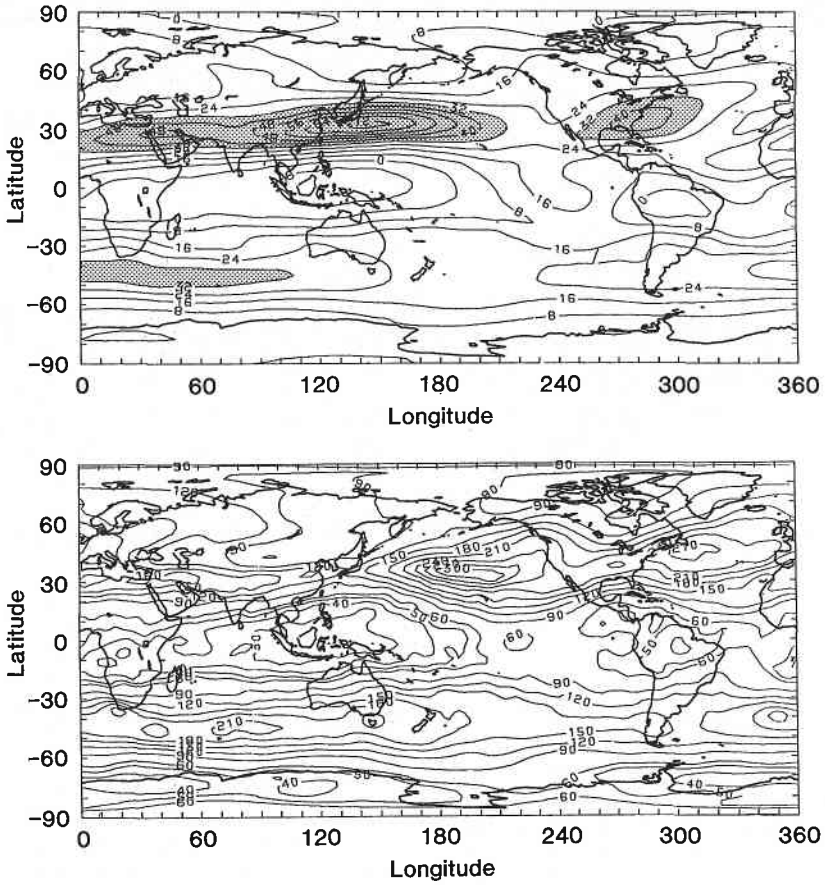

Fig. 5a. Colocation of the mean 200-mbar $\bar{u}$ field (upper panels) and the perturbation kinetic energy (PKE) in $m^2 s^{-2}$ (lower panels) for December-January-February (left panels) and June-July-August (right panels). Regions where $\bar{u} > 32$ m s^{-1} are shaded [after *Arkin and Webster*, 1985].

of strong westerlies but downstream of the mean jet streams. Here are located the slowly varying blocking phenomena. Probably, the unique locations of the two spectral maxima are hinting at a dominance of different physical processes at the different ends of the spectrum.

Unfortunately, because of the inferior quality of the southern hemisphere data sets, fewer studies of the statistics of the southern hemisphere circulation have been attempted. Thus we are forced to use less sophisticated data analysis, such as those attempted by *Arkin and Webster* [1985] or the few other more detailed analyses, such as those by *Trenberth* [1981, 1984] and *Trenberth and Mo* [1985], to gain information about fluctuations in the southern hemisphere.

Figure 6 summarizes the relationships between the mean zonal flow and the PKE with scatter diagrams of point pairs of $\bar{u}$ and PKE for the 5° bands around the latitudes 30°N, 0°, and 30°S for DJF and JJA [*Arkin and Webster*, 1985] using an extended 16-year National Meteorological Center (NMC) data set. Correlations for the equatorial regions are strong and positive, illustrating a direct relationship between the strength of the westerlies at low latitudes and the degree of perturbation. Correlations are 0.838 and 0.717 for DJF and JJA, respectively, compared to the 1% level significance of 0.610 calculated using 15 degrees of freedom. For the same latitude band the correlations between PKE and $\bar{v}$ [see *Arkin and Webster*, 1985, Figure 6] are −0.076 and 0.245, respectively, thus failing any acceptable statistical significance test. A very natural question is why are there regional "centers of action" along the equator?

In the extratropics, $\bar{u}$-PKE relationships show the same general pattern as in the tropics. However, in the winter northern hemisphere, in particular, the very largest values of the $\bar{u}$ field do not coincide with the maximum values of PKE. On the contrary, values are spread over a much wider speed spectrum. This difference may be due to the growth of the transients as they propagate away from the region of maximum local instability, the jet cores, into the regions of lower values of $\bar{u}$ or to the impact of the large longitudinal stretch on the transients in the downstream part of the jet. However, the scatter diagrams for the southern hemisphere winter (and those for the summer extratropics of both hemispheres) do exhibit a structure very similar to that in the tropics. The reasons for the variations between hemisphere and season are not known, although *Webster and Chang* [1988] noted a substantial difference between the longitudinal stretching deformation fields in each hemisphere. It has been suggested by *van Loon* [1980] and *Trenberth* [1984] that the differences may arise from the poorer quality of the data in the southern hemisphere. However, it may also be that the difference arises from the large-scale flow being generated remotely (rather than locally as in the northern hemisphere) and thus possessing a more equivalent barotropic structure.

3.2. *Very Low Frequency Variability: Teleconnection Patterns*

Over one half century after the pioneering work of *Walker* [1924], two major types of teleconnection situations have

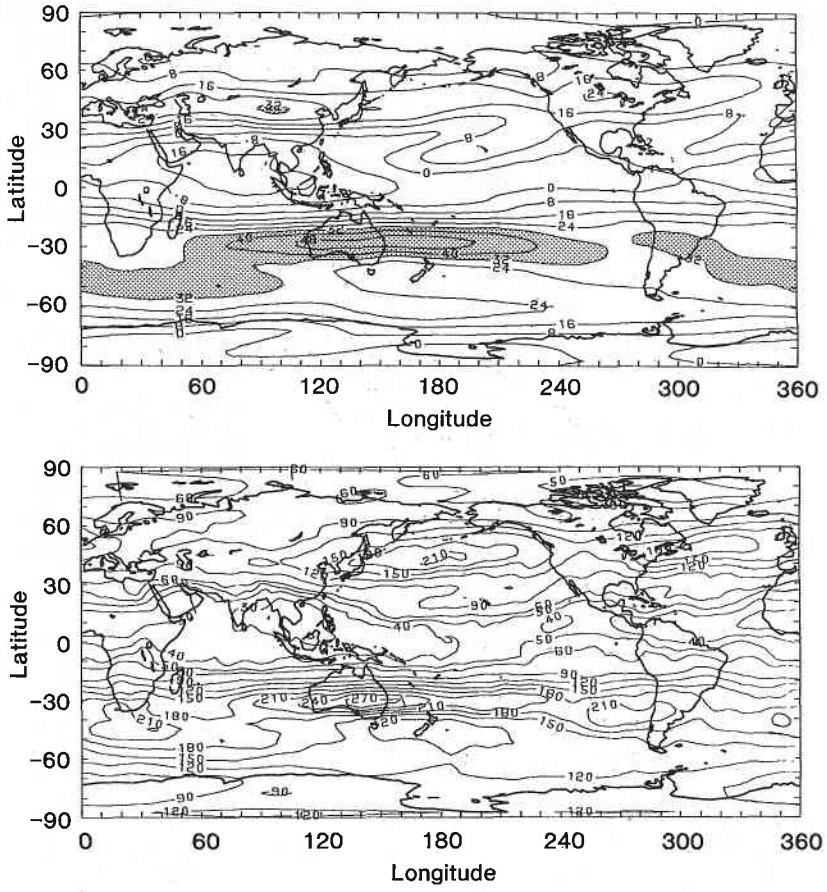

Fig. 5*a*. (continued)

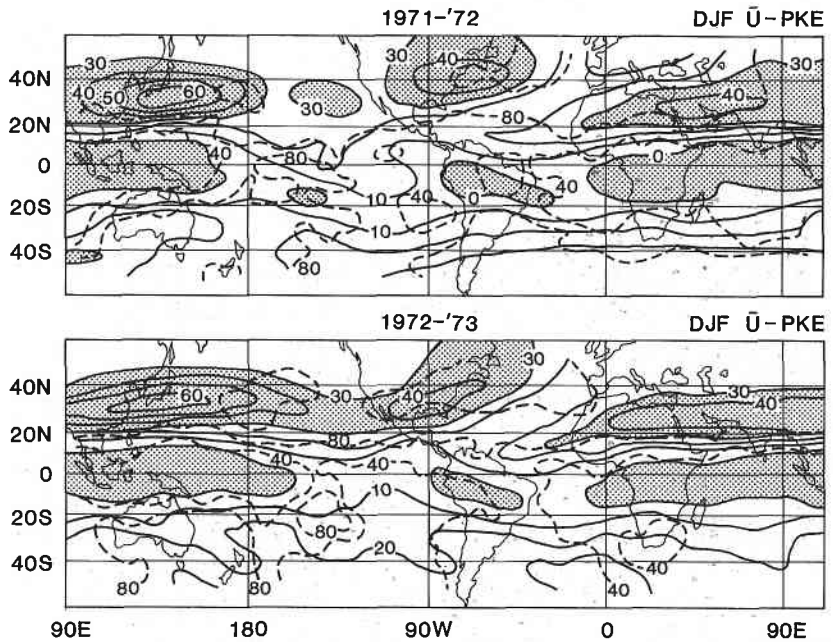

Fig. 5*b*. Comparison of the $\bar{u}$ and perturbation kinetic energy (PKE) distributions for the 1971/1972 and 1972/1973 December-January-February (DJF) periods. The second period coincides with an equatorial warm event [after *Arkin and Webster*, 1985]. Regions where $\bar{u} > 30\ \mathrm{m\ s^{-1}}$ in mid-latitudes and $\bar{u} < 0$ in equatorial regions are shaded.

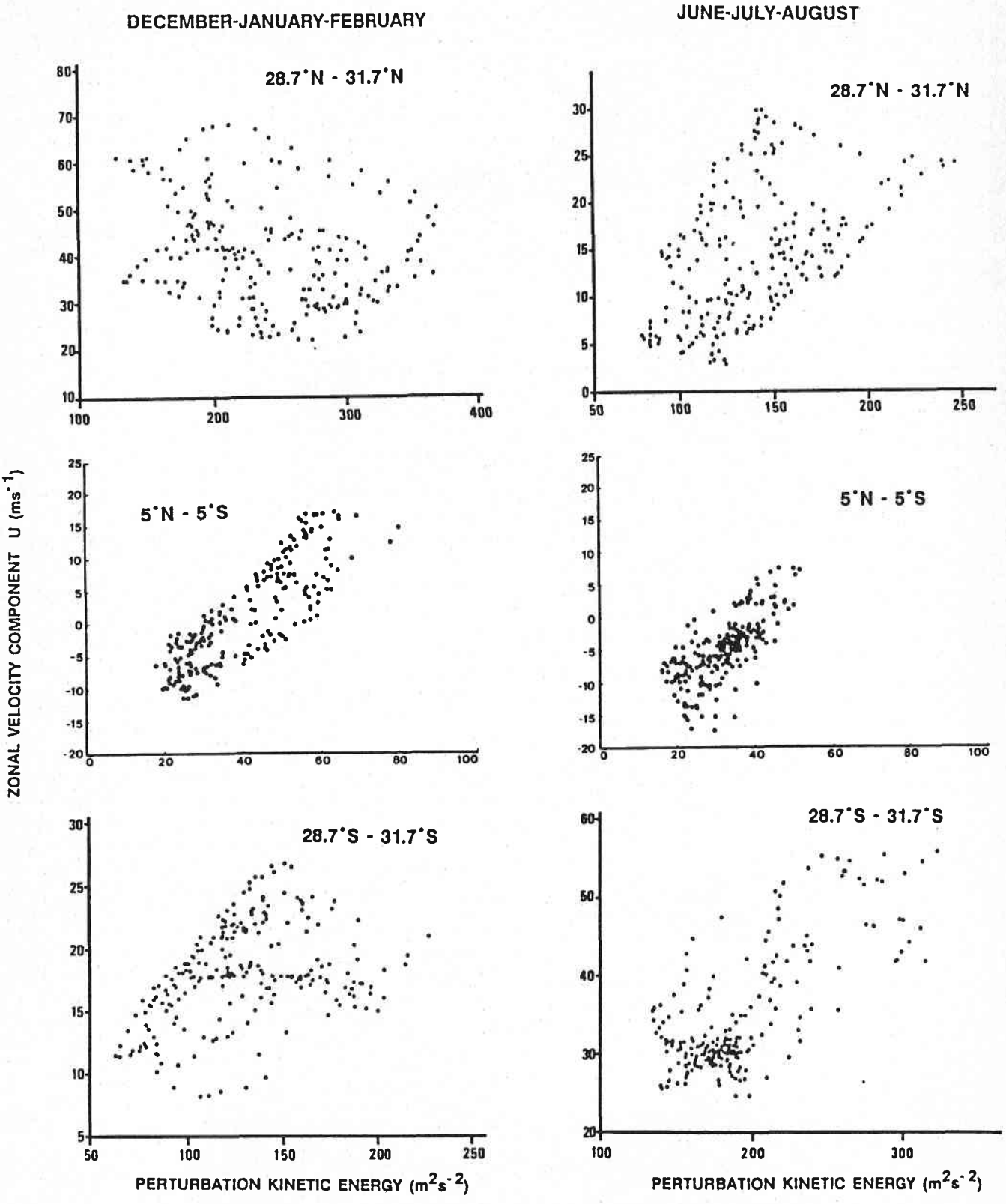

Fig. 6. Scatter diagrams of point pairs for the long-time mean of the two seasons DJF and JJA in the strips 5°N to 5°S and 28.7°–31.7° (N and S). (We are thankful to P. Arkin (unpublished data, 1986) of the Climate Analysis Center, NMC/NOAA, for the compilation of the scatter diagrams for the northern and southern hemisphere extratropics.)

been uncovered. Receiving most attention are teleconnections occurring during times of anomalous tropical heating and their influence on higher latitudes. This is the "tropics to extratropics atmospheric teleconnection." Ususally thought to possess time scales of 2–3 years, the system may exist over a much wider spectral band. *Lau et al.* [1986] have suggested that very similar patterns exist on the intraseasonal 40- to 60-day time scale.

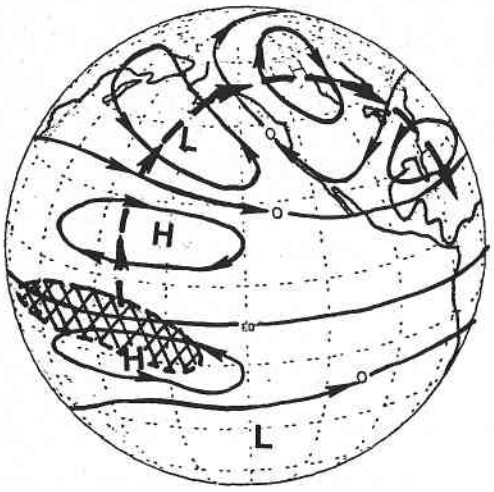

Fig. 7. Composite of the atmospheric anomaly pattern in the upper troposphere during warm events (large negative Southern Oscillation Index in Figure 4) in the Pacific Ocean [from *Horel and Wallace*, 1981].

The second type of teleconnection refers to the influence of extratropical events on the tropics, termed here the "extratropics to tropics teleconnection." This phenomenon has received much less attention than the reverse teleconnection. The evidence that does exist suggests that the teleconnections appear to be strongest at the higher-frequency end of the spectrum.

The third teleconnection type refers to "tropics to tropics" circulation communication. We have discussed the mean or slow mode equatorial teleconnection through the large scale, steady Kelvin wave of *Webster* [1972] and *Gill* [1980]. Here, though, we refer to an equatorial interconnection mechanism caused either by a temporal variation of the slow Kelvin wave or transients that move through the basic state. However, the evidence for such a mechanism arises from theoretical studies and numerical experiments rather than observations. We shall delay the discussion of this third type until section 5.2.

3.2.1. *Tropics to extratropics teleconnections.* Following the initial work of *Walker* [1924] and *Troup* [1965] more detailed studies (*Bjerknes* [1969], *Horel and Wallace* [1981], and many others) linked the extratropical climate variability to the low-frequency oscillation of the tropical ocean. These latter studies estimated the atmospheric variations by subtracting the mean fields of the El Niño years from those of the non–El Niño years, thus isolating significant differences which possess considerable spatial coherence especially in the winter hemisphere. The evidence of teleconnections has raised such interest for them to become a major focus of the World Climate Research Project through the Tropical Ocean Global Atmosphere (TOGA) Programme.

Figure 7 provides a composite of the upper tropospheric atmospheric anomaly pattern in the upper and lower troposphere during El Niño times (or warm events) in the Pacific Ocean from *Horel and Wallace* [1981]. Two anticyclonic eddies exist to the north and south of the equator in the upper troposphere, and stronger than average westerlies and easterlies lie along the equator to the east and west of the anomalous heat source. The circulation is completely out of phase with the lower troposphere (not shown) in the vicinity of the anomalous heating but is in phase away from the source. The figure suggests that the anomalous response is very much like the normal tropospheric circulation that has followed a translated sea surface temperature (cf. Figure 3).

It is likely that the atmosphere is not a passive player in the evolving climate system, but an active partner with an ocean. *Barnett* [1983] suggested that the translation between the two extreme tropical circulations of Figure 3 is part of a cycle where the anomalous convection starts in the eastern Indian Ocean and moves progressively eastward to the eastern Pacific Ocean. In Barnett's scheme the El Niño is only one part of a very long period ocean-atmosphere interaction.

Figure 7 also shows that to the north and east of the tropical heat source, from the northern end of the two upper tropospheric anticyclones, emerges an apparent train of waves that extends into the winter extratropics. This is, in fact, a detail of the SOI pattern shown in Figure 4. The wave train–like phenomena are the physical manifestation of the atmospheric teleconnections first discovered by *Walker* [1924]. Of particular note is the so-called Pacific–North America pattern (denoted PNA) implicitly discussed by *Namias* [1951] and *Bjerknes* [1969], which is one of many anomalous climate circulation patterns of the higher latitudes.

The role of anomalous forcing in producing these patterns, or whether it plays a role at all (the anomalies occurring perhaps as internal fluctuations of the atmosphere), is discussed in detail in section 7.3. But from an observational side, it would appear that *Horel and Wallace* [1981] have presented convincing observational evidence of at least a modest relationship between anomalous forcing in the tropical Pacific and the PNA pattern. However, *Dole* [1986] noted, as have other authors, that the patterns often, and perhaps primarily, grow and decay while the external forcing remains nearly fixed. Also, *Plumb* [1985] finds no evidence of Rossby-like wave trains of tropical origin. *Wallace and Blackmon* [1983] have also reviewed the evidence for the roles of external forcing versus internal dynamics for generating low-frequency variability.

Continuing studies [e.g., *Horel*, 1981; *Mo and White*, 1985; *Mo and Livezey*, 1986] have documented other teleconnection patterns for both the northern and the southern hemisphere, although many of them possess amplitudes that explain far less of the total variance than does the PNA pattern. Clearly, the mean state of the atmosphere is very different during the warm El Niño episodes as shown in Figure 3. However, whether or not the anomalous structure of the extratropics during the episodes can be explained in terms of the shift in the thermal forcing in the tropics or whether it forms as an aggregation of low-frequency (or even high-frequency) fluctuations that are responses to excitation from the perturbed tropics, or even as a combination of both effects, cannot be deciphered from observational studies alone. Accompanying parallel and highly focused theoretical and modeling studies are necessary.

3.2.2. *Extratropics to tropics teleconnections. Riehl* [1954] observed that

> . . . The intermittent appearance of high tropospheric westerlies on the equator . . . is a foreign thought in classical views of the general circulation. Yet . . . [there is evidence] . . . that they do occur . . . Since flow in the high levels is so unsteady, coupling at high altitudes between the circulations of the Northern and Southern Hemispheres promises to provide an important link in the understanding of the fluctuations of the general circulation . . .

Riehl also noted that there was considerable evidence of ". . . an intrusion of extratropical-type disturbances into the heart of the tropics [in the region of the tropical westerlies] . . . ."

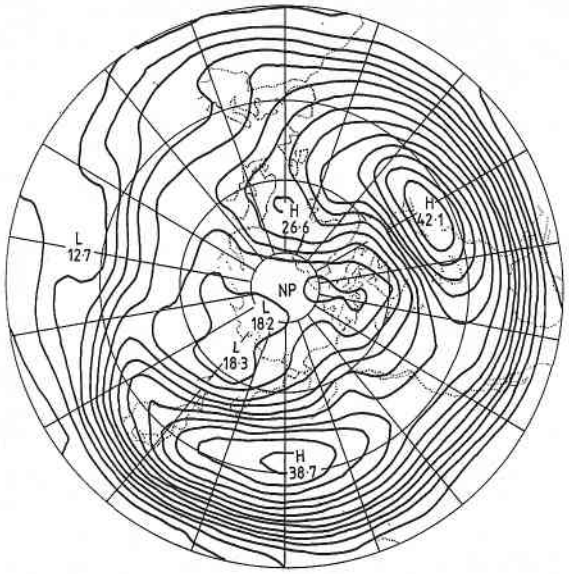

Fig. 8*a*. Band-pass-filtered rms height field at 500 mbar for the northern hemisphere winter [from *Blackmon*, 1976].

Over a decade later, *Murakami and Unninayer* [1977] noted that there were regions of anomalously high PKE along the equator. *Webster and Holton* [1982] observed that these maxima in PKE coincided with the upper tropospheric equatorial westerlies. Further collaboration of Riehl's original observation was made by *Arkin and Webster* [1985] using a much longer data series. Their results have been shown in Figures 5*a*, 5*b*, and 6.

The observational studies mentioned raise a number of interesting questions. Are the regions of anomalously high PKE in the tropics the results of in situ dynamics, such as local instabilities or energy accumulation from the convective regions of the tropics, or the results of propagating disturbances originating at higher latitudes? Furthermore, why are the regions of high PKE colocated with the upper tropospheric equatorial westerlies and not the easterlies? We shall address these questions in section 5.2.

4. THEORIES OF LOW-FREQUENCY VARIABILITY

Concomitant with the large strides that have been made in the observational analysis of the atmosphere has been a flood of attendant numerical experiments and theories. Their aim has been to explain the temporal and spatial structure of the atmospheric fluctuations. In the following paragraphs we will list the various hypotheses that have been posed to explain the observed structure of the subclasses of the low-frequency variance of the atmosphere.

4.1. *Higher-Frequency Variability*

There is now little controversy regarding the basic mechanism operating to produce fluctuations on the shorter (band-passed) time scales. Since the pioneering work of *Charney* [1947] and *Eady* [1949], the generally accepted theory of cyclogenesis has been that of linear baroclinic instability of the large-scale atmospheric flow field. These early investigations, and many others that were to follow, examined the stability of flows that had no zonal variation in their basic states or in the amplitude of the growing disturbances.

Recent theoretical studies of the instability of the atmosphere [e.g., *Frederiksen*, 1979, 1983*a*, *b*, 1986] have focused on three-dimensional basic states such as shown in Figure 5. The relaxation of the constraints on the structure of the basic state showed that the regionality of the storm tracks in both the northern and the southern hemisphere (i.e., the band-pass filter field maxima) could be explained within the context of three-dimensional instability theory. Furthermore, the amplitudes of the fastest growing modes coincide fairly closely with the centers of the storm tracks in the band-pass filter observations of *Blackmon* [1976], *Blackmon et al.* [1977, 1984*a*], *Physick* [1981], and *Trenberth* [1982] (see also *Streten* [1969]) for the northern and southern hemispheres.

Comparisons of the fastest growing instability modes for northern and southern hemisphere climatological flows, obtained using a five-level quasi-geostrophic model with spherical geometry, with observations are shown in Figure 8 and 9, respectively. The amplitudes of the instability modes, of course, do not have the wave train structure of the stream functions [cf. *Frederiksen*, 1983*b*, Figure 10; *Frederiksen*, 1985, Figure 5*b*]. *Blackmon et al.* [1984*a*, Figure 15] have also examined the wave structures of the observed band-pass fluctuations and find that they are very similar to those of the fastest growing instability mode of *Frederiksen* [1982*a*], except that the observed wavelength is slightly longer. Nonlinear effects are expected to be the reason for this, although some of the slower growing monopole cyclogenesis instability modes of *Frederiksen and Bell* [1987] also have longer wavelengths. For both hemispheres, instability theory yields a number of different cyclogenesis modes which make contributions to different geographical regions. Frederiksen and Bell, for example, also discuss modes which correspond to storm tracks across Siberia and across the Mediterranean and Middle East.

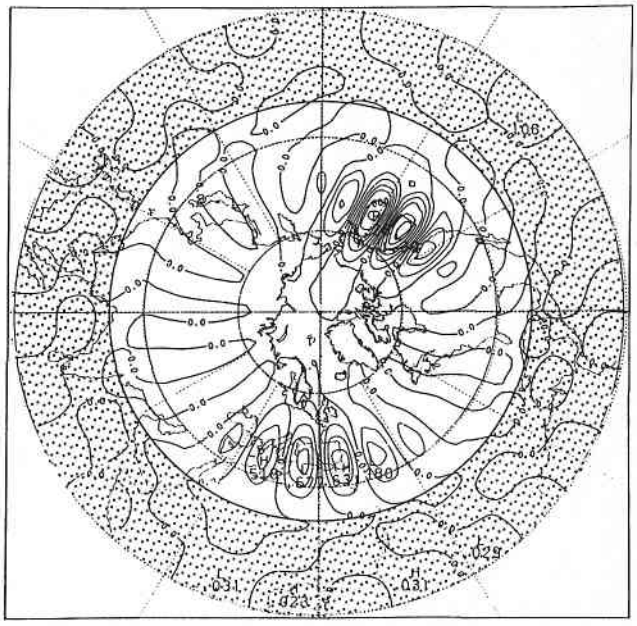

Fig. 8*b*. Disturbance stream function at 700 mbar for the fastest growing instability mode with a monthly averaged three-dimensional basic state for the northern hemisphere in January 1978 [from *Frederiksen*, 1983*b*]. The region between 0° and 20° latitude has been stippled as a reminder of the fact that the observations do not include this region.

4.2. *Lower-Frequency Variability*

For low-pass fluctuations the problem is less clearly defined simply because of the large number of phenomena involved. Arising from a doubt of the existence of a unique solution for the explanation of all low-frequency phenomena, many different mechanisms have been proposed. For example, a great diversity of thought exists for even one low-frequency phenomenon: blocking. Blocking was discussed as early as 1904 by *Garriott* [1904], and its profound effects upon the weather and climate were noted by *Namias* [1947], *Berggren et al.* [1949], and *Rex* [1950]. Many early theories [e.g., *Yeh*, 1949; *Rossby*, 1950; *Rex*, 1950; *Thompson*, 1957] considered blocking as a purely barotropic process. In particular, *Rossby* [1950] and *Rex* [1950] suggested that the development of blocking systems was a process analogous to the formation of hydraulic jumps in open channel flow.

Recent theories of blocking, and of low-frequency behavior of the atmosphere in general, are much more diverse. Within these theories there appear to be three main areas of concern: (1) the onset and development of blocking events and of other low-frequency fluctuations of the atmosphere, (2) the maintenance of the low-frequency fluctuations, and (3) their decay. However, most research appears to have been on the subjects of the first two areas.

Among the theories that have been offered to explain the onset and development of the blocking events (and low-frequency fluctuations in general) are the following:

1. Two-dimensional Rossby wave dispersion theory [*Rossby*, 1945; *Yeh*, 1949], which has been generalized by *Hoskins et al.* [1977] to a spherical geometry. Extensions of the theory have been used to explain the teleconnection patterns observed in the atmosphere, although often with the assumptions of a stable basic state without longitudinal variation.
2. Nonlinear interaction of a forced lee wave and a free traveling wave [*Egger*, 1978].
3. Hemispheric resonant amplification of large-scale planetary waves forced by topography and heating [*Tung and Lindzen*, 1979*a*, *b*].

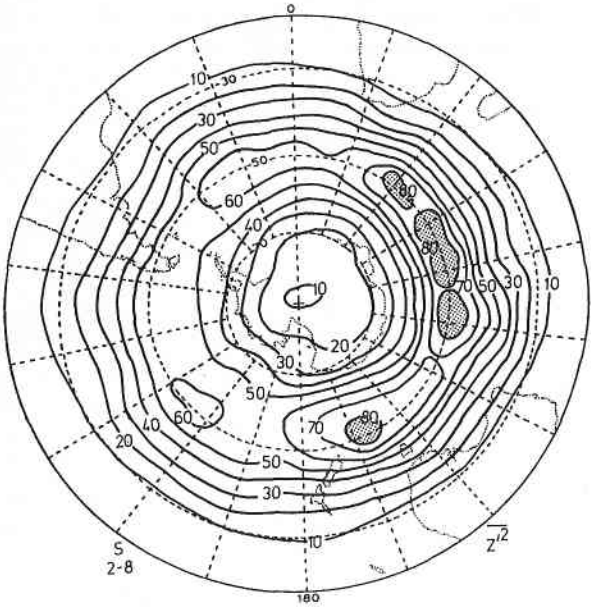

Fig. 9*a*. Geopotential height variance in the 2- to 8-day band at 500 mbar for the southern hemisphere summer [from *Trenberth*, 1982].

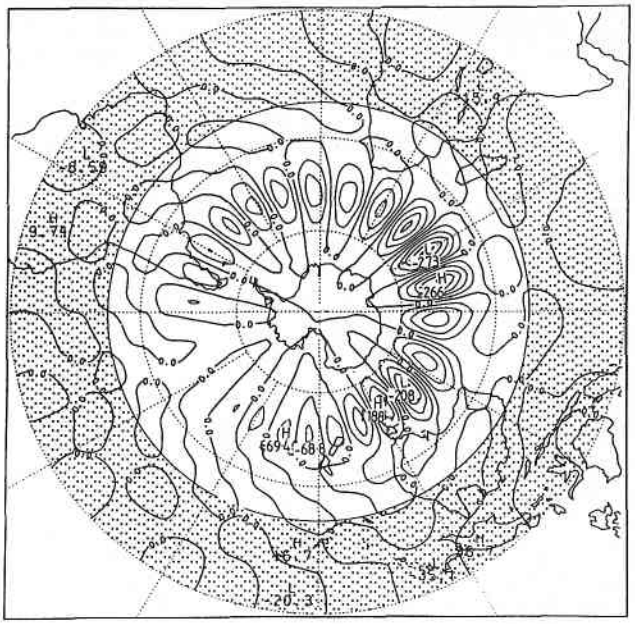

Fig. 9*b*. Disturbance stream function at 700 mbar for the fastest growing instability mode with a monthly and yearly averaged basic state for the southern hemisphere in January 1972–1976 [from *Frederiksen*, 1985].

4. Local response due to Rossby lee waves generated by one forcing region being enhanced by a second source downstream [*Kalnay-Rivas and Merkine*, 1981].
5. Three-dimensional instability of three-dimensional varying basic flow [*Frederiksen*, 1982*a*, 1983*a*, *c*, 1984*a*; *Frederiksen and Bell*, 1987].
6. Barotropic instability of zonally varying flow [*Simmons et al.*, 1983] which is a special case of theory 5 as discussed by *Frederiksen* [1983*c*] and *Frederiksen and Bell* [1987].

Primary mechanisms for the maintenance of blocking that have been proposed are as follows:

7. Multiple equilibria of atmospheric flow [*Charney and De Vore*, 1979; *Hart*, 1979; *Charney and Strauss*, 1980; *Trevisan and Buzzi*, 1980; *Malguzzi and Speranza*, 1981; *Källén*, 1983]. Generalizations to include stochastic forcing and transients have also been proposed [*Egger*, 1981; *Rheinhold and Pierrehumbert*, 1982; *Benzi et al.*, 1984]. The importance of transients in the maintenance of blocks has also been emphasized by *Lejenäs* [1977] and *Green* [1977] and many other authors as discussed in section 6.4.
8. Solitary Rossby wave or modon theory [*Stern*, 1975; *Larichev and Reznik*, 1976; *Flierl et al.*, 1980; *McWilliams*, 1980; *Verkley*, 1984, 1987; *Tribbia*, 1984].

There has been little discussion of theories of the decay of blocking in the literature. However, the sequence of events that leads to the formation high zonal index flows such as those associated with one sign of the PNA pattern is very similar to that which leads to the corresponding low zonal index situation. This was noted on the basis of observations by *Dole* [1982], and the theoretical implications relating to the role of instability mechanisms was discussed by *Frederiksen* [1983*c*]. Thus one might also expect that instability would also play an important role in changes and in particular in the decay of blocks. Evidence that instability theory provides information on the different stages of block development including maintenance and decay is presented by *Frederiksen* [1988].

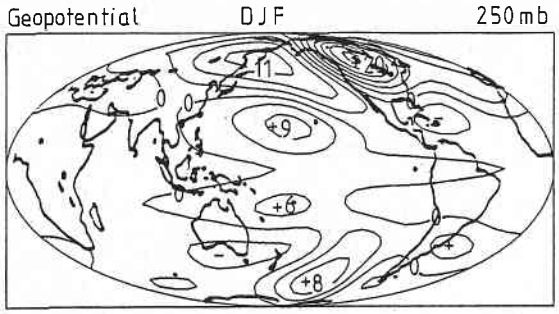

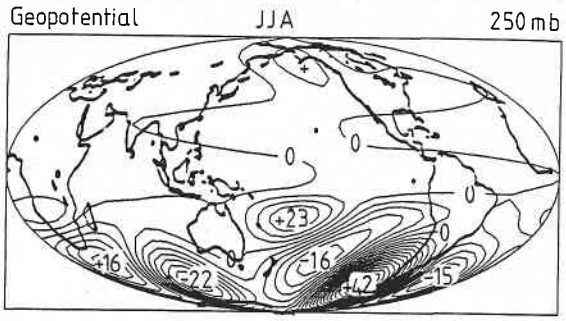

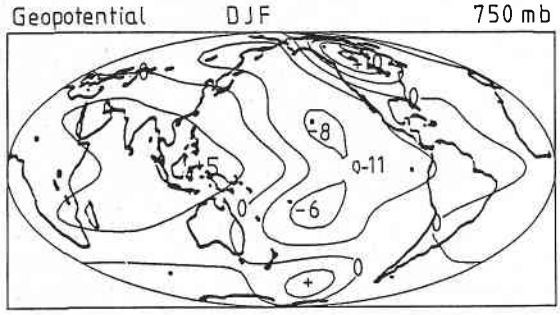

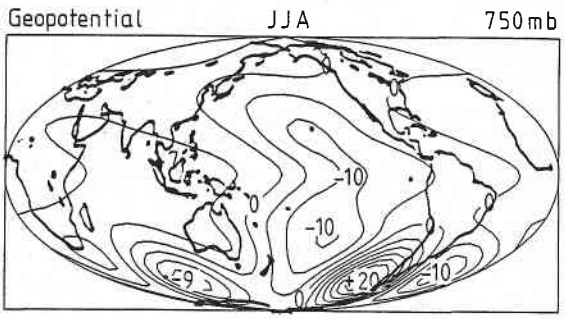

Fig. 10*a*.

Fig. 10*b*.

Fig. 10. Wave trains produced by a linear steady state model perturbed in the tropics for (*a*) December-January-February (DJF) and (*b*) June-July-August (JJA). The basic state was the observed zonally symmetric zonal velocity components. Fields of perturbation geopotential are shown relative to forcing in the equatorial Pacific Ocean. The iterative techniques of *Webster* [1982] were used in solving the steady state set.

5. Rossby Wave Dispersion and Steady State Response Theories

5.1. *Zonally Averaged Basic States*

5.1.1. *Tropical to extratropical teleconnections.* A picture of the variety of techniques used in the examination of low-frequency phenomena may be seen from a review of studies of atmospheric teleconnections. Some studies have assumed a stable time-mean basic flow and have sought steady state linear solutions (*Opsteegh and van den Dool* [1980], *Webster* [1981, 1982], *Hoskins and Karoly* [1981], and many others). This assumption has a long tradition in the study of forced flow in a time-independent medium (*Charney and Eliassen* [1949], *Long* [1952], *Kasahara* [1966], *Webster* [1972, 1973*a*, *b*, 1981, 1982], *Egger* [1976], *Grose and Hoskins* [1979], *Opsteegh and van den Dool* [1980], *Hoskins and Karoly* [1981], *Frederiksen and Sawford* [1981], *Frederiksen* [1982*c*], and many others).

Other studies have used complex numerical general circulation models of the atmosphere, which, beyond the usual caveats applied to all models and to the design of the experiments, presuppose no a priori assumptions regarding the dominant dynamics of the atmospheric response to remote forcing (*Rowntree* [1972], *Keshavamurty* [1983], *Shukla and Wallace* [1983], *Blackmon et al.* [1983], *Geisler et al.* [1985], *Palmer and Zhaobo* [1985], and many others). Their results, like those gained from observational studies of the atmosphere, are decipherable only by an analysis using a guided a priori hypothesis gained either from the analysis of real data or from a simpler, phenomenological model.

However, linear steady state models and general circulation experiments produce results which in some respects are surprisingly similar. Emanating from the low latitudes, where an anomaly source has been specified either as a sea surface temperature anomaly or as a prescribed midtropospheric latent heat source, is a train of waves propagating predominately toward the winter hemisphere higher latitudes. *Opsteegh and van den Dool* [1980], *Hoskins and Karoly* [1981], and *Webster* [1981, 1982] saw these features as dispersing Rossby waves, produced by the anomalous equatorial heat source, forcing rotational modes in the subtropics and extratropics. Examples of emanating wave trains are shown in Figure 10 [from *Webster*, 1982] for DJF and JJA where zonally symmetric basic states with realistic vertical and lateral shear were assumed. The preferential forcing of the winter hemisphere occurs simply because there the upper tropospheric westerlies encroach closest to the equator (see Figure 5), thus facilitating an easier excitation of Rossby waves. The seasonal characteristics may be seen in either the simple steady state results of *Webster* [1982], as shown in Figure 10, or in the general circulation model experiments of, for example, *Shukla and Wallace* [1983].

There are many compelling aspects of the simple forced wave train hypothesis:

1. The theory correctly predicts that the winter hemisphere is most easily perturbed by the equatorial heating anomalies. Observations show that it is the winter hemisphere that possesses the largest amplitude anomalies during warm equatorial episodes.

2. The anomalous response has a strong spectral dependence on latitude. In this context, *Hoskins and Karoly* [1981] showed that the longer waves would propagate further pole-

ward while the shorter waves would possess turning latitudes much more equatorward. This spectral filtering by the basic state is evident in the steady state solutions shown in Figure 10.

3. The wave train dispersion toward the extratropics possesses an equivalent barotropic structure. Again, this was predicted from simple wave theory by *Hoskins and Karoly* [1981]. Both observations and the results of circulation model experiments show this same feature.

But there are also a number of problems that exist with the theory:

4. The theory, depending on steady state assumptions, does not take into account the possibility that the three-dimensional basic state of the atmosphere is inherently unstable.

5. The theory ignores the longitudinal variability of the basic state, although we have seen from Figures 2, 3, and 4 that a considerable longitudinal structure exists both in the basic state and in the low-frequency variance.

6. With point 5 in mind, the theory predicts that the wave train will migrate following the heat source as it moves eastward during equatorial warm episodes. This appears to be contrary to considerable observational and modeling evidence. The general circulation experiment results of *Keshavamurty* [1982] and *Geisler et al.* [1985] showed a very similar response at higher latitudes for different locations of equatorial heating. Specifically, both studies placed anomalous sea surface temperature fields in different regions of the tropics and found the anomalous extratropical response to be relatively independent of their position. Furthermore, *Lau and Phillips* [1986] have found that the location of the extratropical response to tropical forcing on the 40- to 60-day time scale is phase locked irrespective of the phase of the tropical forcing. In a series of experiments with the NMC global spectral model, E. A. O'Lenic et al. found very similar results (E. A. O'Lenic, P. J. Webster, and A. N. Samuel, Effect of uncertainty in the state of the tropics on extended prediction, 1, The experiments, paper submitted to *Monthly Weather Review*, 1988. A draft version may be obtained as Office Note No. 311, Development Section/National Meteorological Center, National Weather Service, Camp Springs, Maryland). We will discuss these observational and modeling results later as part of the *Webster and Chang* [1988] theory on tropical-extratropical energy accumulation region–westerly duct teleconnection mechanism.

7. As pointed out by *Dole* [1986], the observed structures of mature anomalies

> . . . are quite distinct from the vertical structures of disturbances forced by local anomalous heat sources as obtained in simple models of the stationary wave responses to thermal forcing (Hoskins and Karoly, 1981) suggesting that local diabatic heating anomalies are unlikely to be the approximate source for their development . . .

8. If the sign of the anomalous forcing is changed in linear steady state theories, the anomalous circulation produced retains the same structure but with the opposite sign, whereas in general circulation studies the nonlinear response is much more complex [*Geisler et al.*, 1985, and references therein] as mentioned in point 6.

5.1.2. *Extratropical to tropical teleconnections.* Using a zonal averaged basic state, some initial studies of latitudinal wave propagation (especially *Charney* [1969] and *Mak* [1969] and later *Bennett and Young* [1971] and *Webster* [1973*a*]) showed that extratropical modes, which possessed sufficient energy to have a meaningful influence on the tropical atmosphere, were excluded from propagating toward the equator by critical lines (in the studies cited above, which considered a zonally symmetric basic state, these were lines of constant latitude) where the phase speed of the equatorward propagating mode matched the speed of the basic flow. (Poleward of the critical line, wavelike solutions exist, but equatorward there are only exponentially decaying forms possible for a given mode of a particular scale in a certain basic state.) Thus all stationary waves (phase speed $C_p = 0$) would encounter critical lines where the zonally averaged zonal wind component $[\bar{u}]$ was zero. Similarly, all extratropical synoptic waves, possessing relatively slow easterly phase speeds ($C_p < 0$), would encounter critical lines in the weak easterlies. Only very large scale transient Rossby waves ($C_p \ll 0$) could penetrate the tropical easterlies. As these large-scale modes were seen to possess little energy and all other rotational modes were absorbed or reflected at critical lines, *Charney* [1969] concluded that tropical disturbances must develop in situ.

There is some confusion in the literature regarding cross-equatorial flow and the concept of wave propagation and the role of critical lines. The distinction is very clear. Cross-equatorial flow may exist as a response to thermal forcing associated with very low frequency phenomena such as the monsoons. The heating forces a very large scale thermal flow, which may be interpreted as a quasi-stationary mixed Rossby-gravity wave, possessing a cross-equatorial component down the upper tropospheric pressure gradient and the heating gradient. It is this very low frequency flow produced by the monsoon heating distributions, in addition to the Walker circulations formed by the near-equatorial heating, that creates the low-frequency critical lines with which the equatorial transient waves must contend.

The conclusions of these earlier theoretical studies were based on the assumption of a zonally averaged basic state, thus ignoring the considerable longitudinal variation both in the time-averaged flow and in the transient structure relative to that basic state shown in Figure 5. On the basis of these observational studies, *Webster and Holton* [1982], using a free-surface nonlinear barotropic model, tested the hypothesis that the regions of high PKE, existing in regions of the upper tropospheric equatorial westerlies, were formed by the propagation of waves from the extratropics. Figure 5 shows that the westerlies are continuous between the mid-latitudes of the two hemispheres in some regions which, Webster and Holton argued, were waveguides or "ducts." That is, the wave critical lines possessed a distinct longitudinal structure and were no longer lines of constant latitude. Finally, noting that the meridional group velocity component (C_{gy}) behaves like $\bar{u}^{3/2}$, a distinct seasonal bias to extratropical to tropical interaction was shown, as $\bar{u}$ varied throughout the year. During the boreal fall and winter, when the equatorial westerlies are strongest, the transients of one hemisphere could propagate at least to the equator or even through to the other hemisphere. Webster and Holton concentrated on quasi-stationary extratropical disturbances (i.e., $C_p = 0$ but $C_g \neq 0$).

Figures 11*a* and 11*b* show model-produced extratropical-tropical teleconnections in the upper troposphere for basic states with weak and strong equatorial westerlies, respectively, for differently placed extratropical wave source regions [from *Webster and Holton*, 1982]. For a given basic state, the lo-

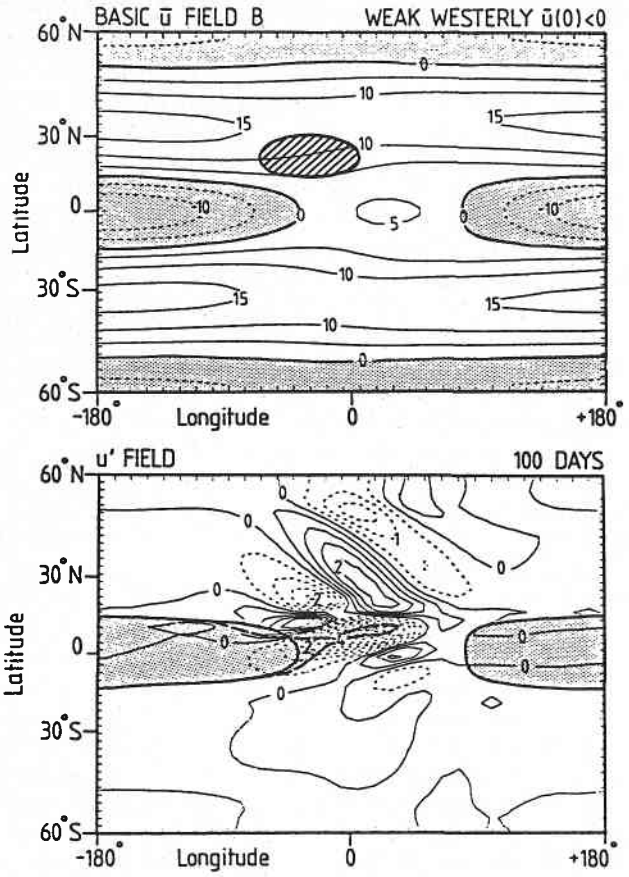

Fig. 11*a*. The quasi-steady state response of a free-surface barotropic atmosphere to perturbation from an energy source (hatched region) in the westerlies of a "weak westerly" basic state (upper panel). The field is the perturbation zonal velocity component in meters per second [from *Webster and Holton*, 1982].

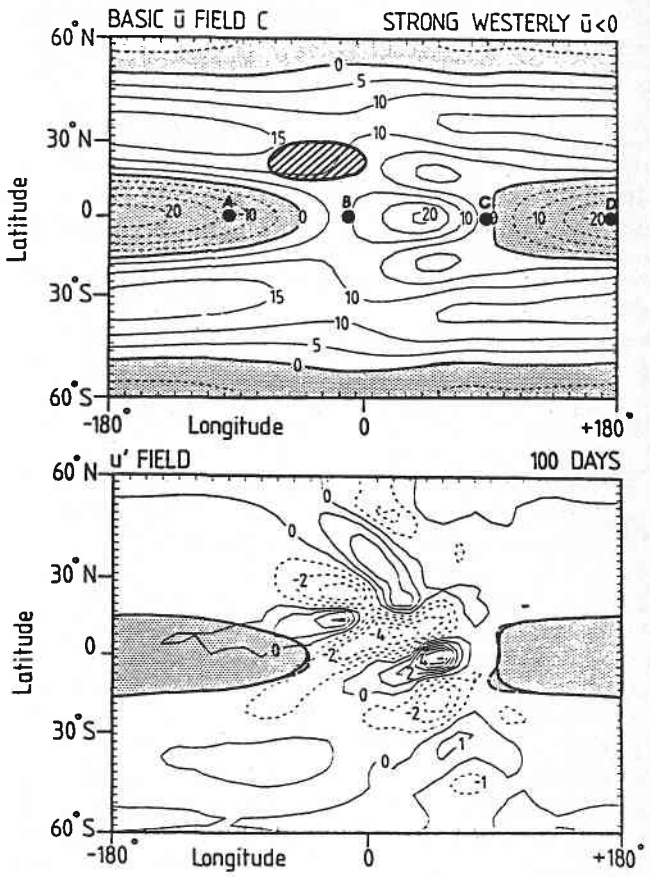

Fig. 11*b*. Same as Figure 11*a* except for a "strong westerly" basic state [after *Webster and Holton*, 1982]. The letters A, B, C, and D will be referred to later in the text.

cation of the source is important, as it determines whether or not the emanating wave train intercepts the equatorial easterlies or westerlies. For waves whose scale is smaller or of the same scale as the region of equatorial westerlies, the sign of the equatorial wind at the point of interception determines whether the wave will propagate through the equatorial regions or, in the case of equatorial easterlies, be absorbed or reflected at the critical line. However, for waves that are substantially larger than the scale of the equatorial westerlies, Webster and Holton showed that the wave may interact with the basic state such that, depending on the phase of the extratropical wave, the westerly region will be either widened or removed. Webster and Holton refer to the upper tropospheric equatorial westerlies as the "westerly duct region" to indicate its importance as a propagation path of extratropical waves.

Held [1983] noted an interesting feature relating to the position of the Himalayan wave train relative to the equatorial westerlies. The stationary wave train produced by the orographic feature intercepted the equator in the region of the equatorial westerlies. He argued that during the time of El Niño (and probably during the boreal summer also), when the east Pacific westerlies are weakest, the Himalayan wave train would encounter a critical line rather than a duct. In this manner the distribution of PKE along the equator would be very different during El Niño (cf. Figure 5*a* and 5*b*). Furthermore, the emanating Himalayan wave would influence the subtropics and extratropics of the northern hemisphere in a different manner because during El Niño (or boreal summer) it could be reflected at the critical line toward the extratropics but could pass through the tropics during the interim times (i.e., during positive Southern Oscillation Index periods or the boreal fall and winter).

The discussion above does not really change the conclusions reached by *Charney* [1963, 1969] regarding whether tropical disturbances develop in situ or are forced remotely. Maximum PKE and strongest westerlies occur together in regions of minimum tropical convection; the propagating convective transients occur in the regions of maximum upper tropospheric easterlies with typical values of PKE of about 20–30 $m^2\ s^{-2}$ compared to twice that value in the westerlies. This may be seen in Figure 12, which presents the time-averaged zonal wind component, the PKE, and the outgoing long-wave radiation (OLR) for boreal winter. Maximum westerlies correlate with maximum PKE and minimum convection (maximum OLR). Easterlies correlate with minimum PKE and maximum convection (minimum OLR). It would be possible that the equatorial modes are produced by the extratropical waves, but this aspect has only been hinted at theoretically by *Webster and Chang* [1988] (see discussion in section 5.2).

However, without theoretical or observational input, the influencing of the deep tropics within the regions of equatorial easterlies by forced equatorial modes from the equatorial westerlies remains, at best, very speculative. But there is some evidence that the reverse influence may take place. In the next

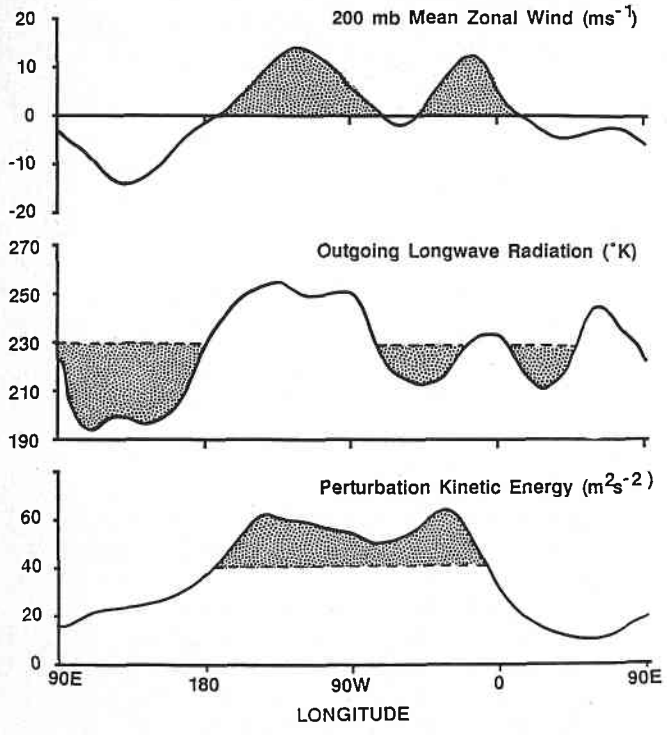

Fig. 12. Sections along the equator of the 200-mbar mean zonal wind (meters per seconds, westerlies shaded), the outgoing long-wave radiation (effective temperatures of <230°K shaded), and the perturbation kinetic energy ($m^2\ s^{-2}$, values of $>40\ m^2\ s^{-2}$ shaded) for the boreal winter [after *Webster and Chang*, 1988].

section we will discuss how, via the effect of the longitudinal stretch within the tropics, the disturbances of the equatorial easterlies may influence the extratropics.

5.2. *Wave Dispersion in a Flow With Longitudinal Variation of the Basic State*

Tropical disturbances are invariably convective and confined to the regions of very warm sea surface temperature (see Figure 3). They possess a deep divergent structure, occupying the entire depth of the troposphere. Furthermore, they are equatorially trapped with an amplitude that decreases exponentially away from the equator. Their northward phase and group speeds are at least an order of magnitude smaller than their respective zonal components [see *Matsuno*, 1966; *Longuet-Higgins*, 1968; *Gill*, 1982; *Webster*, 1972, 1983]. At the same time there may be exceptions. There appears some evidence that hydrodynamical instability of the low-level jet in Africa over dry regions produces disturbances which propagate to the warmer sea surface temperature regions.

Prevailing thought has it that the transient convective systems of the tropics locally aggregate their heating to produce strong local effects which force circulations which directly force the extratropics. However, it is conceivable that there are other effects where the longitudinal variation in the equatorial basic state so determines the behavior of the equatorial transient waves that they impart a significant influence on remote, nonconvective regions of the tropics and, eventually, the extratropics. That is, the geographically removed PKE and convection maxima shown in Figure 12 may be connected by transients controlled by the longitudinally varying basic state. For this to occur, three conditions would need to be satisfied:

1. There must be physical processes that create transient energy within the tropics. Presumably, the regions of convective activity are capable of exciting families of equatorial modes over a wide frequency and scale range [*Lim and Chang*, 1983].

2. There must be a mechanism that allows for the lateral transmission of energy from the sources identified in condition 1 to regions of PKE maxima, identified in Figure 5*a*.

In the following development we consider equatorially trapped Rossby waves because these possess group speeds which are very similar to observed speeds of basic state winds. On the other hand, inviscid Kelvin waves propagate eastward at rates very much faster than those of the basic state winds. Consequently, we ignore transient Kelvin waves in the analysis which follows. From the dispersion relationship for equatorially trapped Rossby waves,

$$\omega_r = -\beta k/[k^2 + \beta(2n+1)/c] \tag{1}$$

where ω_r is the modal frequency, $\beta = df/dy$, k is the longitudinal wave number, n is the latitudinal modal number, and $c = (gH)^{1/2}$ is the phase speed of a shallow water gravity wave. The Doppler-shifted group speed of these modes in a zonal flow $\bar{u}(x, y)$ may be expressed as

$$C_{gd} = \bar{u} - \left\{\frac{\beta[k^2 + \beta(2n+1)/c] - 2k^2\beta}{[k^2 + \beta(2n+1)/c]^2}\right\} \tag{2}$$

Figure 13 shows the longitudinal group velocity as a function of k for the longitudinal scales $n = 1, \cdots, 5$ [*Webster and Chang*, 1988]. Noting the scales and distribution of $\bar{u}$ in Figure 5*a*, it is obvious that the group speeds are of similar magnitude such that one may expect zeros in the modal group speed. However, for mode propagation through a time-independent basic flow there is the constraint that the frequency is conserved. Thus in order for ω_r to be conserved through a zonally varying basic flow, the wave number must change. Following *Lighthill* [1978], this may be written as

$$\frac{dk}{dt} = \frac{\partial k}{\partial t} + \left(\bar{u} + \frac{\partial \omega_r}{\partial k}\right) \cdot \frac{\partial k}{\partial x} = -k\,\frac{\partial \bar{u}}{\partial x} \tag{3}$$

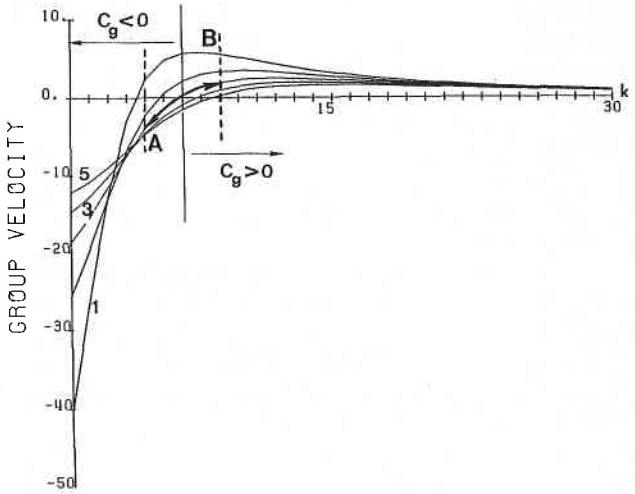

Fig. 13. The group velocity of an equatorially trapped Rossby wave $n = 1, 2, \cdots, 5$, where $H = 2000$ km, as a function of k, the longitudinal wave number. The line perpendicular to the abscissa at $k = 6$ demarks the $C_g = 0$ point for the $n = 3$ mode. Regions of negative and positive group speeds are noted. The points A and B are referenced in the text [from *Webster and Chang*, 1988].

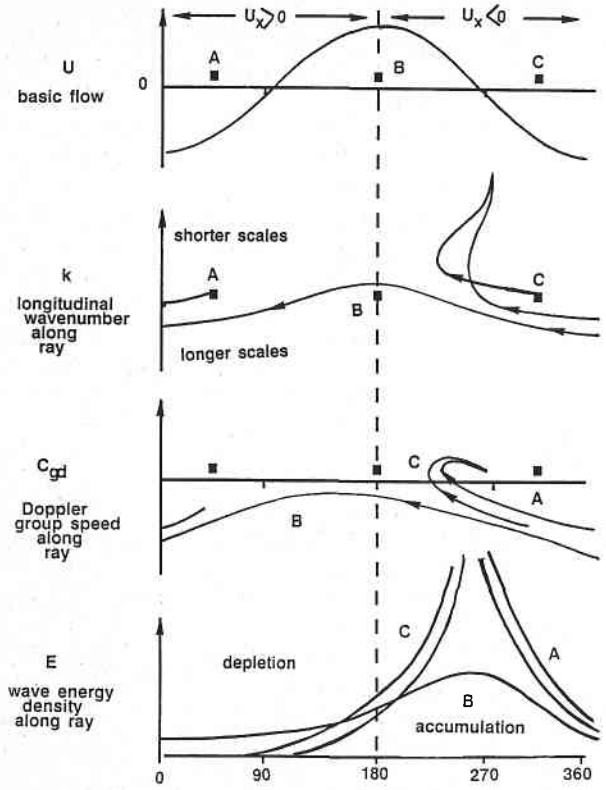

Fig. 14*a*. A schematic diagram representing the results of the WKBJ analysis for equatorially trapped Rossby waves moving through a basic state with longitudinal stretch as shown in the top panel. Wave sources are located at A, B, and C along the equator. The second panel shows the variation of the wave number along the three rays as given by (3). The third panel shows the variation of the Doppler-shifted group speed along the ray according to (2). A and C are longitudinally trapped, whereas B, the exceptional mode which always possesses $C_{gd} < 0$, is free to propagate around the equator. The bottom panel shows the wave energy density variation along the rays from (4). Regions of energy depletion and accumulation along the equator are indicated.

Thus as a wave moves into a region of stronger westerlies, its longitudinal scale must shorten. As it moves into stronger easterlies, the scale must lengthen. Returning to Figure 13, we can see that moving through an equatorial flow with longitudinal stretch is equivalent to moving the position where $C_{gd} = 0$ to larger (toward A) or smaller (toward B) scales depending on the sign of the longitudinal stretch $\partial\bar{u}/\partial x$.

In summary, there is the potential for the transportation of energy away from an energy source region to either the east or the west, although because of the frequency constraint, exotic behavior may be expected.

3. There must be a means of accumulating the transmitted energy through processes described in condition 2 in the regions of the equatorial westerlies.

Following *Whitham* [1965] and *Bretherton and Garrett* [1968], *Webster and Chang* [1988] found that the wave energy density ε could be written as

$$\frac{\partial \varepsilon}{\partial t} + C_{gd}\frac{\partial \varepsilon}{\partial x} = -\varepsilon\frac{\partial \bar{u}}{\partial x} \tag{4}$$

where C_{gd}, the Doppler-shifted group speed, is given by (2) and $\varepsilon = \rho g h^2/2$. The consequence of (4) is that a convergence of wave energy density occurs in regions where $\partial\bar{u}/\partial x < 0$. Regions where $\partial\bar{u}/\partial x > 0$, on the other hand, are divergent regions of wave energy. The ray paths of three modes emanating from points A, B, $\cdots$, F along the equator within a time-independent basic flow $\bar{u}(x, y)$ are shown schematically in Figure 14*a*. The lower panel shows the paths (arrowed lines), and the upper panel shows the change in the longitudinal wave number k from (3) and the wave energy density from (4). We note that the wave energy is shown to accumulate in the region where $\partial\bar{u}/\partial x < 0$ and, specifically, where min $(\partial\bar{u}/\partial x)$ occurs; here $\bar{u} = 0$.

Figure 14*b* shows the wave characteristics as a function of time of various families of waves created at source points A, B, $\cdots$, F along the equator for the $k = 3$, $n = 1$ (3, 1) mode; the (3, 2) mode; and the (3, 3) mode. Within this simple sinusoidal basic state with extreme values of ± 5 m s^{-1} all modes are trapped in the region where $\partial\bar{u}/\partial x < 0$ and min $(\partial\bar{u}/\partial x)$ occurs except for modes originating at C. These extraordinary modes appear free to propagate completely around the equator and correspond to grave modes where $C_g < |\bar{u}|$ at all longitudes.

The extraordinary modes are those which are forced at a particular scale such that their group speed in the first instance is sufficiently large that for a given basic state a zero in their Doppler-shifted group speed is never attained. Figure 15 shows the longitudinal domain (ordinate) from which a mode of a particular scale (k) will propagate through a basic state with longitudinal stretch and a maximum westerly of some prescribed value (curves). The intercept of the $\bar{u}_0$ curves with the ordinate defines the maximum longitudinal wave number k_0 that can just propagate through the westerly maximum. Intercepts with the $\bar{u}_0 = 5$ m s^{-1} curve at longitudes x_1 and x_2 show the scale of those waves that could just pass through a westerly maximum of 5 m s^{-1} if they were to originate from x_1 and x_2, respectively. Note that for very weak westerlies the $k < k_0$ mode may propagate completely around the equator. We expect this behavior to be of importance in defining influence regions for numerical prediction at low latitudes.

Using the same free surface barotropic model of *Webster and Holton* [1982], *Webster and Chang* [1988] designed a series of experiments to test the solutions of the simple analysis described above, but with a model with fewer scale restrictions. With the "strong westerly basic state" of Webster and Holton (see Figure 11*b*, upper panel) a transient energy source with an *e*-folding time scale of 2 days was inserted, successively at points A, B, C, and D along the equator, as shown in Figure 11*b*. Figure 16 shows time sections along the equator of the perturbation response, and Figure 17 the longitude-latitude section of the velocity and height fields.

The time sections show results very similar to the WKBJ solution. Irrespective of the location of the forcing along the equator, the maximum response resides, ultimately, in the region where $\partial\bar{u}/\partial x < 0$. The horizontal sections also show this feature as a short-wave symmetric response about the equator which is also the emanation region for wave trains toward middle latitudes. That is, irrespective of the energy source along the equator, the wave trains emanate from the same longitudinal belt. Presumably, for very different basic states, the accumulation points, and thus the emanation zones, would change. Thus between climatic epochs and seasons the influence of the tropics on the higher-latitude circulation may be expected to be different.

5.3. *Westerly Duct Mechanism*

The weaknesses of the pure wave train theory for atmospheric teleconnections and the understanding of the impor-

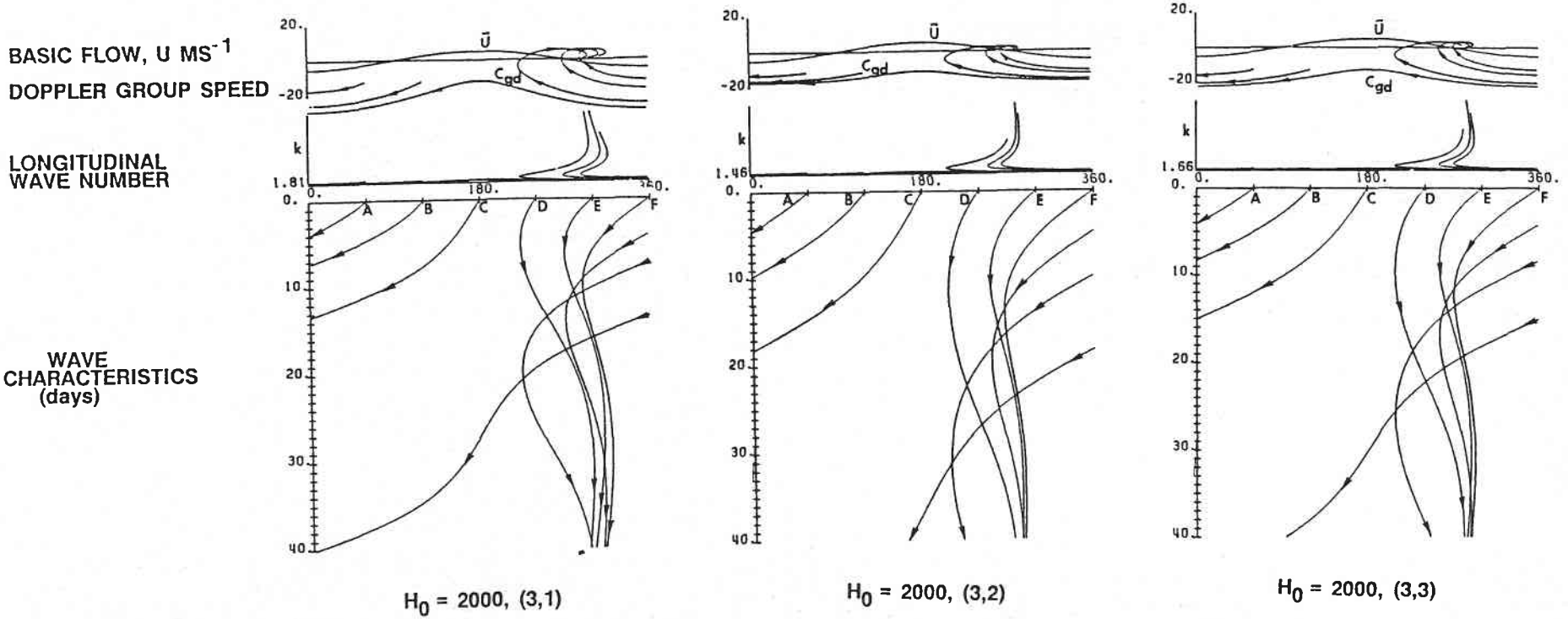

Fig. 14*b*. The wave characteristics of various families of waves created at source points A, B, · · ·, F along the equator for the $k = 3$, $n = 1$ (3, 1) mode, the (3, 2) mode, and the (3, 3) mode. The lower panels are time-longitude plots of the ray paths. The Doppler-shifted group speeds relative to the basic state $\bar{u}$ are shown in the upper panels. The simple basic state has extremes of 5 m s^{-1}. The center panel shows the local longitudinal wave number along the ray path. The equivalent depth is 2000 m.

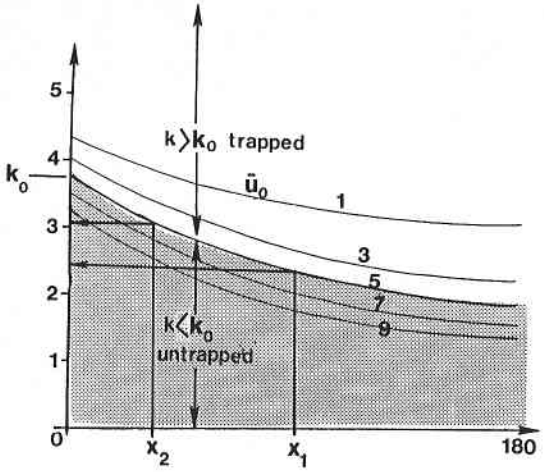

Fig. 15. The loci of k as a function of longitude for various trigonometric basic states with maximum westerly amplitude $\bar{u}_0$. Intercept of the $\bar{u}_0$ curves with the ordinate defines the maximum longitudinal wave number k_0 that can just propagate through the westerly maximum. Intercepts with the $\bar{u}_0 = 5$ m s^{-1} curve at longitudes x_1 and x_2 show the scale of those waves that would just pass through a westerly maximum of 5 m s^{-1} if they were to originate from x_1 and x_2, respectively.

tance of the role of longitudinal shear, together with the identification of the wave saturation and emanation region, allow us to pose a new mechanism for the communication between the tropics and the extratropics. This mechanism calls for the development of transients within the warm sea surface temperature regions of the tropics. The modes propagate westward through the easterlies and the relatively weak westerlies of the Atlantic Ocean until they reach the stronger westerlies of the eastern Pacific Ocean. If the longitudinal stretching deformation is strong enough (or, effectively, if the westerlies are significantly strong), a wave saturation region forms, defining the region of influence of the propagating wave and also the emanation region to the extratropics.

Even though there is a certain attractiveness to the modified mechanism, it still does not take into account the instability of the extratropical basic state. With regard to the stability of the tropical basic flow, *Webster and Chang* [1988] expended considerable effort in showing a robust stability. Thus we will concentrate subsequently on the instability of flow at the higher latitudes.

6. Three-Dimensional Instability Theory and Low-Frequency Variability of the Atmosphere

6.1. *Baroclinic-Barotropic Dipole Instability Mechanism and Climatological Basic States*

The study of *Frederiksen* [1982*a*] showed that instability theory with three-dimensional basic state flows could produce a variety of disturbances in addition to the monopole cyclogenesis modes (such as those shown in Figure 9*b* and 10*b*) associated with the storm tracks. The results suggested that three-dimensional instability theory could provide a similar basis for understanding both blocking and localized cyclogenesis as zonally averaged instability theory has traditionally provided for cyclone scale disturbances. According to this proposition, the formation of mature anomalies such as blocking events is initiated (at least in some cases) by the generation of onset-of-blocking dipole instability modes upstream of the

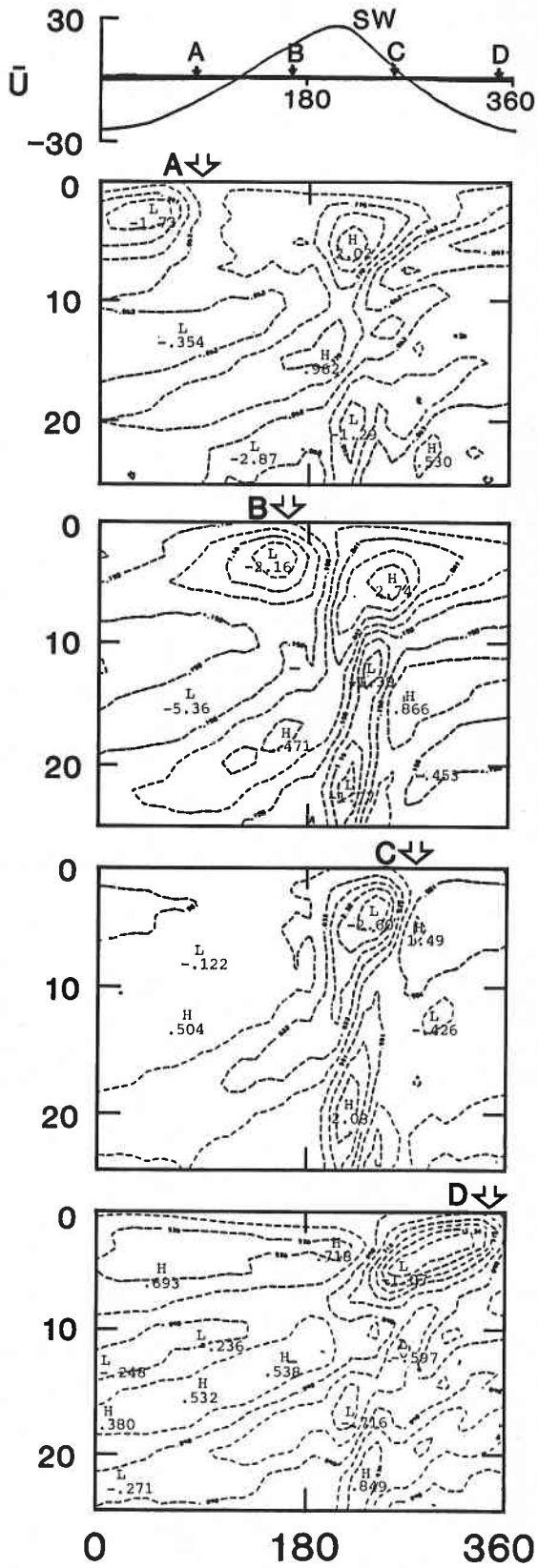

Fig. 16. Longitude-time sections of the perturbation velocity component for the first 25 days along the equator. The top panel shows the mean zonal wind component of the basic state along the equator together with the location of the initial forcing [from *Webster and Chang*, 1988].

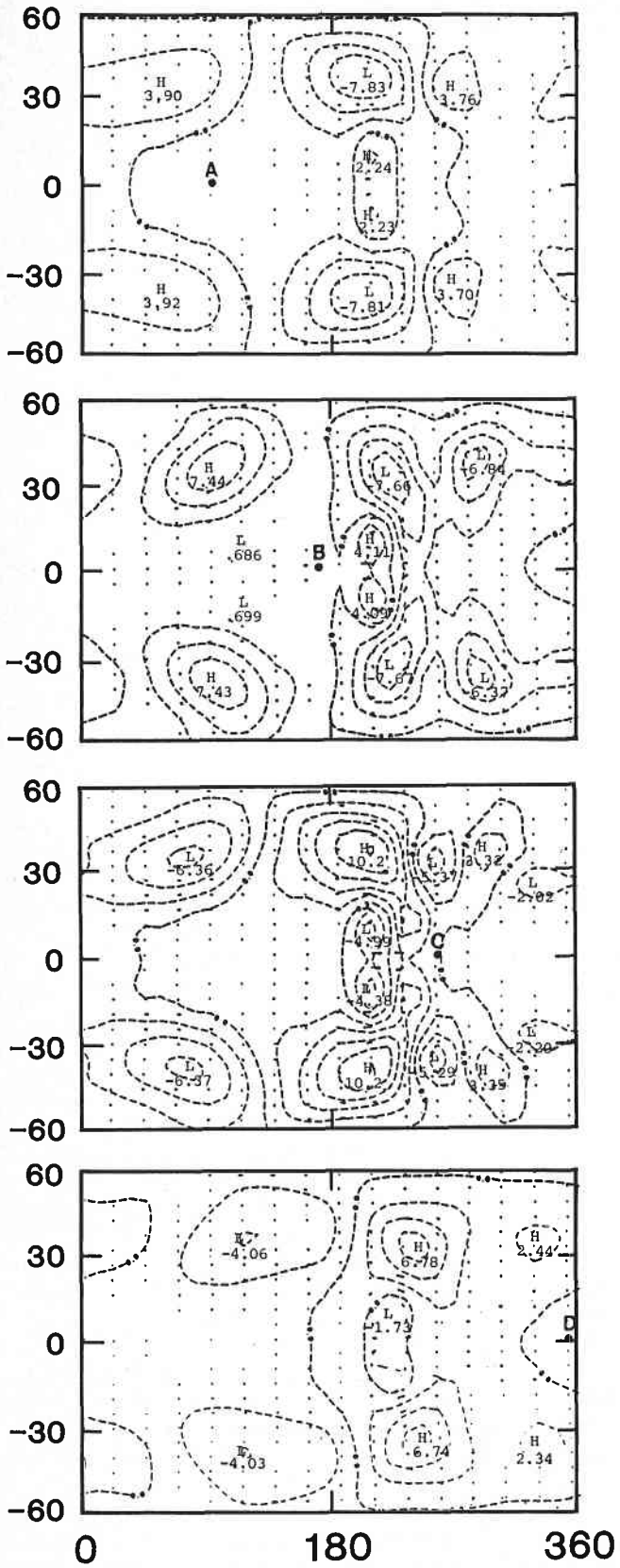

Fig. 17. Longitude-latitude section of the perturbation velocity and height field after 25 days of integration for the strong westerly basic state. The $\bar{u} = 0$ isopleth from Figure 11*b* is shown to demark the easterlies and westerlies. Note the maximum perturbation in the vicinity of the mean equatorial westerlies. The central location of the forcing is indicated by a solid circle and a letter [from *Webster and Chang*, 1988].

regions of maximum amplitude of the mature anomalies. These onset modes have westward tilt with height; baroclinic processes and barotropic processes are relatively important in their formation [*Frederiksen*, 1983*a*]. They propagate eastward, and as they increase in amplitude, they become quasi-stationary and essentially equivalent barotropic. It was suggested that in many qualitative respects the change from onset-of-blocking dipole modes to mature anomaly modes would occur through nonlinear effects in much the same way as is the case with cyclone scale disturbances and as is found in the life cycle experiments of *Gall* [1976], *Simmons and Hoskins* [1978], and *Frederiksen* [1981*a*, *b*] using zonally averaged basic states. Support for this view also comes from the study of *Dole* [1986], who notes that "Indeed in several aspects the structures resemble those of amplifying baroclinic waves although their spatial scales are considerably larger and propagation speeds considerably smaller than for typical disturbances."

Frederiksen [1982*a*, 1983*c*] studied the instability of a three-dimensional flow for northern hemisphere winter (similar to that in Figure 5*a*) in a two-layer quasi-geostrophic model with spherical geometry. A number of cases with different static stability parameters were considered. It was found that there was a close relation between the period of the modes and their structure and baroclinic or barotropic nature. Short periods (high frequencies) are associated with smaller-scale baroclinic modes progressing through increasingly larger-scale more barotropic modes as the period increases. *Frederiksen and Bell* [1987] classified these modes (for a five-level model) into four broad classes: class I, monopole cyclogenesis modes with periods of 2.0–6.5 days; class II, onset-of-blocking dipole modes with periods of 6.5–11 days; class III, intermediate modes with periods of 11–17 days; and class IV, mature anomaly modes with periods greater than 17 days.

Here we shall concentrate on instability modes relevant to blocking in the Pacific–North American regions, since this is the case for which there are most detailed observational data for comparison. Figures 18*a* and 18*b* show upper layer stream functions for the third and twenty-second fastest growing modes for case 1 of *Frederiksen* [1982*a*, 1983*c*] (corresponding to a potential temperature difference between the layers of 23°K). We may identify the mode in Figure 18*a* as a Pacific onset-of-blocking mode which initiates the blocking process and that in Figure 18*b* as a Pacific–North American mature anomaly mode characteristic of the later stages of block development in this region. The onset-of-blocking mode has an *e*-folding time for growth of about 2.5 days and a period of 7.4 days. These values are to be compared with an *e*-folding time of 2.3 days and a period of 3.3 days for the fastest growing monopole cyclogenesis mode (similar to that in Figure 8*b*) for case 1. Like the monopole cyclogenesis modes the onset-of-blocking mode has a westward tilt with height, while the mature anomaly mode is equivalent barotropic, has an *e*-folding time of 5.8 days, and has infinite period. In fact, modes very similar to the mature anomaly mode in Figure 18*b* have been obtained within barotropic models [*Simmons et al.*, 1983; *Frederiksen*, 1983*c*; *Schubert*, 1985] and in five-level models [*Frederiksen and Bell*, 1987].

It is interesting to compare the instability results with the studies of *Dole* [1982, 1983, 1986], which provided important insight into many aspects of observed anomalies including their time evolution. Figure 19 shows time sequences of composite analyses of 15 positive anomaly cases at 500 mbar lead-

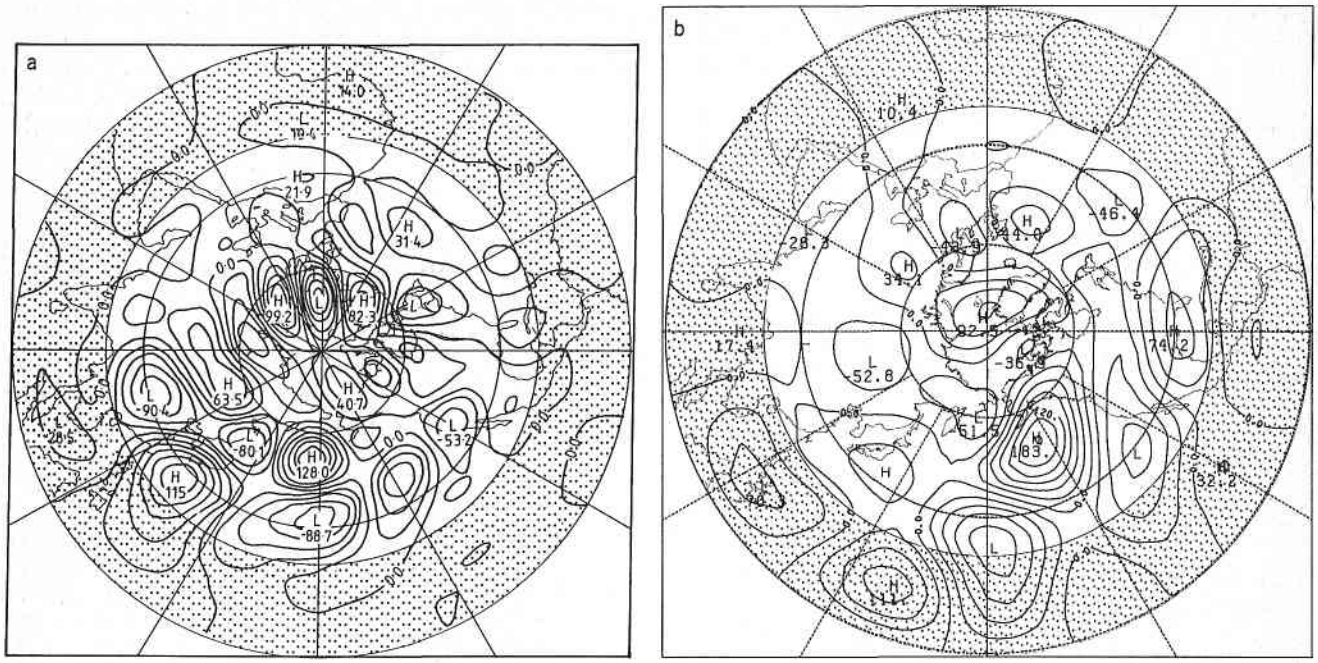

Fig. 18. Disturbance stream function in the upper layer of a two-layer quasi-geostrophic model with northern hemisphere winter basic state for (*a*) the third fastest (Pacific–North America onset of blocking) and (*b*) the twenty-second fastest growing (Pacific–North America mature anomaly) modes [from *Frederiksen*, 1982*a*, 1983*c*].

ing to establishment of a mature Pacific anomaly pattern. Figures 19*a* and 19*b* are unfiltered data on days −3 and 0 before the appearance (on day 0) of the essentially stationary large-scale positive anomaly in the key region in the north central Pacific, while Figure 19*c* shows low-pass-filtered data on day 6.

For the period leading up to the appearance of the positive anomaly in the key region, which we refer to as the onset-of-blocking period, Dole notes that the "sequence of development suggests that the initial rapid growth of the main centre is primarily associated with the propagating intensifying disturbance which originates in mid-latitudes near Japan." He also notes that "this disturbance continues to intensify as it becomes quasi-stationary over the key region." The dipole wave train across east Asia and into the Pacific that appears in Figure 19*a* at day −3 is qualitatively very similar to that in Figure 18*a* (as well as to that in Figure 6*a* of *Frederiksen* [1982*a*]). We note that *Schubert* [1986] has also found fluctuations like the onset-of-blocking modes by filtering observed data.

Further evidence that baroclinic onset-of-blocking instability modes are involved in the initial period may be obtained from Figure 20 (taken from *Dole* [1986]), which shows longitude-pressure cross sections at 45°N and 20°N of the unfiltered Pacific composite anomalies at days −3 and 0.

The dipole nature of the developing anomaly is clearly evident, particularly at day −3, and the zonal scale of the anomaly at day −3 is practically the same as shown in Figure 18*a*. The developing anomaly has a definite westward tilt with height, as do the onset-of-blocking instability modes. Dole notes: "... This feature has pronounced westward tilts with height during this period, suggesting that a substantial baroclinic contribution is involved in its amplification ... ."

Following day 0 the development of the 500-mbar height anomaly follows that shown by *Dole* [1986], with the anomalies being largely equivalent barotropic during this period. Intensification of the centers occurs with little phase propagation, and by day 4, and especially at day 6, the Pacific–North American pattern is established as shown in Figure 19*c*.

The observational and theoretical results described above suggest that the development of mature anomalies, such as blocks, may be thought of as consisting basically of two stages. For the Pacific–North American pattern the baroclinic-barotropic dipole instability mechanism may be summarized as follows:

1. A rapidly growing and relatively rapidly eastward propagating onset-of-blocking dipole disturbance mode which tilts westward with height forms in the east Asia–Pacific Ocean region through the combined baroclinic-barotropic instability of the three-dimensional basic state. As the disturbance grows, the regions of largest amplitude propagate into the central Pacific, and the disturbance increases its zonal scale, becoming quasi-stationary and essentially equivalent barotropic through the operation of nonlinear effects. At this stage the mode has a structure reminiscent of the mature Pacific–North American pattern instability mode.

2. The (nonlinear analogue of the) mature anomaly instability mode amplifies without phase propagation and through the operation of largely equivalent barotropic effects to form the large-amplitude mature Pacific–North American anomaly pattern.

The change from the initial onset-of-blocking mode to the formation of the large-amplitude mature anomaly pattern mode is, in fact, a continuous one, and the separation into two distinct stages is to some extent arbitrary, if convenient. The fact that the mode continually changes its structure in a gradual manner to optimize its growth, as nonlinear effects become increasingly important, is also clearly shown in the numerical simulation of *Frederiksen and Puri* [1985], which will be discussed in section 8.

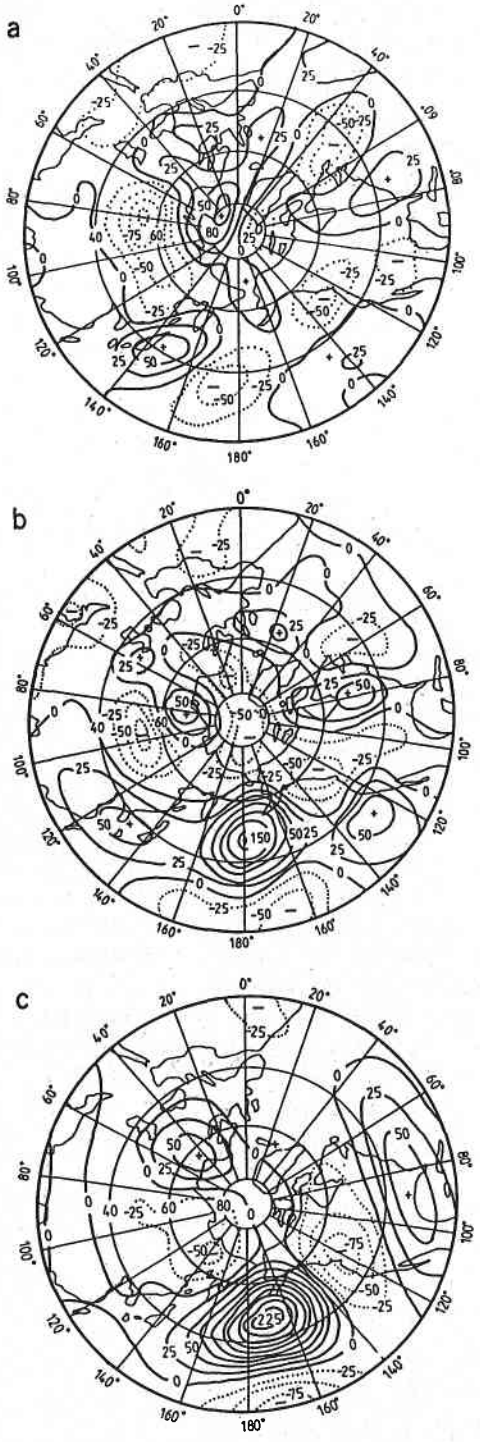

Fig. 19. Composites of heights (meters) of unfiltered anomalies at 500 mbar on (*a*) day −3 and on (*b*) day 0 and low-pass-filtered anomalies on (*c*) day 6 for 15 Pacific positive cases [from *Dole*, 1983].

Further observational evidence for the existence of onset-of-blocking dipole modes with periods between about 6 and 10 days and intermediate modes with periods between about 10 and 20 days was presented by *Schubert* [1986] using filtered data rather than the composite approach of Dole. Figure 21 shows one of Schubert's modes with periods between 6 and 10 days which is quite similar to the onset-of-blocking instability mode in Figure 18*a* and to Dole's observed onset mode in Figure 19*a*.

Instability modes corresponding to onset-of-blocking and mature anomalies in the Atlantic region were also found in the two-level model [*Frederiksen*, 1982*a*, 1983*c*]. *Dole* [1982] showed that similar sequences of events leading to blocking in the Atlantic and north USSR regions also occurred. The study of *Frederiksen and Bell* [1987] using a five-level model found a wide variety of modes, including new modes corresponding to onset-of-blocking and mature anomalies in the north USSR region. Some modes also had similarities to a number of teleconnection patterns described in the work of *Wallace and Gutzler* [1981]. One particular large-scale mode with infinite period has some similarities to the western Atlantic teleconnection pattern of Wallace and Gutzler. The mode is a largely zonal wave number one disturbance whose structure is consistent with a ducting of wave activity from near the Himalayas in the Asian region at the surface into the polar stratosphere. Thus it also appears to have the right properties such that if it were produced with sufficient amplitude, it would produce a stratospheric sudden warming. It seems interesting that instability theory should reflect the fact that stratospheric sudden warmings occur in association with atmospheric blocking, although not necessarily vice versa [*O'Neill and Taylor*, 1979, and references therein; *Hunt*, 1978].

6.2. *Instantaneous Basic States*

Frederiksen [1984, 1988] examined the instability of three-dimensional instantaneous synoptic flows in the southern and northern hemispheres in a quasi-geostrophic five-level model incorporating spherical geometry. As noted there, instability theory literally gives information about linear error growth; however, in practice, the growth of errors tends to be rapid where dynamical development of storms, blocks, etc. is greatest. This seems to be the primary reason why instability theory is relatively successful in predicting the geographical regions of the storm tracks, blocking and other mature anomalies.

Frederiksen [1988] made a study of the three-dimensional instability properties of a sequence of daily northern hemisphere flow fields for the period November 1 to November 16, 1979. During the second week of November, rapid development of a major block occurred off the west coast of North America in the Gulf of Alaska. On November 6 the blocking process was evident in the observations, but distinct high-low dipole pairs only formed a few days later. Figure 22*a* shows the stream function of the 500-mbar surface for 1200 UT on November 9, 1979; a very distinct dipole with the high centered over the Gulf of Alaska is evident at this stage. After about November 12 the blocking ridge weakened and moved eastward.

Figures 22*b*, 22*c*, and 22*d* show the 500-mbar stream function for instability modes at 1200 UT on November 2, 4, and 6 which are relevant to the formation of the Gulf of Alaska block. Figure 22*b* is for the ninth fastest growing mode on November 2, which has a period of 6.7 days and an *e*-folding time of 3.2 days; it consists of a wave train of high-low dipoles upstream of the blocking region. This mode has significant westward tilt with height indicating the importance of baroclinic (as well as barotropic) processes and appears to correspond to an onset-of-blocking mode. Figure 22*c* is for the ninth fastest growing mode on November 4, which has a period of 12.4 days and an *e*-folding time of 3.4 days; it again has some westward tilt with height and corresponds to a slightly later stage of block formation. Finally, on November 6

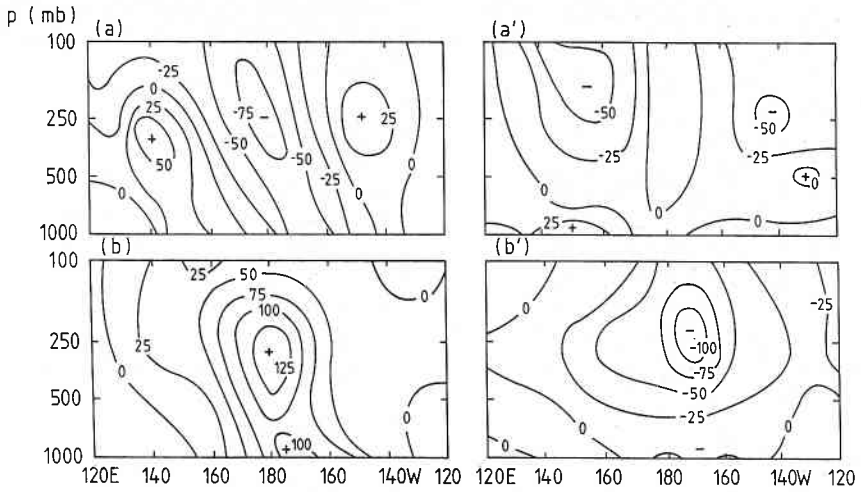

Fig. 20. Composite longitude-pressure cross sections of heights (meters) of unfiltered anomalies for 15 Pacific positive cases at 45°N on (*a*) day −3 and (*b*) day 0. Parallel analyses at 20°N are presented in (*a'*) and (*b'*) [from *Dole*, 1986].

the mode in Figure 22*d* is the fastest growing mode with an *e*-folding time of only about 1.6 days and an infinite period.

In the late stage of block formation on November 6, the nature of instability is essentially barotropic. This was established by carrying out the instability calculation using a barotropic model with the basic state field taken at the 300-mbar level. The fastest growing instability mode thus obtained has virtually the same structure as that for the five-level model at 300 mbar. It again has zero phase frequency and a somewhat smaller *e*-folding time of about 1.1 days.

One of the southern hemiphere basic states considered by *Frederiksen* [1984, Figure 1] was the observed flow field at 2300 UT on August 24, 1975. This is a few days before a blocking dipole wave train first occurred in the Tasman Sea region between Australia and New Zealand. For this basic state the fastest growing mode [*Frederiksen*, 1984, Figure 10] has a tendency toward the formation of dipole structures corresponding to the very early stages of the onset of blocking in the southeast Australian–Tasman Sea area.

6.3. *Discussion*

Simmons et al. [1983] proposed an alternative instability theory for the development of mature anomalies which contrasted with the previously described baroclinic-barotropic dipole instability mechanism of *Frederiksen* [1982*a*]. The Simmons et al. mechanism is direct barotropic instability of the climatological basic state flow. They recognize, however, that the global growth rates for direct barotropic instability may only be about one-third those for the baroclinic-barotropic dipole instability mechanism. In order for their path of development to be competitive, they propose that the local growth rate (i.e., at a particular point) due to barotropic instability may be enhanced (during one-quarter period) over the global growth rate due to phase propagation. However, for this mechanism to work, the mode must be propagating, and Simmons et al. suggest that as a consequence, stationary growing modes may be difficult to excite in reality. In contrast, we note that both the fastest growing equivalent barotropic mode in Figure 22*d* and the corresponding barotropic mode are in fact nonpropagating but nevertheless are very rapidly growing. Their growth rates are about 5 times that of barotropic modes growing on climatological flows typical for northern hemisphere winter. Although the instability calculation used to obtain the mode in Figure 22*d* is a linear one, nonlinear processes have been responsible for distorting the flow to the extent that barotropic instability has become the dominant process at this late stage of block development.

The life cycle experiments with zonally averaged basic states discussed in section 6.1 have demonstrated the importance of barotropic conversions in the late stages of development. This is also the case in similar experiments using climatological basic states [*Frederiksen and Puri*, 1985]. It appears from the results of section 6.2 that linear instability studies of instantaneous flows may (at least in some cases) produce modes with reasonable structures and growth rates and phase speeds, including cases where barotropic conversion is the dominant mechanism. In this way one can study the nonlinear process through a series of linear instability calculations.

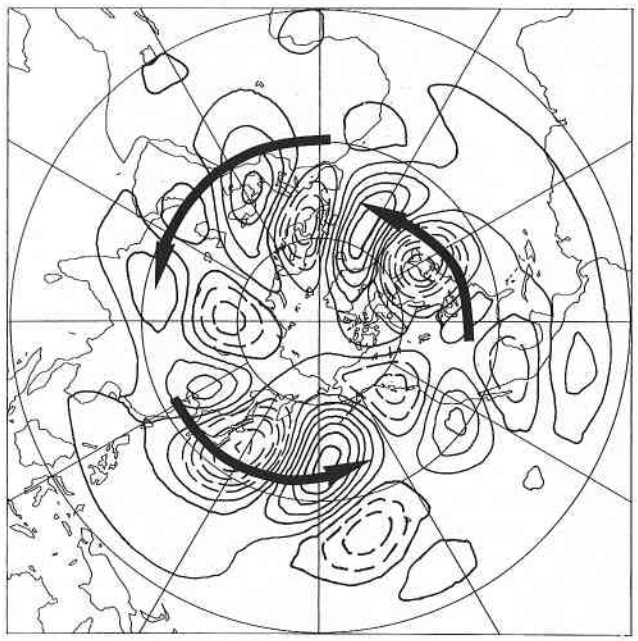

Fig. 21. The 500-mbar stream function of a particular empirical orthogonal function (D3) with time scales between 6 and 10 days [from *Schubert*, 1986].

A question that comes to mind at this stage is whether it is also useful to regard the statistics of various classes of atmospheric fluctuations as arising from linear instability of climatological flows for particular months or seasons. That is, to what extent can one replace doing an ensemble of instability calculations for instantaneous flows with a single instability calculation for a climatological flow corresponding to the same ensemble of instantaneous flows? The success of the baroclinic instability theory of cyclone scale disturbances would seem to indicate that such a replacement is reasonable for these disturbances. That is, the baroclinicity of the atmosphere is fairly robust as we change from instantaneous to climatological and even to zonally averaged flows. For the onset-of-blocking modes, baroclinic processes are also very important, and therefore one might again expect that the replacement would not be an unreasonable one. However, for modes characterized by barotropic instability the horizontal shears may be quite different in instantaneous and climatological flows. The northern hemisphere winter flow preserves a reasonable amount of wave structure in its climatological average, and for this reason, modes like the Pacific–North American anomaly mode (see Figure 18*b*) are captured in instability calculations. However, the growth rates may be too small by a factor of about 5, and the detailed structures may differ significantly from corresponding blocking modes growing on instantaneous flows. In the southern hemisphere, with its more zonal climatological flows, one would expect the replacement to be considerably worse for modes arising from barotropic instability. On the basis of his observational studies, *Dole* [1986] makes the comment: "These observations raise the distinct possibility that barotropic or equivalent barotropic models will be inadequate for modelling important aspects of the initial developments."

6.4. *Other Studies*

The composite results of *Dole* [1983, 1986] present a very clear-cut example of the change in the horizontal and vertical structure of the anomaly pattern starting upstream of the key region with the formation of westward tilting smaller-scale dipole disturbances. The importance of baroclinic transients in the development of blocks has also been pointed out by many other authors [e.g., *Lejenäs*, 1977; *Green*, 1977; *Tucker*, 1979; *Austin*, 1980; *Youngblutt and Sasamori*, 1980; *Illari and Marshall*, 1983; *Colucci*, 1985, 1987; *Hansen and Chen*, 1982; *Shutts*, 1983, 1986]. Hansen and Chen, in particular, note that intense upstream cyclogenesis preceded the growth of the blocking ridge in their observational studies of blocking. Further, "the nonlinear transfer of kinetic energy from baroclinically active cyclone-scale waves to the planetary-scale waves provided the major source of kinetic energy for the block." *Lejenäs* [1977] notes the importance of the combination of barotropic and baroclinic instability during the formation of blocks (see also *Schilling* [1986]). *Barnett* [1984], in an observational study, also finds support for instability normal modes playing important roles in the generation of anomaly patterns. The study of *Colucci* [1985, 1987], in which the dynamics of individual cases of observed block formations are examined, also supports the generation of blocks through the three-dimensional instability of the flow. He argues that heat sources serve only an indirect role in the blocking processes. For one particular case of northern hemisphere blocking during 1980, *Colucci* [1987] notes, "This evolution resembles the development of certain of Doles' (1982) persistent anomalies, and of certain onset-of-blocking structures evolving linearly (Frederiksen, 1982*a*) and nonlinearly (Frederiksen and Puri, 1985)".

In retrospect, the study of *Joung and Hitchman* [1982] also seems to support the existence of onset-of-blocking modes in the atmosphere and their role in the blocking process. Joung and Hitchman, for example, find that the east Asia polar air outbreaks are associated with the formation of baroclinic dipole structures in the east Asian–west Pacific region. Further, they note that in many of their cases the disturbance led to the formation of blocks in the Pacific Ocean.

Lejenäs [1984], in an observational study of southern hemisphere blocking, also finds support for dipole instability modes being responsible for the majority of blocking episodes, while the additional influence of forcing controls the duration. *Baines* [1983] carried out a survey of blocking mechanisms and discussed their application to the Australian region. He found that the most promising mechanism which was consistent with the observations in the Australian region was the three-dimensional instability mechanism leading to dipole modes.

The above observational, numerical, and theoretical studies would appear to the authors to present convincing evidence in favor of the three-dimensional instability mechanism (modified by nonlinearity) being of primary importance for the development of mature anomalies. However, a number of observational studies, for example, those of *Horel and Wallace* [1981], *Wallace and Gutzler* [1981], *Dole* [1983], and *Blackmon et al.* [1984*a*, *b*], have noted the importance of two-dimensional Rossby wave dispersion for low-frequency anomalies. In some studies, the structure and time variation of such disturbances have been interpreted in terms of the theory of Rossby wave dispersion on a sphere. *Dole* [1983] nevertheless describes some discrepancies between Rossby wave dispersion from a localized source and the observations. He notes in particular that

> the near simultaneity of development, the almost north-south orientation of the centers and the absence of tilts in the anomaly axis over the Pacific make interpretation of the development in this region more difficult . . . The time scale for changes in such forcing, however, is presumably much longer than the time scales that we typically find for the development and decay of persistent anomalies . . .

As discussed in section 5 the theory of Rossby wave dispersion, initially proposed by *Rossby* [1945] and *Yeh* [1949], describes how an initial localized source of vorticity in a barotropic atmosphere, with a simple stable zonal eastward flow, can produce a series of troughs and ridges for which the energy is dispersed with the group velocity. This theory has been developed further by a number of authors, including *Hoskins et al.* [1977], *Karoly* [1983], and *Branstator* [1985], and for the tropics by *Webster and Chang* [1988]. The resulting wave trains obtained by a number of authors, including *Hoskins and Karoly* [1981] and *Karoly* [1983], have been likened to observed teleconnection patterns.

In view of the above apparently conflicting evidence in support of three-dimensional instability theory and two-dimensional Rossby wave dispersion, it would perhaps be interesting to examine the relationship between the two theories in more detail; we do that in the next section.

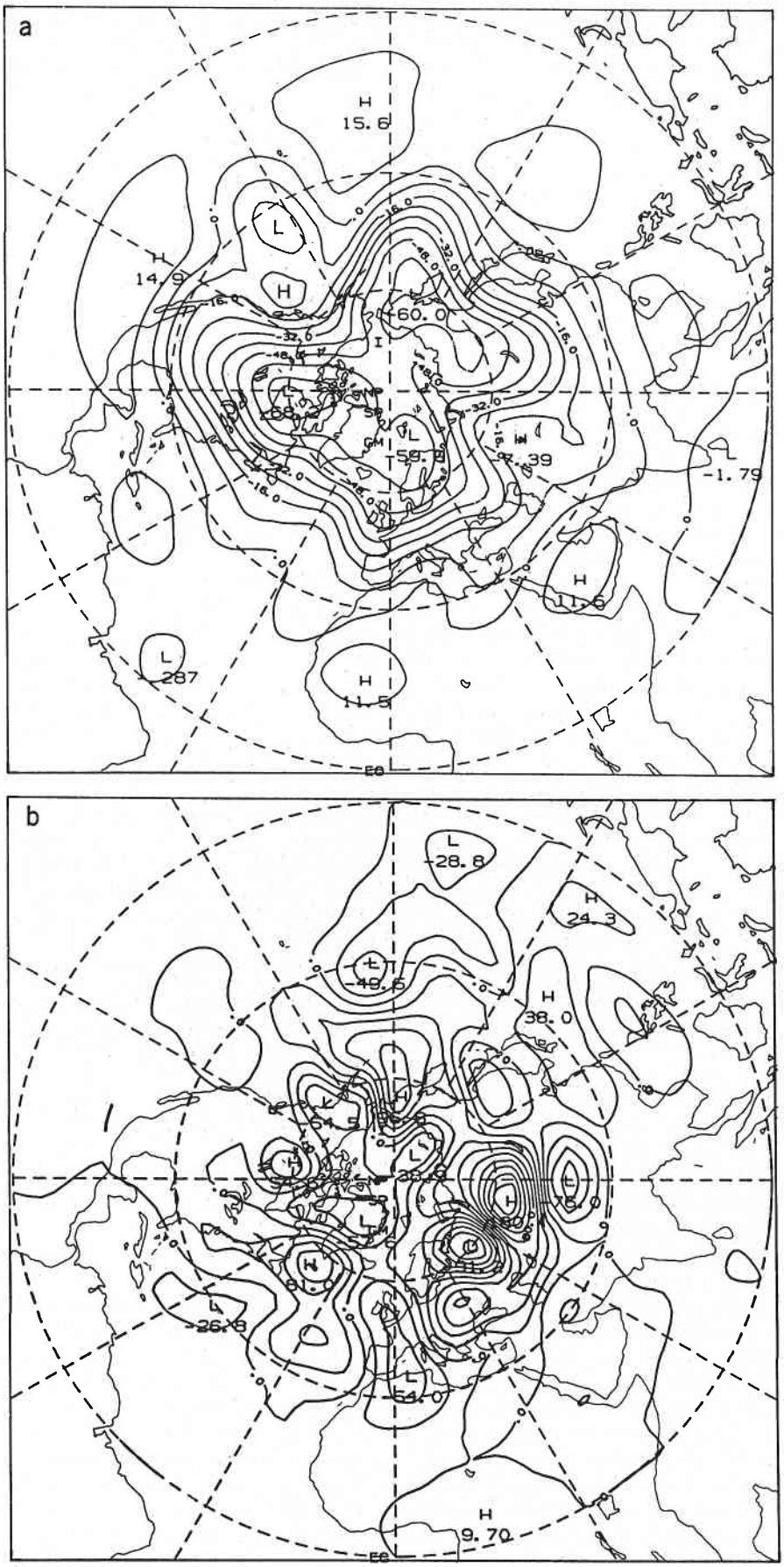

Fig. 22. The stream function ($km^2\ s^{-1}$) of the 500-mbar surface for 1200 UT on November 9, 1979, in the northern hemisphere. (*a*) Instantaneous disturbance stream function at 500 mbar for (*b*) the ninth fastest growing mode at 1200 UT on November 2, (*c*) the ninth fastest growing mode at 1200 UT on November 4, and (*d*) the fastest growing mode at 1200 UT on November 6 [from *Frederiksen*, 1988].

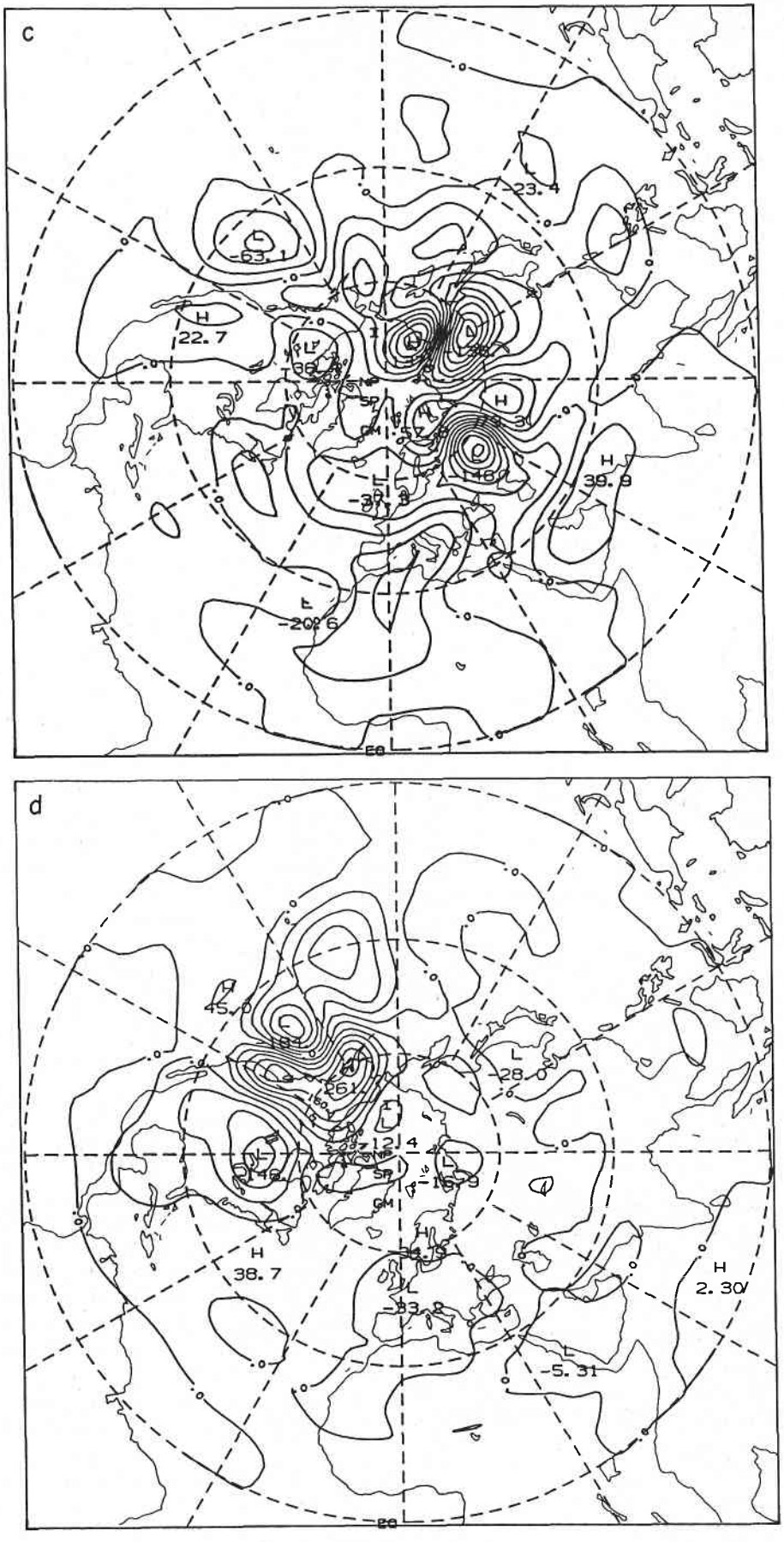

Fig. 22. (continued)

7. Basic State Instability and Rossby Wave Dispersion

7.1. *Theory*

The growing perturbations in three-dimensional instability calculations (on a sphere) have stream functions of the form

$$\psi^j(\lambda, \mu, t) = \mathrm{Re} \sum_{m=-\infty}^{\infty} \sum_{n=|m|}^{\infty} \psi_{mn}{}^j P_n{}^m(\mu) \exp\,[i(m\lambda - \omega t)] \quad (5)$$

Here j refers to the level of the multilevel model, m is the zonal wave number, n is the total wave number, $\omega = \omega_r + i\omega_i$ is the complex angular frequency, λ is longitude, μ is sin (latitude), t is time, and $P_n{}^m(\mu)$ are Legendre functions.

Suppose now that we have an initial state consisting of two or more growing modes of the form (5) with different ω and, in particular, different ω_r. Further, at a given point, suppose the two modes interfere constructively to give maximum amplitude. Then, as time evolves, we find that just as in the case of neutral modes, there is Rossby wave dispersion.

We also note that for single disturbances of the form (5), the global growth rate of the disturbance is ω_i; however, because a given mode consists of many wave numbers, these can conspire at different stages of the mode's period to give either very little amplitude or maximum amplitude at a given point. Hence if the disturbance happened to be aligned so that initially the amplitude was small at the given point, the amplitude could increase at that point both through phase propagation (nonzero ω_r) and through the global growth rate ω_i giving a local growth rate which is larger than the global growth rate. Conversely, at a later stage the fact that the phase speeds ω_r/m of the different scales are different leads to a smaller than global growth rate if the mode is initially primarily concentrated in one region. Of course, the disturbance will be reconstructed there (with larger amplitude) after a full period. This effect of surges in the local growth rate is most noticeable for some of the larger-scale modes, although it is of less importance for the monopole cyclogenesis modes as discussed by *Frederiksen* [1983*c*].

In fact, within the linear context the normal modes of the three-dimensional instability problem form a natural way for analyzing both the growth and dispersion of an initial disturbance and the response to imposed anomalous forcing. To see this, we note that in terms of spectral components, the linear (quasi-geostrophic) multilevel equations for these problems take the form

$$\mathsf{A} \frac{\partial}{\partial t} \boldsymbol{\psi}(t) = -i\mathsf{B}\boldsymbol{\psi}(t) + \mathbf{f} \quad (6)$$

with $\boldsymbol{\psi}(t=0) = \boldsymbol{\psi}_0$. Here $\boldsymbol{\psi}(t)$ is a column vector of stream function spectral coefficients $\psi_{mn}{}^j$ of length N, and A and B are $N \times N$ complex matrices [see *Frederiksen*, 1982*b*]. The matrices A and B contain information about the basic state used in the problem and dissipation parameterizations. The vector $\mathbf{f}$ represents stream function or thermal forcing or, in the case of topographic forcing, contains linear products of the basic state and topographic spectral coefficients. Here N is the total number of spectral components obtained from the number of levels and zonal and total wave numbers used in the truncation scheme.

Then for nonzero ω_α the solution to (6) is

$$\boldsymbol{\psi}(t) = \sum_{\alpha=1}^{N} K_\alpha \boldsymbol{\phi}_\alpha \exp\,(-i\omega_\alpha t) + \sum_{\alpha=1}^{N} \left(\frac{\eta_\alpha \boldsymbol{\phi}_\alpha}{-i\omega_\alpha}\right)[\exp(-i\omega_\alpha t) - 1] \quad (7)$$

[*Coddington and Levinson*, 1955, chapter 3, section 4]. In the absence of an initial perturbation or forcing the first or second terms on the right-hand side of (7), of course, vanish. Here ω_α are the eigenvalues and $\boldsymbol{\phi}_\alpha$ the right-hand column eigenvectors which satisfy

$$(\omega_\alpha \mathsf{I} - \mathsf{C})\boldsymbol{\phi}_\alpha = 0 \qquad \alpha = 1, \cdots, N \quad (8)$$

In (8), $\boldsymbol{\phi}_\alpha$ for $\alpha = 1, \cdots, N$ are precisely the eigenmodes of all the growing (Im $\omega_\alpha > 0$), neutral (Im $\omega_\alpha = 0$), and decaying (Im $\omega_\alpha < 0$) normal modes of the three-dimensional instability problem. Also, $\mathsf{C} = \mathsf{A}^{-1}\mathsf{B}$ and I is the unit matrix and

$$K_\alpha = \boldsymbol{\chi}_\alpha{}^T \boldsymbol{\psi}_0 / \boldsymbol{\chi}_\alpha{}^T \boldsymbol{\phi}_\alpha \quad (9)$$

$$\eta_\alpha = \boldsymbol{\chi}_\alpha{}^T \mathsf{A}^{-1} \mathbf{f} / \boldsymbol{\chi}_\alpha{}^T \boldsymbol{\phi}_\alpha \quad (10)$$

where $\boldsymbol{\chi}_\alpha{}^T$ is the left-hand row eigenvector of C corresponding to eigenvalue ω_α. The left- and right-hand eigenvectors form a bi-orthogonal system [*Wilkinson*, 1965, section 1.4; *Gantmacher*, 1959, chapter 9, section 8]. Equation (7) is valid for all basic states (and dissipations) corresponding to nondegenerate eigenvalues, that is, except for a set having zero volume (assuming sufficient numerical accuracy) in the phase space of basic state spectral coefficients [*Wilkinson*, 1965, section 1.4]. More generally, if the eigenvalues are degenerate, one could include or change the dissipation to remove the degeneracy or do a least squares fit to the initial data in terms of the eigenfunctions associated with the nondegenerate eigenvalues.

For the case of solid body rotation flow over topography in a barotropic atmosphere, the second term on the right-hand side of (7) reduces to the usual expression for Rossby wave dispersion [cf. *Frederiksen*, 1982*c*, equations (2.10)–(2.13)]. Then the modes are neutral in the absence of dissipation and decaying with dissipation, and the ususal problem of Rossby wave dispersion in a (linearly) stable atmosphere is recovered.

The steady state solutions of the studies listed in section 5 may be generalized as the time-independent term on the right-hand side of (7), namely,

$$\boldsymbol{\psi}^s = -i\mathsf{B}^{-1}\mathbf{f} = -i \sum_{\alpha=1}^{N} \frac{\eta_\alpha \boldsymbol{\phi}_\alpha}{\omega_\alpha} \quad (11)$$

7.2. *Linear and Nonlinear Steady State Theories in an Unstable Atmosphere*

Next we consider the implications of (11) within the context of linear theory and in relation to the climate response, i.e., the nonlinear time average or statistical ensemble average response. First, within linear theory we see from (7) that if for all ω_α, Im $(\omega_\alpha) < 0$ then $\boldsymbol{\psi}^s = \boldsymbol{\psi}$ $(t \to \infty)$. That is, $\boldsymbol{\psi}^s$ is the asymptotic value obtained in a linear initial value problem if the dissipation is sufficiently large for all the transients to be damped asymptotically. That would be the case, for example, in a barotropic atmosphere with a stable basic state such as solid body rotation. Then the normal modes change from neutral to damped in the presence of any dissipation. However, in a more realistic baroclinic atmosphere the linear initial value problem would be swamped by rapidly growing baroclinic disturbances with large growth rates [see *Frederiksen*, 1983*c*, Table 2].

In order to damp such modes and obtain (11) as an asymptotic solution, one would have to increase the dissipation to the extent that one would be left with an atmosphere with the consistency of treacle or molasses. That is, unless one increases the dissipation to the extent that all transients are damped, (11) does not have meaning as an asymptotic linear steady

state solution. One can, of course, still solve (11) (as done, for example, in some of the studies mentioned in section 5.1) and hope that the solution gives some indication of what the time-averaged flow in a nonlinear model or the atmosphere should be. The extent to which (11) yields realistic results depends on how successfully one can replace the effects of transients by eddy drag and diffusion coefficients. Given that approximately half the kinetic energy in the atmosphere is due to transients, one would, of course, expect the solution of (11) without appropriately chosen eddy drag and diffusion coefficients to be substantially different from that without such "tuning." The results of *Opsteegh and Vernekar* [1982] and *Egger and Schilling* [1983] in which the transients are treated explicitly rather than as eddy drag and diffusion coefficients clearly shows that this is the case.

In general, it is not possible to give an a priori estimate of how well the linear steady state solution (11) will approximate the nonlinear response; the successes and limitations of this approach for zonally averaged basic states were discussed in section 5.1. *Frederiksen and Carnevale* [1986] have, however, examined the conditions under which the linear steady state solution (11) is also the nonlinear climate solution for the simple case of inviscid solid body rotation flow over topography in a barotropic model. They find that in the case when the solid body rotation component corresponds to westward flow, the linear steady state solution is also the nonlinear climate solution. However, in the more realistic case of eastward solid body rotation flow, the linear steady state solution is unstable, and the linear and nonlinear climate states are considerably different.

7.3. *Internal Fluctuations or Responses to Anomalous External Forcing?*

The three-dimensional instability theory described in section 7.1 provides a formalism for treating both internal "noise" amplification and the response to forcing. As such, it is neutral as to the importance of either in reality, although some of the mechanisms described in earlier sections are not. For example, in the baroclinic-barotropic dipole instability mechanism of section 6, changes in external forcing are not seen as playing a crucial role in the development process.

In this subsection we examine some of the observational and model studies which throw light on the role of internal fluctuations and external forcings in generating anomalies. It is probably fair to say that for band-pass-filtered fluctuations it is generally accepted that the role of anomalous external forcing is minimal except, of course, in determining the distribution of the basic state. In the linear regime we have the initial value problem with the solution given by the first term on the right-hand side of (7). For the lower-frequency fluctuations it may be that anomalous external forcings such as sea surface temperature anomalies play an increasingly important role. There have, of course, been numerous simulation experiments in which realistic circulation anomalies have been produced through the specification of, for example, sea surface temperature anomalies [e.g., *Rowntree*, 1972; *Julian and Chervin*, 1978; *Keshavamurty*, 1982; *Shukla and Wallace*, 1983; *Blackmon et al.*, 1983; *Geisler et al.*, 1985; *Lau*, 1985; *Palmer and Zhaobo*, 1985, and references therein] or mass sources [e.g., *Lau and Lim*, 1984]. *Horel and Wallace* [1981] have presented convincing observational evidence of a modest relationship between interannual variability in tropical Pacific sea surface temperature anomalies and the Pacific–North American teleconnection pattern. They interpret the extratropical atmospheric circulation anomalies as essentially a forced stationary Rossby wave response to the tropical heating anomalies over the central equatorial Pacific. *Dole*'s [1986] observational study, however, indicates that "... the patterns may often and perhaps primarily, grow and decay while the external forcing remains nearly fixed ..." Further, his results "... provide no clear indication for Rossby wave trains propagating northward from this region immediately prior to development ..."

There are also many theoretical and simulation studies which indicate that anomalous circulations such as low zonal index circulations may be achieved purely through internal dynamics. No anomalous external forcing is assumed in the multiple equilibria models proposed independently by *Charney and DeVore* [1979] and *Wiin-Nielsen* [1979] and in generalizations of these models to include baroclinic effects and more modes [*Charney and Strauss*, 1980; *Källén*, 1983; *Malguzzi and Speranza*, 1981; *Trevisan and Buzzi*, 1980; *Wiin-Nielsen*, 1984, 1986; *Speranza*, 1986]. The same is true of generalizations including stochastic forcing [*Egger*, 1981; *Benzi et al.*, 1984] and in numerical simulations with relatively simple numerical models [*Källén*, 1981, 1982; *Legras and Ghil*, 1984]. The results of *Frederiksen and Puri* [1985] using a five-level primitive equation model with fixed boundary conditions (discussed in section 8) and the work of *Lau* [1981] on analyzing anomalies generated within general circulation models also indicate that quite realistic anomalies may be generated without anomalous forcings such as sea surface temperature anomalies. But, on the other hand, the forcing anomaly experiments described above indicate the production of realistic

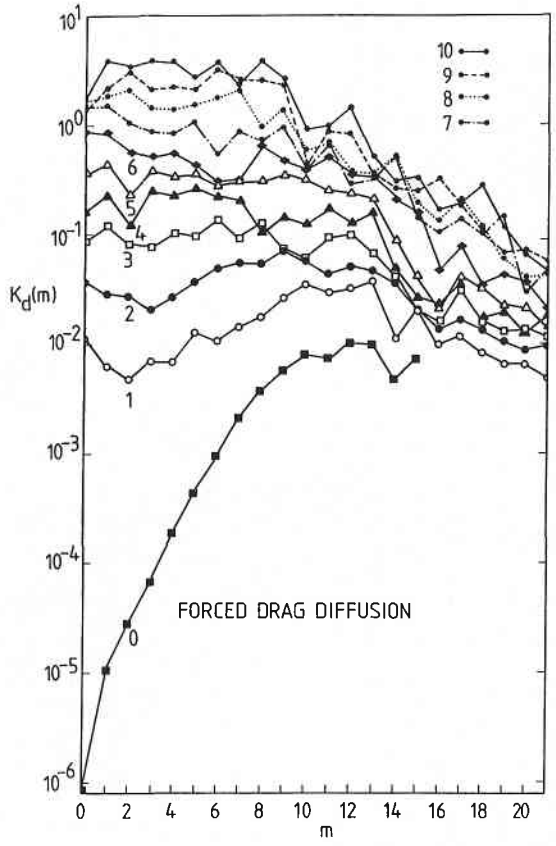

Fig. 23. Vertically averaged disturbance kinetic energy spectra per unit mass in $m^2\ s^{-2}$ as functions of zonal wave number m and days [from *Frederiksen and Puri*, 1985].

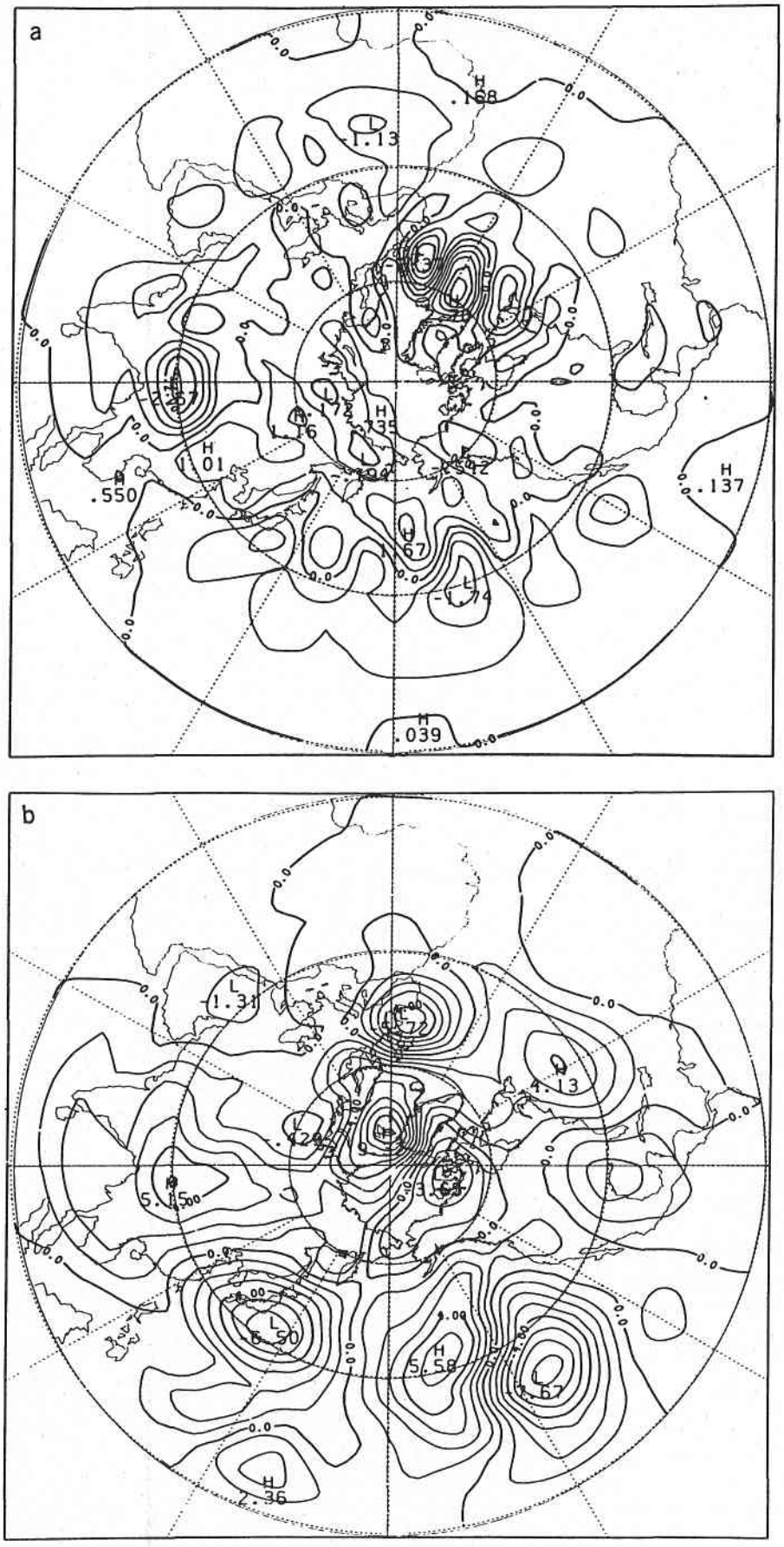

Fig. 24. Disturbance stream function in $km^2\ s^{-1}$ for forced run with drag diffusion at (*a*) $\sigma = 0.7$ on day 2, (*b*) $\sigma = 0.1$ on day 6, and (*c*) $\sigma = 0.1$ on day 10 [from *Frederiksen and Puri*, 1985].

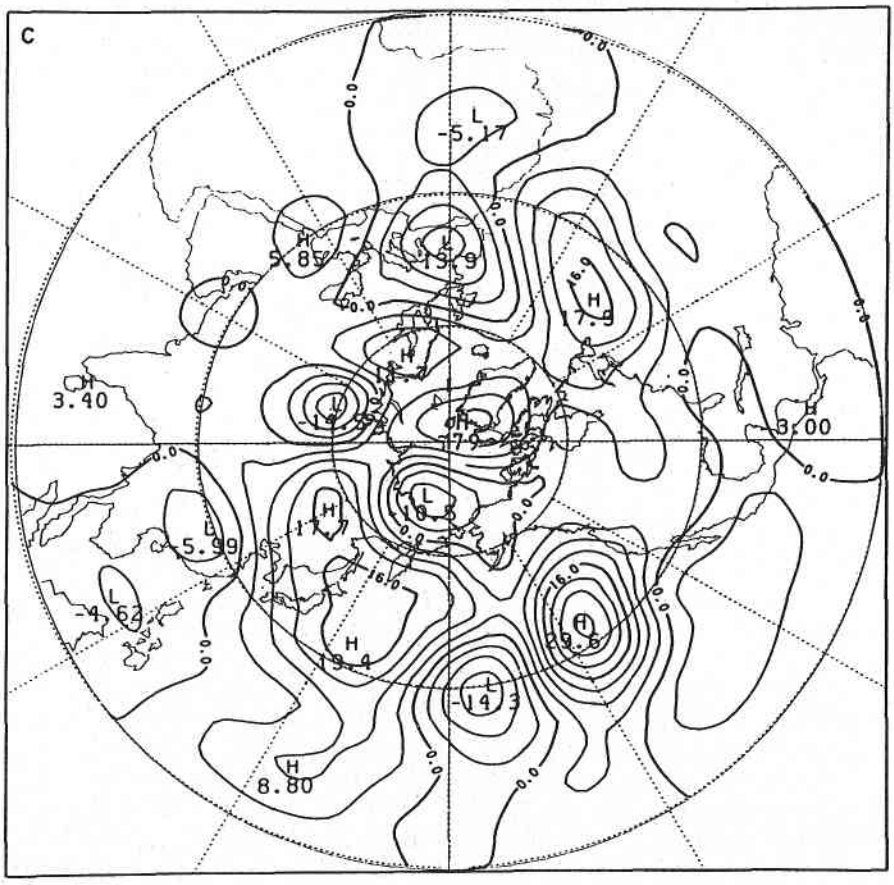

Fig. 24. (continued)

anomalies. In view of the discussion in section 7.1 it is, of course, not surprising that since the atmosphere has preferred modes of oscillation, these can be excited through either "noise" amplification or forcing.

Thus for "free" simulation studies, the anomalies must grow and decay purely through internal dynamics with fixed boundary conditions. As mentioned above and noting the caveats, *Dole* [1983] also suggests that this may be largely true in the case of his observed anomalies. During the growth phase they would project clearly onto growing normal mode solutions rather than neutral modes. Thus it would appear that a linear theory of these (nonlinear) results would require an understanding of the three-dimensional instability problem. We also note that in studying the behavior of observed low-pass-filtered observations, the higher-frequency modes, which are left out, would appear as an effective time-dependent force on the lower-frequency fluctuations as discussed by *Leith* [1973], *Holopainen* [1984], *Holopainen and Fortelius* [1987], *Mullen* [1987], and many others. The work of *Opsteegh and Vernekar* [1982] and *Egger and Schilling* [1983] indicates the importance of this effective force of the transients in obtaining realistic stationary wave patterns. *Hansen and Chen* [1982] also note that in their observational studies a ". . . blocking high over Greenland in December 1978 was, in fact, forced by intense baroclinic cyclone-scale waves . . ." It may not be easy, in general, to separate the role of the transient cyclone scale disturbances in forcing the larger scales [*Gall et al.*, 1979] from that of time-dependent external forcings, such as sea surface anomalies, unless these terms are measured separately. *Kok and Opsteegh* [1985] have recently performed a linear model study in which the effects of transients, diabatic heating and orography in producing anomalous circulations are treated separately. They note that

> the amplitudes of the anomalies in the extratropics forced by the observed tropical heat sources are small even for seasons when the 1982/83 El Niño event was at its maximum. The pattern correlations are close to zero. The signal from the tropics seems by far not as important as the effect of the transient eddies. . . .

There is a further phenomenon which occurs in numerical models and observations which seems to indicate the importance of the unstable modes in dispersion from a source. In linear barotropic model studies of wave trains generated by an equatorial source the wave paths start from the source [e.g., *Simmons*, 1982], especially with the simple basic states usually employed. In contrast, when instability is possible, such as in baroclinic models [*Geisler et al.*, 1985] and in the observations [e.g., *Wallace and Gutzler*, 1981], the wave path is to the north and west of the equatorial source. In the barotropic models, the transient modes are decaying in the presence of dissipation, and hence, as may be inferred from (7) and as found in numerical experiments (*Kasahara*, [1966], *Webster* [1972, 1973*b*, 1981, 1982], *Opsteegh and van den Dool* [1980], *Hoskins and Karoly* [1981], and others), in order to obtain a large-amplitude wave train away from the source, the disturbance must have large amplitude near the source. That is, the wave path starts from the source. However, in an unstable atmosphere where there are growing modes, the source can generate an initially small-amplitude disturbance which dis-

perses and then grows to large amplitude in the unstable region away from the source to form the observed wave train. It may, of course, be that, as in some of the experiments discussed above, it is not necessary for the source to actually generate the initial disturbance. One could think of the slowly varying (unbalanced) forcing function as slowly changing the mean flow instability properties with the formation of the wave trains arising from initial disturbances, which are always present, and occurring on a faster time scale. This hypothesis, which *Dole* [1983, 1986] suggests is most likely on the basis of his observations, is consistent with the wave paths to the north of equatorial sources.

8. Evolution of Anomalies in Baroclinic Models With Longitudinal Variation of the Basic State

As discussed in the previous sections, there have been many model studies which have examined the atmospheric response to anomalous forcing or imposed disturbances. Few, however, have concentrated on the time dependence of the transient response. Here we consider two such studies, one of which examines the evolution of an initial mid-latitude disturbance and the other of an initial equatorial disturbance.

8.1. *Development of Large-Scale Anomaly From Mid-Latitude Disturbance*

Frederiksen and Puri [1985] conducted a series of numerical simulations in which the changes in an initial mid-latitude perturbation, growing on a three-dimensional northern hemisphere climatological flow, were studied. A five-level primitive equation model was used in which the climatological flow was for January 1978 (qualitatively similar to that shown in Figure 5*a*). The perturbation was the instability mode shown in Figure 8*b*. Suitable forcing was included in the model so that the climatological basic state was an exact solution in the absence of the perturbation.

Figure 23 shows the developments of the disturbance kinetic energy zonal wave number m spectra over a 10-day period of integration. We see that there is a gradual and continual change in the energy spectra from being peaked at relatively small scales initially until, by day 10, the disturbance energy preferentially populates the large scales.

Figures 24*a*, 24*b* and 24*c* show the disturbance stream functions on day 2 at the sigma surface $\sigma = 0.7$, on day 6 at the sigma surface $\sigma = 0.1$, and on day 10 at $\sigma = 0.1$. The disturbance starts as a rather shallow feature on day 0 and penetrates increasingly into the upper atmosphere during the integration. On days 6 and 10 the disturbances at lower levels have some of the same features that are shown in Figures 24*b* and 24*c* but have more small-scale structure. During the early stages of development the monopole cyclogenesis wave train splits into dipoles in both the Pacific Ocean and the Atlantic Ocean as seen in Figure 24*a* for the Pacific; in the Atlantic the dipoles are mainly evident at higher levels on day 2. There are also wave trains emanating from the Himalayan and Greenland areas which appear to be due to interaction of the large-scale flow with the topography. By day 6 we see the emergence of an equivalent barotropic large-scale feature in the Atlantic-Arctic region; it has some qualitative features in common with the North Atlantic Oscillation pattern. On day 10 the large-scale equivalent barotropic feature in the Pacific produces strongly diffluent flow characteristic of blocked flow off the west coast of America.

The appearance of baroclinic dipole structures as the precursors to the formation of mature anomalies agrees in qualitative terms with the instability theory results and observations discussed in section 6.1. *Frederiksen and Puri* [1985] also performed error growth experiments in which the difference between two time-dependent fields, one of which was disturbed by the perturbation in Figure 8*b*, was considered. Again, the formation of large-scale anomalies was preceded by the development mid-latitude baroclinic dipole disturbances.

8.2. *Development of Large-Scale Extratropical Anomaly From Equatorial Disturbance*

In the work by E. A. O'Lenic et al. (submitted manuscript, 1988) (see section 5.1.1) a series of experiments designed to assess the impact of the uncertainty of the initial data fields in the tropics tends to lend credence to the results of *Webster and Chang* [1988] described in section 5.2. Such corroboration is important, as it comes from the fully nonlinear, global National Meteorological Center forecasting model and allows the abandonment of some of the caveats that we had to attach to the simpler phenomenological model described in section 5. Instead of wave sources, the model was forced by inserting regional data uncertainty or error. The difference fields at the nine analysis levels were used to perturb the NMC initial data set in the regions shown in Figure 25. The model was then run for a series of 10-day forecasts for both summer and winter cases and difference fields were generated by subtracting the perturbed run from an unperturbed control forecast. The eastern Pacific Ocean, the Indian Ocean, and the western Pacific Ocean were successively perturbed in three experiments. In a fourth experiment the entire tropics were perturbed. The locations of the four perturbation regions are shown in Figure 25 and are referred to as the EPO, the IO, the WPO, and the TT, respectively. The regions were chosen as they are areas of particularly poor atmospheric data.

There is no real method of judging the degree of "uncertainty" that exists in a data set. Our assessment was made by comparing, and subtracting, two different estimates of the same fields. We chose two sets of analyses of the First GARP Global Experiment (FGGE) Special Observing Periods; one by NMC and the other by the European Centre for the Medium Range Weather Forecasting (ECMWF). Root-mean-square differences of 5–10 m s^{-1} over broad areas were found between the two analyses in the deep tropics.

Figure 26 shows three longitude-time sections of anomaly velocity magnitude along the equator corresponding to experiments using June 27, 1979, initial data and the regional perturbations shown in Figure 25. Anomalies move away from the perturbed region and establish a maximum location in the vicinity of the upper tropospheric westerlies irrespective of the location of the initial perturbation. In sections along 20°N (not shown) there is little or no perturbation for the first few days. However, later the anomaly field grows substantially, not at the longitudes of the initial perturbation but at those longitudes adjacent to the strong equatorial westerlies. Thus the experiments with the NMC model support the concept of a wave energy accumulation region, and also show that the equatorial westerlies act as emanation regions to the extratropics. The latter important point supports the notion of the wave emanation region which may be remote to the tropical excitation zone, as suggested by *Webster and Chang* [1988]. The similarity of the response in the cases where the anomaly grows from either imposed forcing, as in section 5, or an initial error, as in the present experiments, seems to indicate the

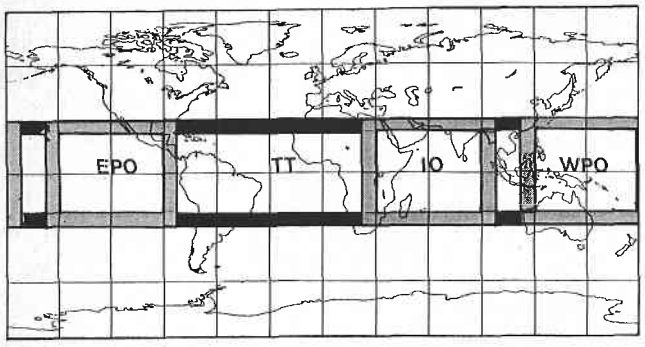

Fig. 25. The transplant regions for the IO (Indian Ocean), WPO (west Pacific Ocean), EPO (east Pacific Ocean), and TT (total tropics) experiments (after E. A. O'Lenic et al., unpublished data, 1988).

importance of projection onto the unstable modes of the system as discussed in sections 6 and 7, as the waves disperse to higher latitudes.

The impact of the same wave energy emanation region occurring for very different distributions of uncertainty (or forcing) along the equator has a very dramatic effect on the response in the extratropics. For a given initial data set, irrespective of which region along the equator is perturbed, essentially the same response occurs at higher latitudes. This is to be expected, of course, as the wave train will have the same reference point along the equator. This may be seen in Figure 27, where northern hemisphere 200-mbar height difference fields (m), after 10 days, are plotted for the June 27, 1979, IO, EPO, WPO, and TT experiments. The response also possesses an equivalent barotropic structure. The amplitude of the anomalies is about one third of the average amplitude of a synoptic wave at 200-mbar!

Experiments with initial conditions for the preceding and succeeding days show a remarkable robustness, although this may be expected. If the hypothesis regarding the control of the equatorial accumulation and emanation regions by the longitudinal variation of the basic state is true, then we would expect the extratropical response to change only with the slow variation of the large-scale basic state. Although the experiments with the NMC model only extend to 10 days, it is worth noting that the constancy of the response is very similar to the *Keshavamurty* [1983] and *Geisler et al.* [1985] results from longer-term climate experiments with general circulation models.

The westerly duct teleconnection mechanism or hypothesis, described in section 5, calls for the focusing of transient wave energy in the equatorial regions at a "wave energy accumulation region," defined by the longitudinal stretch of the basic state. The hypothesis then suggests that this region acts as the emanation region for the wave train to the extratropics. However, in the last section we have seen that the instability of the basic flow must be taken into account in the wave dispersion process into the higher latitudes. The dispersion through the basic state has the potential of triggering the low-frequency modes discussed in sections 6 and 7. The low-frequency nature of these growing modes and the very slow propagation during their major amplification phase is such that a time average would have the appearance of a steady state wave train. Figure 28 shows a schematic of the modified wave train hypothesis: the westerly duct mechanism. In the background the basic flow with longitudinal stretching and shearing deformation is shown as velocity vectors. The regions of easterlies are enclosed by the heavy line. The heavy arrows (PR) show the propagation of the equatorially trapped transient Rossby waves moving toward the accumulation region (AC) in the region along the equator where $\partial\bar{u}/\partial x < 0$. The stippled arrows show the emanation of the wave trains to higher latitudes. It might be remembered that *Webster and Holton* [1982] speculated that the equatorial westerlies could act as waveguides to the propagation of extratropical waves to the deep tropics or through to the other hemisphere. *Webster and Chang* [1988] do not refute this possibility and see the equatorial westerlies as a region of strong two-way interaction (i.e.,

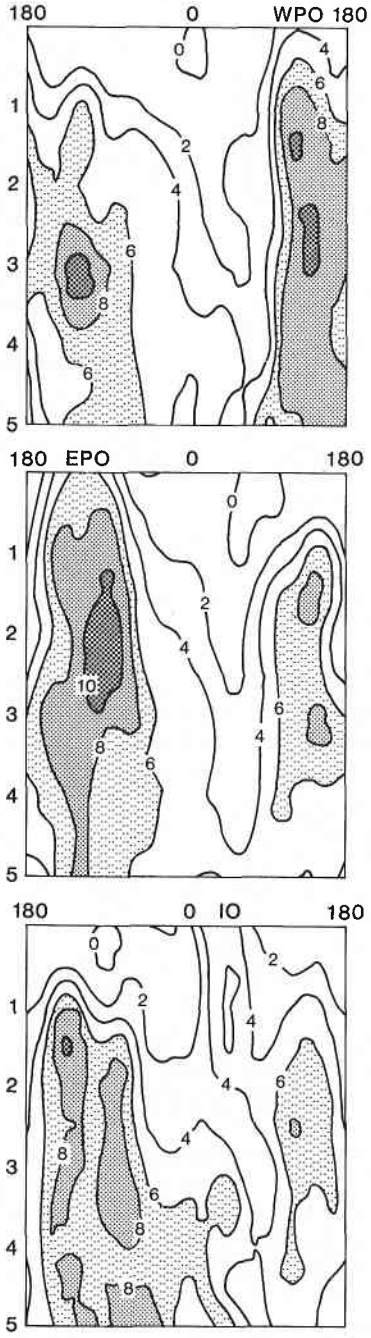

Fig. 26. Time-longitude plots at 200 mbar of the anomalous wind speed along the equator for the west Pacific Ocean (WPO), the east Pacific Ocean (EPO) and the Indian Ocean (IO) experiments of E. A. O'Lenic et al. (unpublished data, 1988) using the National Meteorological Center global spectral model.

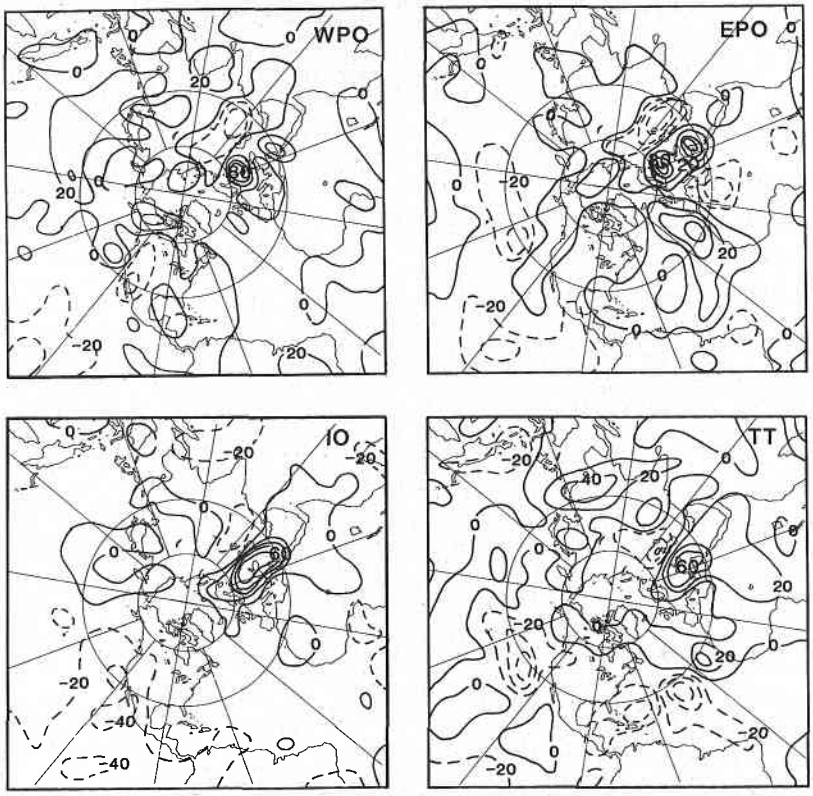

Fig. 27. The 200-mbar height anomalous northern hemisphere response to the perturbation of the eastern Pacific Ocean (EPO), the Indian Ocean (IO), and the western Pacific Ocean (WPO) in the National Meteorological Center model for June 27, 1979. The response to the perturbation of the entire tropics (TT) is also shown (after E. A. O'Lenic et al., unpublished data, 1988).

both extratropics to tropics and tropics to extratropics) between remote regions on the globe.

9. Summary and Conclusions

Throughout this paper we have discussed and reviewed observations and theoretical and modeling studies that pertain to the low-frequency structure of the global atmosphere. Without doubt, a very rich structure has been found in all sections of the globe, including the tropics. The variety of low-frequency modes depends, to a great extent, on the evolving three-dimensional structure of the atmospheric circulation. We have argued that this structure can be explained in terms of the annual variation of the low-latitude heating and the distribution of orography. The importance of the former forcing is seen clearly from the location and variation of the boreal winter subtropical jet stream that exists relative to the equatorial heating. It was also pointed out that there are significant variations of the annual cycle that are linked, in part, to the Southern Oscillation.

The existence of low-frequency "centers of action" within the tropical regions, as distinct from those of the extratropics that have been acknowledged in the literature since *Rossby* [1949], is a new concept and one, it would seem, that may be of some consequence. *Webster and Holton* [1982], *Arkin and Webster* [1985], and *Webster and Chang* [1988] have shown through empirical, theoretical, and modeling studies that the regions of negative longitudinal stretch in the basic flow at low latitudes is a region of transient energy accumulation. Such regions of negative stretch occur in the eastern Pacific Ocean and, to a lesser extent, in the Atlantic Ocean in the upper troposphere. Energy accumulates in these regions either from the middle latitude disturbances [*Webster and Holton*, 1982; *Arkin and Webster*, 1985] or from the regions of convection in the equatorial easterlies [*Webster and Chang*, 1988]. The transfer of energy from one region of the tropics to another suggests the possibility of an equatorial teleconnection mechanism. Again, this is distinct from the tropical-extratropical teleconnection mechanisms of *Hoskins and Karoly* [1981] and *Webster* [1981, 1982].

Throughout this paper we have argued that simple linear steady state and Rossby wave dispersion theories fail to predict several aspects of mature anomalies. For example, the observed structures of these anomalies are quite often different from the vertical structures predicted by these theories. Further, in general circulation model studies, the sign of the nonlinear response is not simply related to the sign of the anomalous forcing as would be the case in linear steady state theories. We have suggested that these theories require refinement from two points of view. First, the full three-dimensional complexity of the basic state needs to be considered to explain the fact that the response of the middle latitudes is phase-locked relative to the three-dimensional flow and less dependent on the location of the anomalous forcing in, for example, the tropics. Second, the inherent instability of the basic flow needs to be considered, and this also leads to the recognition that mature anomalies can be generated either through the amplification of internal "noise" or as the response to anomalous heating.

We have shown that three-dimensional instability theory provides a natural generalization and union of the zonally

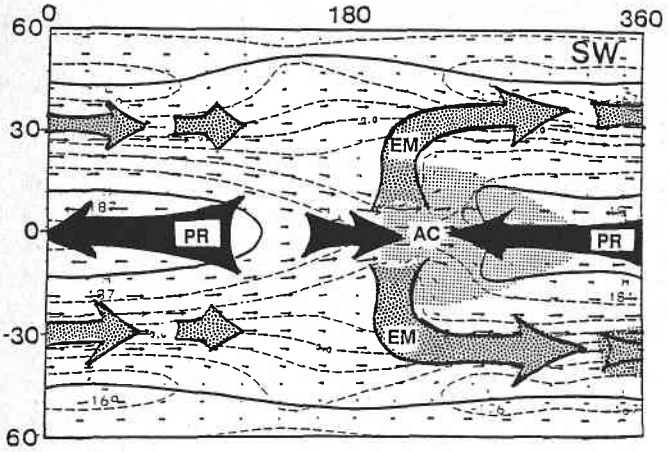

Fig. 28. Schematic of the westerly duct teleconnection mechanism. The diagram shows the propagation of equatorial trapped waves (broad arrows) along the equator and to higher latitudes relative to a background basic state containing both stretching and shearing deformation. Regions of easterlies are indicated by a heavy line. Velocity vectors of the basic flow are also shown. Transients formed in the convective regions of the tropics as equatorially trapped modes are ducted westward along the equator (PR) to regions of equatorial westerlies. If the westerlies are sufficiently strong, a wave saturation point is produced. As the waves are nondispersive, an accumulation of wave energy occurs (AC). The upper tropospheric westerlies act as emanation regions (EM) for wave trains that must disperse through a potentially unstable basic state.

averaged instability theory of Charney and Eady and the Rossby wave dispersion and linear steady state theory of Rossby and Yeh. Perhaps one of the useful functions of this study is to question and to place into a proper perspective the results of steady state climate models such as those used by *Opsteegh and van den Dool* [1980], *Hoskins and Karoly* [1981], *Webster* [1981, 1982], and many others. Clearly, since the atmosphere is inherently unstable, the linear steady state solutions must be inaccurate to some extent.

Three-dimensional instability theory, as we have formulated it in section 7, provides a formalism for studying both the amplification of internal "noise" and the response to anomalous forcing. It is also neutral as to the importance of either of these for generating mature anomalies in the atmosphere, although some of the mechanisms described in this paper are not. For example, in the baroclinic-barotropic dipole mechanism, changes in the external forcing are not seen as playing an important role in the development process. In this mechanism the formation of blocks (and "antiblocks" such as high zonal index situations) is seen (at least in some cases) as being initiated by the upstream formation of mid-latitude eastward propagating dipole wave trains which arise through the combined baroclinic-barotropic instability of the three-dimensional atmospheric flows. Nonlinear effects then are responsible for increasing the scale of the disturbance and slowing down the phase propagation until eventually the mode amplifies through the operation of largely equivalent barotropic effects. This is seen as occurring on a time scale which is much shorter than that associated with changes in anomalous forcing such as sea surface temperature anomalies. The fact that mature anomalies may have *e*-folding times as short as about one and a half days during parts of their life cycle makes it seem very unlikely that changes in sea surface temperatures would play a crucial role.

The other mechanism we have considered in detail is the westerly duct mechanism. In this, the initiation of low-frequency variability is seen as caused (at least in some cases) by tropical disturbances. These may be generated either through amplification of internal "noise" or through changes in boundary forcing such as sea surface temperature anomalies. According to this hypothesis, the longitudinal variation of the basic atmospheric flow near the equator causes a ducting of wave energy generated in the tropics to specific zones in the upper tropospheric westerlies. These zones then act as source regions for the emanation of waves into the extratropics.

We have produced observational, theoretical, and modeling evidence in favor of both of these specific mechanisms.

REFERENCES

Arkin, P. A., and P. J. Webster, Annual and interannual variability of tropical-extratropical interaction: An empirical study, *Mon. Weather Rev., 113*, 1510–1522, 1985.

Austin, J. F., The blocking of middle latitude westerly winds by planetary waves, *Q. J. R. Meteorol. Soc., 106*, 327–350, 1980.

Baines, P. G., A survey of blocking mechanism, with application to the Australian region, *Aust. Meteorol. Mag., 31*, 27–36, 1983.

Barnett, T. P., Interaction of the monsoon and Pacific trade wind systems at interannual time scales, I, The equatorial zone, *Mon. Weather Rev., 111*, 756–773, 1983.

Barnett, T. P., Variations in near-global sea level pressure, *J. Atmos. Sci., 42*, 478–501, 1984.

Bennett, J. J., and J. Young, The influence of latitudinal wind shear upon large-scale wave propagation into the tropics, *Mon. Weather Rev., 99*, 202–214, 1971.

Benzi, R., A. R. Hansen, and A. Sutera, On stochastic perturbation of simple blocking models, *Q. J. R. Meteorol. Soc., 110*, 393–409, 1984.

Berggren, R., B. Bolin, and C.-G. Rossby, An aerological study of zonal motion, its perturbation and break-down, *Tellus, 1*, 14–37, 1949.

Bjerknes, J., Atmospheric teleconnections from the equatorial Pacific, *Mon. Weather Rev., 97*, 162–172, 1969.

Blackmon, M. L., A climatological spectral study of the 500 mb geopotential height of the northern hemisphere, *J. Atmos. Sci., 33*, 1607–1623, 1976.

Blackmon, M. L., J. M. Wallace, N. Lau, and S. L. Mullen, An observational study of the northern hemisphere wintertime circulation, *J. Atmos. Sci., 34*, 1040–1053, 1977.

Blackmon, M. L., J. E. Geisler, and E. J. Pitcher, A general circulation model study of January climate anomaly patterns associated with interannual variation of equatorial Pacific sea surface temperature, *J. Atmos. Sci., 40*, 1410–1425, 1983.

Blackmon, M. L., Y. H. Lee, and J. M. Wallace, Horizontal structure of 500 mb height fluctuations with long, intermediate and short time scales, *J. Atmos. Sci., 41*, 961–979, 1984*a*.

Blackmon, M. L., Y. H. Lee, J. M. Wallace, and H. H. Hsu, Time variation of 500 mb height fluctuations with long, intermediate and short time scales as deduced from lag-correlation statistics, *J. Atmos. Sci., 41*, 981–991, 1984*b*.

Branstator, G., Analysis of general circulation model sea-surface temperature anomaly simulations using a linear model, II, Eigenanalysis, *J. Atmos. Sci., 42*, 2242–2254, 1985.

Bretherton, F. P., and C. J. R. Garrett, Wave trains in inhomogeneous moving media, *Proc. R. Soc. London, Ser. A, 362*, 529–554, 1968.

Charney, J. G., The dynamics of long waves in a baroclinic westerly current, *J. Meteorol., 4*, 135–162, 1947.

Charney, J. G., A note on the large-scale motions in the tropics, *J. Atmos. Sci., 20*, 607–609, 1963.

Charney, J. G., A further note on large scale motions in the tropics, *J. Atmos. Sci., 26*, 182–185, 1969.

Charney, J. G., and J. G. DeVore, Multiple flow equilibria in the atmosphere and blocking, *J. Atmos. Sci., 36*, 1205–1216, 1979.

Charney, J. G., and A. Eliassen, A numerical method for predicting the perturbations of the middle latitude westerlies, *Tellus, 1*, 38–54, 1949.

Charney, J. G., and D. M. Straus, Form-drag instability and multiple equilibria in baroclinic, orographically forced planetary wave systems, *J. Atmos. Sci., 37*, 1157–1176, 1980.

Coddington, E. A., and N. Levinson, *Theory of Ordinary Differential Equations*, 429 pp., McGraw-Hill, New York, 1955.

Colucci, S. J., Explosive cyclogenesis and large scale circulation changes: Implications for the onset of blocking, *J. Atmos. Sci.*, *42*, 2701–2719, 1985.

Colucci, S. J., Comparative diagnosis of blocking versus non-blocking planetary-scale circulation changes during synoptic-scale cyclogenesis, *J. Atmos. Sci.*, *44*, 124–139, 1987.

Dole, R. M., Persistent anomalies of the extratropical northern hemisphere wintertime circulation, Ph.D. thesis, 225 pp., Dep. of Meteorol., Mass. Inst. of Technol., Cambridge, 1982.

Dole, R. M., Persistent anomalies of the extratropical northern hemisphere wintertime circulation, in *Large-Scale Dynamical Processes in the Atmosphere*, edited by B. J. Hoskins and R. P. Pearce, pp. 95–109, Academic, San Diego, Calif., 1983.

Dole, R. M., The life cycles of persistent anomalies and blocking over the North Pacific, *Adv. Geophys.*, *29*, 31–69, 1986.

Eady, E. T., Long waves and cyclone waves, *Tellus*, *1*, 33–52, 1949.

Egger, J., The linear response of a hemispheric two-level primitive equation model to forcing by topography, *Mon. Weather Rev.*, *104*, 351–364, 1976.

Egger, J., Dynamics of blocking highs, *J. Atmos. Sci.*, *35*, 1788–1801, 1978.

Egger, J., Stochastically driven large-scale circulations with multiple equilibria, *J. Atmos. Sci.*, *38*, 2606–2618, 1981.

Egger, J., and H. D. Schilling, Predictability of atmospheric low-frequency motion, in *Predictability of Fluid Motions*, edited by G. Holloway and B. J. West, pp. 149–157, American Institute of Physics, New York, 1983.

Flierl, G., V. Larichev, J. McWilliams, and G. Reznik, The dynamics of baroclinic and barotropic solitary eddies, *Dyn. Atmos. Oceans*, *104*, 841–872, 1980.

Frederiksen, J. S., The effect of long planetary waves on the regions of cyclogenesis: Linear theory, *J. Atmos. Sci.*, *36*, 195–204, 1979.

Frederiksen, J. S., Growth and vacillation cycles of disturbances in southern hemisphere flows, *J. Atmos. Sci.*, *38*, 1360–1375, 1981*a*.

Frederiksen, J. S., Scale selection and energy spectra of disturbances in southern hemisphere flows, *J. Atmos. Sci.*, *38*, 2573–2584, 1981*b*.

Frederiksen, J. S., A unified three-dimensional instability theory of the onset of blocking and cyclogenesis, *J. Atmos. Sci.*, *39*, 969–987, 1982*a*.

Frederiksen, J. S., Instability of the three-dimensional distorted stratospheric polar vortex at the onset of the sudden warming, *J. Atmos. Sci.*, *39*, 2313–2329, 1982*b*.

Frederiksen, J. S., Eastward and westward flows over topography in nonlinear and linear barotropic models, *J. Atmos. Sci.*, *39*, 2477–2489, 1982*c*.

Frederiksen, J. S., The onset of blocking and cyclogenesis: Linear theory, *Aust. Meteorol. Mag.*, *31*, 15–26, 1983*a*.

Frederiksen, J. S., Disturbances and eddy fluxes in northern hemisphere flows: Instability of three-dimensional January and July flows, *J. Atmos. Sci.*, *40*, 836–855, 1983*b*.

Frederiksen, J. S., A unified three-dimensional instability theory of the onset of blocking and cyclogenesis, II, Teleconnection patterns, *J. Atmos. Sci.*, *40*, 2593–2609, 1983*c*.

Frederiksen, J. S., The onset of blocking and cyclogenesis in southern hemisphere synoptic flows: Linear theory, *J. Atmos. Sci.*, *41*, 1116–1131, 1984.

Frederiksen, J. S., The geographical locations of southern hemisphere storm tracks: Linear theory, *J. Atmos. Sci.*, *42*, 710–723, 1985.

Frederiksen, J. S., Instability theory and nonlinear evolution of blocks and mature anomalies, *Adv. Geophys.*, *29*, 277–303, 1986.

Frederiksen, J. S., The role of instability during the onset of blocking and cyclogenesis in northern hemisphere synoptic flows, *J. Atmos. Sci.*, in press, 1988.

Frederiksen, J. S., and R. C. Bell, Teleconnection patterns and the roles of baroclinic, barotropic and topographic instability, *J. Atmos. Sci.*, *44*, 2200–2218, 1987.

Frederiksen, J. S., and G. F. Carnevale, Stability properties of exact nonzonal solutions for flow over topography, *Geophys. Astrophys. Fluid Dyn.*, *15*, 173–207, 1986.

Frederiksen, J. S., and K. Puri, Nonlinear instability and error growth in northern hemisphere three-dimensional flows: Cyclogenesis, onset-of-blocking and mature anomalies, *J. Atmos. Sci.*, *42*, 1374–1397, 1985.

Frederiksen, J. S., and B. L. Sawford, Statistical dynamics of two-dimensional inviscid flow on a sphere, *J. Atmos. Sci.*, *37*, 717–732, 1980.

Gall, R., A comparison of linear baroclinic instability theory with the eddy statistics of a general circulation model, *J. Atmos. Sci.*, *33*, 349–373, 1976.

Gall, R., R. Blackeslee, and R. C. J. Sommerville, Cyclone-scale forcing of ultra-long waves, *J. Atmos. Sci.*, *36*, 1692–1698, 1979.

Gantmacher, F. R., *The Theory of Matrices*, vol. 1, 374 pp., Chelsea, New York, 1959.

Garriott, E. B., Long range forecasts, *U.S. Weather Bur. Bull. 35*, Natl. Weather Serv., Washington, D. C., 1904.

Geisler, J. E., M. L. Blackmon, G. T. Bates, and S. Muñoz, Sensitivity of January climate response to the magnitude and position of equatorial Pacific sea surface temperature anomalies, *J. Atmos. Sci.*, *42*, 1037–1049, 1985.

Gill, A., Some simple solutions for heat induced tropical circulation, *Q. J. R. Meteorol. Soc.*, *106*, 447–462, 1980.

Gill, A., *Atmosphere-Ocean Dynamics*, *Int. Geophys. Ser.*, vol. 30, 662 pp., Academic, San Diego, Calif., 1982.

Green, J. S. A., The weather during July, 1976: Some dynamical considerations on the drought, *Weather*, *32*, 120–126, 1977.

Grose, W. L., and B. J. Hoskins, On the influence of orography on large scale atmospheric flow, *J. Atmos. Sci.*, *36*, 223–234, 1979.

Hansen, A. P., and T. C. Chen, A spectral energetics study of atmospheric blocking, *Mon. Weather Rev.*, *110*, 1146–1165, 1982.

Hart, J. E., Barotropic quasi-geostrophic flow over anisotropic mountains, *J. Atmos. Sci.*, *36*, 1736–1746, 1979.

Held, I. M., Stationary and quasi-stationary eddies in the extratropical troposphere: Theory, in *Large Scale Dynamic Processes in the Atmosphere*, edited by B. J. Hoskins and R. P. Pearce, pp. 127–167, Academic, San Diego, Calif., 1983.

Holopainen, E., Statistical local effect of synoptic-scale transient eddies on the time-mean flow in the northern hemisphere winter, *J. Atmos. Sci.*, *41*, 2505–2515, 1984.

Holopainen, E., and C. Fortelius, High-frequency transient eddies and blocking, *J. Atmos. Sci.*, *44*, 1632–1645, 1987.

Horel, J. D., A rotated principal component analysis of the interannual variability of northern hemisphere 500 mb height field, *Mon. Weather Rev.*, *109*, 2080–2092, 1981.

Horel, J. D., and J. M. Wallace, Planetary-scale atmospheric phenomena associated with the Southern Oscillation, *Mon. Weather Rev.*, *109*, 813–829, 1981.

Hoskins, B. J., and D. J. Karoly, The steady linear response of a spherical atmosphere to thermal and orographic forcing, *J. Atmos. Sci.*, *38*, 1179–1196, 1981.

Hoskins, B. J., A. J. Simmons, and D. G. Andrews, Energy dispersion in a barotropic atmosphere, *Q. J. R. Meteorol. Soc.*, *103*, 553–567, 1977.

Hunt, B. G., Atmospheric vacillations in a general circulation model, II, Tropospheric-stratospheric coupling and stratospheric variability, *J. Atmos. Sci.*, *35*, 2052–2067, 1978.

Illari, L., and J. C. Marshall, On the interpretation of eddy fluxes during a blocking episode, *J. Atmos. Sci.*, *40*, 2232–2242, 1983.

Joung, C. H., and M. H. Hitchman, On the role of successive downstream development in the east Asian polar air outbreaks, *Mon. Weather Rev.*, *110*, 1224–1237, 1982.

Julian, P. R., and R. M. Chervin, A study of the Southern Oscillation and Walker circulation phenomenon, *Mon. Weather Rev. 106*, 1433–1451, 1978.

Källén, E., The nonlinear effects of orographic momentum forcing in a low-order, barotropic model, *J. Atmos. Sci.*, *38*, 2150–2163, 1981.

Källén, E., Bifurcation properties of quasi-geostrophic, barotropic models and their relations to atmospheric blocking, *Tellus*, *34*, 255–265, 1982.

Källén, E., A note on orographically induced instabilities in two-layer models, *J. Atmos. Sci.*, *40*, 500–505, 1983.

Kalnay-Rivas, E., and L. O. Merkine, A simple mechanism for blocking, *J. Atmos. Sci.*, *38*, 2077–2091, 1981.

Karoly, D. J., Rossby wave propagation in a barotropic atmosphere, *Dyn. Atmos. Oceans*, *7*, 111–125, 1983.

Kasahara, A., The dynamical influence of orography on the large scale motion of the atmosphere, *J. Atmos. Sci.*, *23*, 259–270, 1966.

Keshavamurty, R. N., Response of the atmosphere to sea surface temperature anomalies over the equatorial Pacific and the teleconnections of the Southern Oscillation, *J. Atmos. Sci.*, *39*, 1241–1259, 1982.

Keshavamurty, R. N., Southern Oscillation: Further studies with a GFDL general circulation model, *Mon. Weather Rev., 111*, 1988–1997, 1983.

Kok, K., and T. D. Opsteegh, On the possible causes of anomalies in seasonal mean circulation patterns during the 1982/83 El Niño event, *J. Atmos. Sci., 42*, 677–694, 1985.

Kushnir, Y., Retrograding wintertime low-frequency disturbances over the North Pacific Ocean, *J. Atmos. Sci., 44*, 2727–2742, 1987.

Larichev, V., and G. Reznik, Two-dimensional Rossby solution: An exact solution, *POLYMODE News, 19*, 1–5, 1976. (Simultaneous publication in Russian, *Rep. U.S.S.R. Acad. Sci., 231*(5), 1077–1079, 1976.)

Lau, K. M., and H. Lim, On the dynamics of equatorial forcing of climate teleconnections, *J. Atmos. Sci., 41*, 161–176, 1984.

Lau, K. M., and T. J. Phillips, Coherent fluctuations of extratropical geopotential height and tropical convection in interseasonal time scales, *J. Atmos. Sci., 43*, 1164–1181, 1986.

Lau, N., A diagnostic study of recurrent meteorological anomalies appearing in a 15-year simulation with a GFDL general circulation model, *Mon. Weather Rev., 109*, 2287–2311, 1981.

Lau, N., Modelling the seasonal dependence of the atmospheric response to observed El Niños in 1962–76, *Mon. Weather Rev., 113*, 1970–1996, 1985.

Legras, B., and M. Ghil, Persistent anomalies, blocking and variations in atmospheric predictability, *J. Atmos. Sci., 42*, 433–471, 1984.

Leith, C. E., The standard error of time averaged estimates of climatic means, *J. Appl. Meteorol., 12*, 1066–1069, 1973.

Lejenäs, H., On the breakdown of the westerlies, *Atmosphere, 15*, 89–113, 1977.

Lejenäs, H., Characteristics of southern hemisphere blocking as determined from a time series of observational data, *Q. J. R. Meteorol. Soc., 110*, 967–979, 1984.

Lighthill, J., *Waves in Fluids*, 504 pp., Cambridge University Press, New York, 1978.

Lim, H., and C. P. Chang, Dynamics of teleconnections and Walker circulations forced by equatorial heating, *J. Atmos. Sci., 40*, 1847–1915, 1983.

Long, R. R., The flow of a liquid past a barrier in a rotating spherical shell, *J. Meteorol., 9*, 187–199, 1952.

Longuet-Higgins, M. S., The eigenfunctions of Laplace's tidal equations, *Philos. Trans. R. Soc., London, Ser. A, 262*, 511–607, 1968.

Mak, M., Laterally driven stochastic motions in the tropics, *J. Atmos. Sci., 26*, 41–46, 1969.

Malguzzi, P., and A. Speranza, Local multiple equilibria and regional atmospheric blocking, *J. Atmos. Sci., 38*, 1939–1948, 1981.

Matsuno, T., Quasi-geostrophic motions in the equatorial area, *J. Meterol. Soc. Jpn., 44*, 25–42, 1966.

McWilliams, J. C., An application of equivalent modons to atmospheric blocking, *Dyn. Atmos. Oceans, 5*, 43–66, 1980.

Metz, W., Transient eddy forcing of low-frequency atmospheric variability, *J. Atmos. Sci., 44*, 2407–2417, 1987.

Mo, K. C., and R. E. Livezey, Tropical-extratropical geopotential height teleconnections during the northern hemisphere winter, *Mon. Weather Rev., 114*, 2488–2501, 1986.

Mo, K. C., and G. H. White, Teleconnections in the southern hemisphere, *Mon. Weather Rev., 113*, 22–37, 1985.

Mullen, S. L., Transient eddy forcing of blocking flows, *J. Atmos. Sci., 44*, 3–22, 1987.

Murakami, T., and M. S. Unninayer, Atmospheric circulation during December 1970 through February 1971, *Mon. Weather Rev., 105*, 1024–1038, 1977.

Namias, J., Characteristics of the general circulation over the northern hemisphere during the abnormal winter 1946–1947, *Mon. Weather Rev. 75*, 145–152, 1947.

Namias, J., The great Pacific anticyclone of the winter 1949–50: A case study in the evolution of climatic anomalies, *J. Meteorol., 8*, 251–261, 1951.

O'Neill, A., and B. F. Taylor, A study of the major stratospheric warming of 1976/77, *Q. J. R. Meteorol. Soc., 105*, 71–92, 1979.

Oort, A. H., and E. M. Rasmussen, Atmospheric circulation statistics, *NOAA Prof. Pap. 5*, 323 pp., U.S. Dep. of Commer., Washington, D. C., 1971. (Available as NTIS COM-72-50295 from the National Technical Information Service, Springfield, Va.)

Opsteegh, J. D., and H. M. van den Dool, Seasonal differences in the stationary response of a linearized primitive equation model: Prospects for long range weather forecasting?, *J. Atmos. Sci., 37*, 2169–2185, 1980.

Opsteegh, T. D., and A. D. Vernekar, A simulation of the January standing wave pattern including the effects of transient eddies, *J. Atmos. Sci., 39*, 734–744, 1982.

Palmer, N., and S. Zhaobo, A modelling and observational study of the relationship between sea surface temperature in the north-west Atlantic and the atmospheric general circulation, *Q. J. R. Meteorol. Soc., 111*, 947–975, 1985.

Physick, W. L., Winter depression tracks and climatological jet streams in the southern hemisphere during the FGGE year, *Q. J. R. Meteorol. Soc., 107*, 883–898, 1981.

Pittock, A. B., On the reality, stability and usefulness of southern hemisphere teleconnections, *Aust. Meteorol. Mag., 32*, 75–82, 1984.

Plumb, R. A., On the three-dimensional propagation of stationary waves, *J. Atmos. Sci., 42*, 217–229, 1985.

Rex, D., Blocking action in the middle troposphere and its effect upon regional climate, *Tellus, 2*, 196–211, 1950.

Rheinhold, B. B., and R. T. Pierrehumbert, Dynamics of weather regimes: Quasi-stationary waves and blocking, *Mon. Weather Rev., 110*, 1105–1145, 1982.

Riehl, H., *Tropical Meteorology*, 392 pp., McGraw-Hill, New York, 1954.

Rossby, C. G., On the propagation of frequencies and energy in certain types of oceanic and atmospheric waves, *J. Meteorol., 2*, 187–203, 1945.

Rossby, C. G., On the dispersion of planetary waves in a barotropic atmosphere, *Tellus, 1*, 54–58, 1949.

Rossby, C. G., On the dynamics of certain types of blocking waves, *J. Chin. Geophys. Soc., 2*, 1–13, 1950.

Rowntree, P. R., The influence of tropical east Pacific Ocean temperatures on the atmosphere, *Q. J. R. Meteorol. Soc. 98*, 290–321, 1972.

Schilling, H., On atmospheric blocking types and blocking numbers, *Adv. Geophys., 29*, 71–99, 1986.

Schubert, S. D., A statistical-dynamical study of empirically determined modes of atmospheric variability, *J. Atmos. Sci. 42*, 3–17, 1985.

Schubert, S. D., The structure, energetics and evolution of the dominant frequency-dependent three dimensional atmospheric modes, *J. Atmos. Sci., 43*, 1210–1237, 1986.

Shulka, J., and J. M. Wallace, Numerical simulation of the atmospheric response to equatorial Pacific sea surface temperature anomalies, *J. Atmos. Sci., 40*, 1613–1630, 1983.

Shutts, G. J., The propagation of eddies in diffluent jetstreams: Eddy vorticity forcing of 'blocking' flow fields, *Q. J. R. Meteorol. Soc., 109*, 737–761, 1983.

Shutts, G. J., A case study of the eddy forcing during an Atlantic blocking episode, *Adv. Geophys., 29*, 135–162, 1986.

Simmons, A. J., The forcing of stationary wave motion by tropical diabatic heating, *Q. J. R. Meteorol. Soc., 108*, 503–534, 1982.

Simmons, A. J., and B. J. Hoskins, The life cycles of some nonlinear baroclinic waves, *J. Atmos. Sci., 35*, 414–432, 1978.

Simmons, A. J., J. M. Wallace, and G. W. Branstator, Barotropic wave propagations and instability, and atmospheric teleconnection patterns, *J. Atmos. Sci., 40*, 1363–1392, 1983.

Speranza, A., Deterministic and statistical properties of northern hemisphere, middle latitude circulation: Minimal theoretical models, *Adv. Geophys., 29*, 199–225, 1986.

Stern, M. E., Minimal properties of planetary eddies, *J. Mar. Res., 33*, 1–13, 1975.

Streten, N. A., A note on the frequency of closed circulations between 50°S and 70°S in summer, *Aust. Meteorol. Mag., 17*, 228–234, 1969.

Thompson, P. D., A heuristic theory of large-scale turbulence and long period velocity variations in barotropic flow, *Tellus, 9*, 69–91, 1957.

Trenberth, K. E., Observed southern hemisphere eddy statistics at 500 mb: Frequency and spatial dependence, *J. Atmos. Sci., 38*, 2585–2605, 1981.

Trenberth, K. E., Seasonality in southern hemisphere eddy statistics at 500 mb, *J. Atmos. Sci., 39*, 2507–2520, 1982.

Trenberth, K. E., Interannual variability of the southern hemisphere circulations: Representativeness of the Year of the Global Weather Experiment, *Mon. Weather Rev., 112*, 108–123, 1984.

Trenberth, K. E., and K. C. Mo, Blocking in the southern hemisphere, *Mon. Weather Rev., 113*, 3–21, 1985.

Trevisan, A., and A. Buzzi, Stationary response of barotropic weakly

nonlinear Rossby waves to quasi-resonant orographic forcing, *J. Atmos. Sci.*, *37*, 947–957, 1980.

Tribbia, J. J., Modons in spherical geometry, *Geophys. Astrophys. Fluid Dyn.*, *30*, 131–168, 1984.

Troup, A. J., The Southern Oscillation, *Q. J. R. Meteorol. Soc.*, *91*, 490–506, 1965.

Tucker, G. B., Transient synoptic systems as mechanisms for the meridional transport: An observational study in the southern hemisphere, *Q. J. R. Meterol. Soc.*, *105*, 657–672, 1979.

Tung, K. K., and R. S. Lindzen, A theory of stationary long waves, I, A simple theory of blocking, *Mon. Weather Rev.*, *107*, 714–734, 1979*a*.

Tung, K. K., and R. S. Lindzen, A theory of stationary long waves, II, Resonant Rossby waves in the presence of realistic vertical shears, *Mon. Weather Rev.*, *107*, 735–750, 1979*b*.

van Loon, H., Transfer of sensible heat by transient eddies in the southern hemisphere: An appraisal of the data before and during the FGGE, *Mon. Weather Rev.*, *108*, 1774–1781, 1980.

van Loon, H., and K. Labitzke, The Southern Oscillation, V, The anomalies in the lower stratosphere of the northern hemisphere in winter and a comparison with the quasi-biennial oscillation, *Mon. Weather Rev.*, *115*, 357–369, 1987.

van Loon, H., and R. A. Madden, The Southern Oscillation, I, Global associations with pressure and temperature in northern winter, *Mon. Weather Rev.*, *109*, 1150–1162, 1981.

van Loon, H., and J. C. Rogers, The seasons in winter temperatures between Greenland and northern Europe, I, General description, *Mon. Weather Rev.*, *106*, 296–310, 1978.

van Loon, H., and J. C. Rogers, The Southern Oscillation, II, Associations with changes in the middle troposphere in the northern winter, *Mon. Weather Rev.*, *109*, 1163–1168, 1981.

Verkley, W. T. M., The construction of barotropic modons on a sphere, *J. Atmos. Sci.*, *41*, 2492–2504, 1984.

Verkley, W. T. M., Stationary barotropic modons in westerly background flows, *J. Atmos. Sci.*, *44*, 2383–2398, 1987.

Walker, G. T., World weather, II, in *Memoirs of Indian Meteorological Department*, vol. *24*, part 9, Indian Meteorological Department, 1924.

Wallace, J. M., The climatological mean stationary waves: Observationary evidence, in *Large-Scale Dynamical Processes in the Atmosphere*, edited by B. J. Hoskins and P. A. Pearce, 397 pp., Academic, San Diego, Calif., 1983.

Wallace, J. M., and M. L. Blackmon, Observations of low-frequency atmospheric variability, in *Large-Scale Dynamical Processes in the Atmosphere*, edited by B. J. Hoskins and P. A. Pearce, pp. 95–109, Academic, San Diego, Calif., 1983.

Wallace, J. M., and D. S. Gutzler, Teleconnections in the geopotential height field during the northern hemisphere winter, *Mon. Weather Rev.*, *109*, 784–812, 1981.

Webster, P. J., Response of the tropical atmosphere to local, steady forcing, *Mon. Weather Rev.*, *100*, 518–540, 1972.

Webster, P. J., Remote forcing of the time-independent tropical atmosphere, *Mon. Weather Rev.*, *101*, 58–68, 1973*a*.

Webster, P. J., Temporal variation of low latitude zonal circulations, *Mon. Weather Rev.*, *101*, 803–816, 1973*b*.

Webster, P. J., Mechanisms determining the atmospheric response to sea surface temperature anomalies, *J. Atmos. Sci.*, *38*, 554–571, 1981.

Webster, P. J., Seasonality in the local and remote atmospheric response to sea surface anomalies, *J. Atmos. Sci.*, *38*, 554–571, 1982.

Webster, P. J., Large-scale structure of the tropical atmosphere, in *Large-Scale Dynamical Processes in the Atmosphere*, edited by B. J. Hoskins and P. A. Pearce, pp. 235–330, Academic, San Diego, Calif., 1983.

Webster, P. J., The interactive monsoons, in *Monsoons*, edited by J. Fein and P. L. Stephens, pp. 269–330, John Wiley, New York, 1987.

Webster, P. J., and H. R. Chang, Dispersion of equatorial waves in a flow with longitudinal flow: Implications to teleconnections theory, *J. Atmos. Sci.*, *45*, 803–829, 1988.

Webster, P. J., and J. R. Holton, Low latitude and cross equatorial response to middle-latitude forcing in a zonally varying basic state, *J. Atmos. Sci.*, *39*, 722–733, 1982.

White, G. H., An observational study of northern hemisphere extratropical general circulation, *J. Atmos. Sci.*, *38*, 28–40, 1982.

Whitham, G. R., A general approach to linear and non-linear dispersive waves using a Lagrangian, *J. Fluid Mech.*, *22*, 273–283, 1965.

Wiin-Nielsen, A., Steady states and stability properties of a low-order, barotropic system with forcing and dissipation, *Tellus*, *31*, 375–386, 1979.

Wiin-Nielsen, A., Low and high-index steady states in a low order model with vorticity forcing, *Contrib. Atmos. Phys.*, *57*, 291–306, 1984.

Wiin-Nielsen, A., Global scale circulations—A review, *Adv. Geophys.*, *29*, 3–27, 1986.

Wilkinson, J. H., *The Algebraic Eigenvalue Problem*, 662 pp., Oxford University Press, New York, 1965.

Yeh, T. C., On energy dispersion in the atmosphere, *J. Meteorol.*, *6*, 1–16, 1949.

Youngblutt, C. E., and T. Sasamori, The nonlinear effects of transient and stationary eddies on the winter mean circulation, I, The diagnostic analysis, *J. Atmos. Sci.*, *37*, 1944–1957, 1980.

J. S. Frederiksen, CSIRO Division of Atmospheric Research, Station Street, Aspendale, 3195, Australia.

P. J. Webster, Department of Meteorology, The Pennsylvania State University, University Park, PA 16801.

(Received August 14, 1987;
accepted April 22, 1988.)